

**DELIVERY AND EXOCYTOSIS OF NEUROPEPTIDE VESICLES AT THE NERVE
TERMINAL**

by

Man Yan Wong

BSc, University of Hong Kong, 2004

Submitted to the Graduate Faculty of
University of Pittsburgh in partial fulfillment
of the requirements for the degree of
Doctor of Philosophy

University of Pittsburgh

2011

UNIVERSITY OF PITTSBURGH
SCHOOL OF MEDICINE

This dissertation was presented

by

Man Yan Wong

It was defended on

March 08, 2012

and approved by

William Chet deGroat, Distinguished Professor, Dept. of Pharmacology and Chemical Biology

Michael J. Palladino, Associate Professor, Dept. of Pharmacology and Chemical Biology

Yang Hong, Assistant Professor, Dept. of Cell Biology and Physiology

Guillermo Romero, Associate Professor, Dept. of Pharmacology and Chemical Biology

Dissertation Advisor: Edwin S. Levitan, Professor and Vice Chair of Research, Dept. of of

Pharmacology and Chemical Biology

Copyright © by Man Yan Wong

2012

DELIVERY AND EXOCYTOSIS OF NEUROPEPTIDE VESICLES AT THE NERVE TERMINAL

Man Yan Wong, PhD

University of Pittsburgh, 2012

Neuropeptides, which control emotion, behavior and body homeostasis, are released at nerve terminals through the exocytosis of dense-core vesicles (DCVs). Because neuropeptides are synthesized and packaged exclusively at the cell body, accurate and timely delivery of DCV to the distant nerve terminal, as well as tight regulation of neuropeptide release should be ensured to prevent the deprivation of releasable DCVs during activity. Traditionally, it was believed that DCVs are delivered to the nerve terminal exclusively through anterograde fast axonal transport. However, it is now known that DCVs continuously transit bidirectionally at nerve terminals that are highly branched with release sites located along strings of varicosities called *en passant* boutons. Therefore, it is not clear how DCV logistics operates to support neurosecretion. In addition, little is known about the release properties of neuropeptides in fully differentiated neurons.

To address these issues, GFP-tagged neuropeptides were imaged in *Drosophila melanogaster* neuromuscular junction (NMJ) to study the routing and exocytosis behavior of DCVs *in vivo*. By using a newly developed optical technique, simultaneous photobleaching and imaging (SPAIM), to track single DCVs, it was found that DCVs circulate between the most distal bouton and the proximal axon. Neuropeptides are constantly delivered to *en passant* boutons via sporadic bidirectional capture of DCVs. These newly arrived DCVs can become releasable within minutes. Surprisingly, neuropeptides are discharged only partially and slowly

from DCVs, suggesting that “kiss-and-run” mode of exocytosis predominates over full fusion. Interestingly, these partially emptied DCVs can undergo multiple rounds of exocytosis, allowing some local recycling of DCVs and minimizing the need for the supply of new DCVs. Finally, it was found that DCVs are reloaded into *en passant* boutons after depolarization evoked-neuropeptide release by activity-dependent capture that is regulated through the ryanodine receptor-CamKII signaling pathway.

Altogether, this thesis describes some elegant mechanisms utilized by the neuron that efficiently maintain neuropeptide stores at the distant and morphologically complex nerve terminal.

TABLE OF CONTENTS

PREFACE.....	XIII
1.0 INTRODUCTION.....	1
1.1 NEUROPEPTIDES AND DENSE-CORE VESICLES.....	1
1.2 DCV DELIVERY TO THE NERVE TERMINAL	3
1.2.1 Neuronal compartmentalization.....	3
1.2.2 Supply of neuropeptides from the soma	5
1.2.3 Axonal transport of DCVs	7
1.2.4 Bidirectional DCV transport	11
1.2.5 Axonal transport and neurodegenerative diseases	12
1.3 ACTIVITY-DEPENDENT NEUROPEPTIDE RELEASE AT NERVE	
TERMINALS.....	14
1.3.1 Releasability of DCVs.....	15
1.3.2 Kiss and run exocytosis	16
1.3.3 Fusion pore and neuropeptide release kinetics	17
1.3.4 Role of kiss and run exocytosis is controlling release	19
1.4 THE EXPERIMENTAL SYSTEM : <i>IN VIVO</i> DCV IMAGING IN	
NEURONS.....	21
1.4.1 Tools to study DCV transport and exocytosis	21

1.4.2	Animal models and experimental systems:.....	23
1.5	THESIS GOAL	26
2.0	NEUROPEPTIDE DELIVERY TO SYNAPSES BY LONG RANGE VESICLE CIRCULATION AND SPORADIC CAPTURE	28
2.1	ABSTRACT	28
2.2	INTRODUCTION	29
2.3	RESULTS	30
2.3.1	Preferential anterograde transport of DCVs to the most distal bouton	30
2.3.2	Retrograde DCV transport delivers neuropeptide to proximal boutons	36
2.3.3	Uncaptured retrograde DCVs stop just before reentering the soma	41
2.3.4	Retrograde DCVs circulate back into the axon	46
2.4	DISCUSSION	48
2.4.1	Supplying <i>en passant</i> boutons by vesicle circulation	48
2.4.2	SPAIM: a new tool for studying traffic	50
2.5	MATERIALS AND METHDOS	52
2.5.1	Drosophila.....	52
2.5.2	Immunocytochemistry and Antibodies	53
2.5.3	Imaging	53
2.5.4	Image Analysis	54
3.0	CHARACTERIZATION OF DCV EXOCYTOSIS AT NERVE TERMINALS	56
3.1	ABSTRACT	56
3.2	INTRODUCTION	57
3.3	RESULTS	59

3.3.1	Single DCVs exocytosis at the nerve terminal by SPAIM tracking	59
3.3.2	Releasability of DCVs as measured by probability and size of release..	61
3.3.3	Release kinetics of neuropeptides	65
3.4	DISCUSSION	67
3.4.1	Releasability is independent of transport direction age and mobility ...	67
3.4.2	Kiss and run exocytosis as the predominant role of release.....	67
3.4.3	Imaging single DCV exocytosis at a live nerve terminal	69
3.5	MATERIALS AND METHODS	70
4.0	PRESYNAPTIC RYANODINE RECEPTOR-CAMKII SIGNALING IS REQUIRED FOR ACTIVITY-DEPENDENT CAPTURE OF TRANSITING VESICLES.	
	72	
4.1	ABSTRACT	72
4.2	INTRODUCTION	73
4.3	RESULTS	75
4.4	DISCUSSION	79
4.5	MATERIALS AND METHODS	81
5.0	DISCUSSION	83
5.1	SUMMARY AND SIGNIFICANCE OF FINDINGS	83
5.2	EFFECTIVE SUPPLY OF NEUROPEPTIDES THROUGH A CELLULAR CONVEYOR SYSTEM	87
5.3	CONSERVED NEUROPEPTIDE USE VIA PROGRESSIVE KISS-AND- RUN EXOCYTOSIS	88

5.4	POTENTIAL MECHANISM FOR CONSTITUTIVE AND ACTIVITY-DEPENDENT CAPTURE	89
5.5	SIGNIFICANCE OF THE STUDY	92
5.5.1	New insight into neurodegenerative diseases	92
5.5.2	Technology Advancement	92
5.6	FUTURE DIRECTIONS.....	93
	BIBLIOGRAPHY	97

LIST OF TABLES

Table 1. Common neuropeptides classified by tissue specificity	2
--	---

LIST OF FIGURES

Figure 1 Neurons are highly polarized and differentiated	4
Figure 2 Life of the neurotransmitter	6
Figure 3 Anterograde and Retrograde motors for DCV transport	10
Figure 4 Kiss-and-run versus full collapse fusion	20
Figure 5 Common tools to study DCV exocytosis	23
Figure 6 A dissected fly larval preparation.....	26
Figure 7 Neuropeptide accumulates initially in the most distal bouton.....	32
Figure 8 Complex anterograde DCV traffic in the terminal	35
Figure 9 Retrograde transport of excess DCVs out of the distal bouton	38
Figure 10 Retrograde DCV traffic and capture in the terminal	40
Figure 11 Uncaptured retrograde DCVs leave the terminal to enter the axon.....	42
Figure 12 Accumulation of retrograde DCVs in the proximal axon	45
Figure 13 Retrograde DCVs reverse in the proximal axon to reenter the axon.....	47
Figure 14 Vesicle circulation model for synaptic neuropeptide delivery	49
Figure 15 Measuring neuropeptide release from single DCVs by SPAIM	60
Figure 16 Releasability of DCVs in relation to their transport directions, time of residence, mobility and bouton locations.....	62

Figure 17 Neuropeptides are released partially and slowly independent of DCV transport directions and bouton locations 64

Figure 18 DCVs can undergo multiple rounds of exocytosis with release persisted long after stimulation..... 66

Figure 19 Activity-dependent neuropeptide capture following electrical stimulation 76

Figure 20 CamKII inhibition abolishes activity-dependent DCV capture..... 77

Figure 21 CamKII and presynaptic Ca²⁺ release by ER RyRs are required for activity-dependent DCV capture 79

PREFACE

Acknowledgements

First, I would like to express greatest gratitude to my advisor, Dr. Edwin Levitan, for his continuous guidance and support. His insightful ideas and skeptical thinking have led my research to success. His optimistic attitude was the best encouragement for me to overcome difficulties and challenges in finishing the dissertation. I would like to sincerely thank all the dissertation committee members, who have generously offered their time and expertise to better my work. Thanks to Dinara Shakiryanova, who has trained me with knowledge and fine skills in microscopy imaging. I also appreciate Chaoming Zhou for generating genetic constructs for many new fly lines. I am grateful to have worked in the same lab with Lesley Colgan, Ilva Putzier, Sam Covolo and Kristal Tucker. It has been the most peaceful and enjoyable work environment. Heartfelt thanks to my good friends in Pittsburgh, I would not be able to survive living so far away from home without their encouragement and companionship through these years. Last but not least, I would like to thank my dearest parents and brothers, who have always been very supportive and understanding to let me explore my passions in life. They have provided me with the greatest support, love and care to finish the dissertation.

1.0 INTRODUCTION

1.1 NEUROPEPTIDES AND DENSE-CORE VESICLES

Neuropeptides are neurohormones or neurotransmitters that consist of 3 to 100 amino acids and are expressed in various neuroendocrine cells and neurons. They are released into the extracellular fluid through the exocytosis of dense-core vesicles (DCVs). The name DCVs came from their electron-dense appearance under electron micrographs. They are much larger (diameter 100-500 nm) than classical small synaptic vesicles (SSVs; diameter 30-50 nm) that carry exclusively classical small molecule neurotransmitters (e.g. biogenic amines and amino acids). Neuropeptides are densely packaged in DCVs, in a less osmotically active form (such as sol-gel or crystalline state), which allows more contents to be stored and transported by DCVs (Michael et al., 2006).

Neuropeptides exert effects on diverse tissue systems. They control emotions, behavior, growth, and body homeostasis. Neuropeptides generally bind to G protein-coupled receptors (GPCRs), with the exception of a peptide-gated ionotropic receptor, which is a Na⁺ channel gated by the neuropeptide FMRFamide (Zhainazarov and Cottrell, 1998). Unlike classical small molecule neurotransmitters, secreted neuropeptides have longer half-lives and they often access their corresponding receptors at distant, non-synaptic sites (Agnati et al., 1995). Upon binding and activation of a neuropeptide receptor, downstream second messengers usually modulate

gating probabilities of ion channels and in turn, regulate neuron excitability (Salio et al., 2006), gene transcription (Landgraf and Neumann, 2004), synaptogenesis, and vasodilation (Cauli et al., 2004). The first neuropeptide was identified about 30 years ago and since then 120 neuropeptides have been identified in humans (Salio et al., 2006). Immunocytochemistry and *in situ* hybridization studies revealed their expression in specific neuron subpopulations in both the central nervous system (CNS) as well as the peripheral tissues (Table 1). An increasing number of neuropeptide receptor antagonists and agonists have been developed for treatment of psychiatric diseases.

Table 1 Common neuropeptides classified by tissue specificity

<p>Hypothalamic releasing factors</p> <p>CRH: corticotropin releasing hormone GHRH: growth hormone releasing hormone GnRH: gonadotropin releasing hormone Somatostatin TRH: thyrotropin releasing hormone</p>	<p>Opiate peptides</p> <p>β-endorphin Dynorphin Leu-enkephalin Met-enkephalin</p>
<p>Pituitary hormones</p> <p>ACTH: adrenocorticotrophic hormone αMSH: α-melanocyte stimulating hormone β-endorphin GH: growth hormone PRL: prolactin FSH: follicle stimulating hormone LH: luteinizing hormone TSH: thyrotropin [thyroid stimulating hormone]</p>	<p>Neurohypophyseal peptides</p> <p>Oxytocin Vasopressin</p>
<p>GI and brain peptides</p> <p>CCK: cholecystokinin Gastrin GRP: gastrin releasing peptide Motilin Neurotensin Substance K; substance P (tachykinins)</p>	<p>Neuronal and endocrine</p> <p>ANF: atrial natriuretic peptide CGRP: calcitonin gene-related peptide VIP: vasoactive intestinal peptide</p>
	<p>Neurons only?</p> <p>Galanin Neuromedin K NPY: neuropeptide Y PYY: peptide YY</p>

Adapted from (Siegel, 1999)

1.2 DCV DELIVERY TO THE NERVE TERMINAL

1.2.1 Neuronal compartmentalization

Unlike any other cell types, neurons are highly differentiated and polarized with extended processes (Figure 1). They are also one of the largest cells in humans, with the axonal compartment occupying more than 99% of their total cell volume (Morfini et al., 2009). Neuronal functions are compartmentalized in specific subcellular regions. Information flows unidirectionally in the form of action potentials from the somatodendritic region to the axon and down to the synaptic terminal, where information is relayed to effector cells through the exocytosis of chemical neurotransmitters.

The soma encloses the cell nucleus, rough endoplasmic reticulum (ER) and Golgi apparatus. Proteins and lipids are predominantly synthesized and packaged in this region to supply other compartments of the neuron. Together with the soma, diverse projections of dendrites receive synaptic inputs through the activation of excitatory or inhibitors receptors, which leads to the opening of ion channels. Action potentials are initiated at the axon initial segment (AIS), located at the most proximal part of the axon. Threshold to excitation is remarkably smaller at the AIS than that at the somato-dendritic region (Kole et al., 2008), due to its high abundance of voltage gated Na^+ channels at the AIS. The axon is often the longest process in an organism, its length can be up to 10,000 times the diameter of the cell body (Goldstein and Yang, 2000), transmitting signals possibly meters away. Vertebrate axons are commonly myelinated, allowing action potentials to propagate along the axon rapidly by activating Na^+ channel clusters at the nodes of Ranvier. The axon is also a highway to deliver recourses synthesized at the cell body to the terminal. Unlike the classical textbook picture, the

nerve terminal is highly branched with synaptic release sites located at sequential varicosities called *en passant* boutons. Here, activation of voltage-gated Ca^{2+} channels by action potentials elicits the release of neurotransmitters.

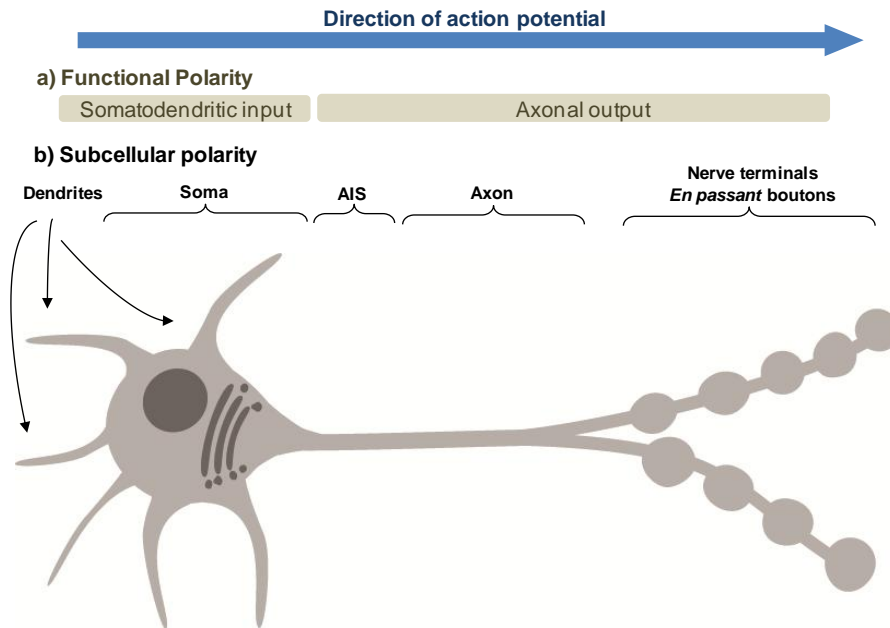


Figure 1 Neurons are highly polarized and differentiated

a) Neurons are compartmentalized into functional units to propagate action potentials unidirectionally. Excitatory and inhibitory synaptic inputs are received and integrated at the somatodendritic area. At the AIS, new action potentials are generated. The resulting action potential then propagates along the axon. Finally, the electrical signal is transformed into chemical signals through the release of neurotransmitters. **b)** Subcellular localization of different molecular components at each functional domain. Dendrites are enriched with post-synaptic receptors that can be activated by neurotransmitters from the upstream neuron. Receptor activation elicits ion influx as well as other signaling cascades. Resources are synthesized at the soma and then transported to other compartments through microtubule-based transport. The AIS is characterized by high densities of voltage-gated sodium and potassium channels that generate and modulate action potentials. Ion channels along the axon rapidly propagate action potentials. Finally, at the nerve terminal, activation of voltage-gated Ca^{2+} channels by action potentials elicits the release of neurotransmitters at specialized release sites (active zones) in *en passant* boutons. The signal is then sent across the synaptic cleft by neurotransmitters to the post-synaptic partner.

1.2.2 Supply of neuropeptides from the soma

The most fundamental difference between neuropeptides and classical neurotransmitters is their site of biosynthesis (Figure 2). Classical neurotransmitters are synthesized and packaged locally at the nerve terminal. Biosynthetic enzymes, transmitter precursors and other SSV components are synthesized at the soma and transported by axonal transport to the nerve terminal. Newly synthesized neurotransmitters are then packaged into SSVs (size: 20 nm radius) that originate from the intermediate endosomal compartment or plasma membrane. A synaptic vesicle cycle involving membrane endocytosis and transmitter repackaging operates at the nerve terminal to rapidly replenish SSVs for repeated rounds of transmitter release. Following release into the synaptic cleft, undegraded classical neurotransmitters are subject to reuptake into the nerve terminal and are repackaged into SSVs for another round of release.

In contrast, since the biosynthetic machinery for neuropeptides is absent in the nerve terminal, the supply of neuropeptides requires the delivery of DCVs from the soma. Neuropeptides are synthesized as precursor peptides in the rough ER, and packaged into immature DCVs at the TGN. The newly budded DCVs fuse with other immature DCVs, missorted materials are then removed through budding (Park and Loh, 2008). After that, DCVs are believed to be delivered to the nerve terminal through one-way anterograde microtubule-based fast-axonal transport (Goldstein and Yang, 2000). During the transport process, DCVs may undergo maturation that involves the proteolytic processing of neuropeptides. Upon arrival at the nerve terminal, DCVs are loaded onto the actin network (Huang et al., 1999), and are transferred to release sites on the plasma membrane either by diffusion or myosin-based transport (Eichler et al., 2006). The arrival of action potentials triggers the exocytosis of readily

releasable DCVs. Released neuropeptides are not subjected to reuptake and reuse through endocytosis.

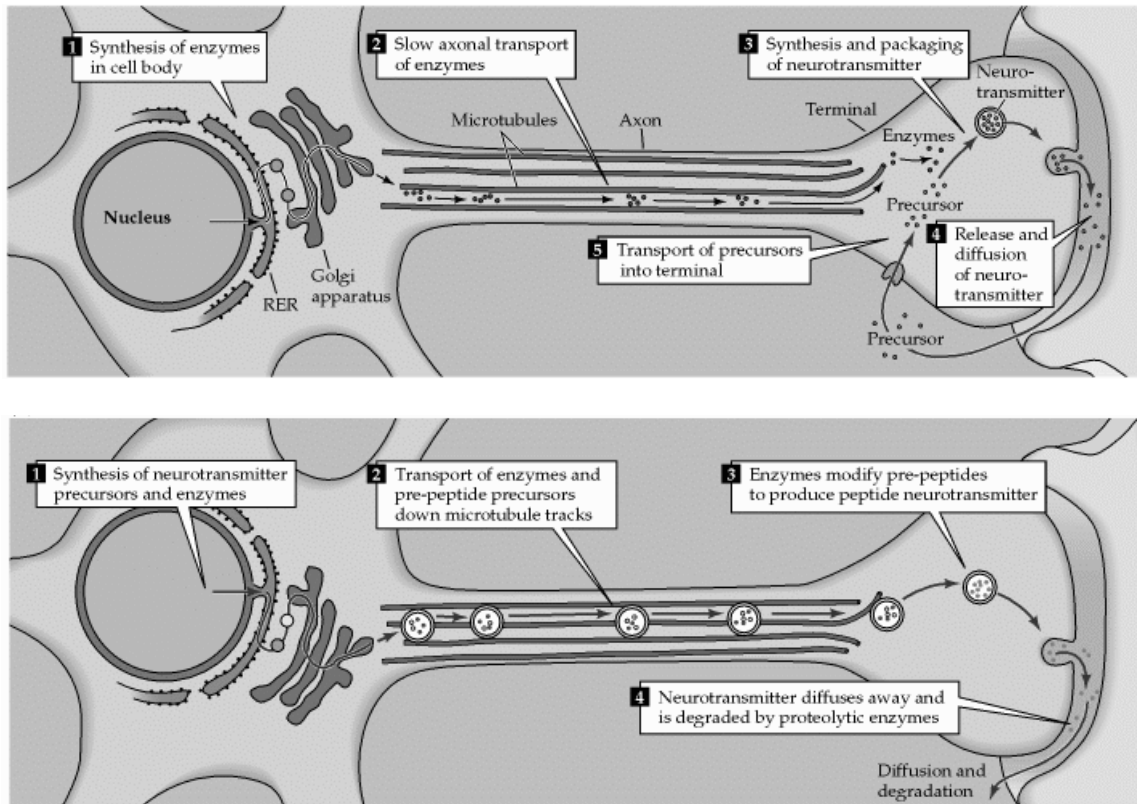


Figure 2 Life of the neurotransmitter

Small molecule neurotransmitters and neuropeptides are synthesized and packaged, released and removed very differently. **Top.** Local synthesis and recycling of small molecule neurotransmitters. **Bottom.** Long distance secretory pathway of neuropeptides. [Modified from (Purves, 2001)]

1.2.3 Axonal transport of DCVs

Long range axonal DCV transport takes place along the polarized microtubule track. A microtubule polymer is made of many α and β tubulins. It has a dynamic plus-end undergoing continuous polymerization and depolymerization. In the axon, microtubules are plus-end oriented (i.e. the fast growing dynamic end is uniformly pointed towards the terminal) (Park et al., 2009). At the nerve terminal, microtubules may be organized as an array of irregular branches if the synapse is still plastic and dynamic. On the other hand, the formation of microtubule loops is indicative of an arrest in synaptic growth and bouton formation (Conde and Caceres, 2009). Microtubule-based motors serve as engines to move cargos along the track in specific direction. Typically, membranous organelles such as vesicles and mitochondria are transported by fast ($\sim 1 \mu\text{m/s}$) axonal transport, whereas cytoskeletal components and other soluble proteins are transported by slow axonal transport that is approximately 100 times slower ($\sim 1 \text{ mm/day}$).

The kinesin superfamily proteins (KIFs) are plus-end directed motors for anterograde transport. KIF1A/Unc-104 related kinesin-3, a monomeric processive motor molecule (Figure 3, left), is the key anterograde motor in the neuron for transport of synaptic vesicle precursor proteins (Okada et al., 1995) as well as neuropeptide containing DCVs (Barkus et al., 2008; Lo et al., 2011; Pack-Chung et al., 2007a; Zahn et al., 2004). In the *Drosophila unc104* mutant, *imac*, GFP-labeled neuropeptide DCVs are absent in both the axon and the neuromuscular junction (NMJ), but an abnormal accumulation was seen at the cell body. Not much is known about how KIF1A/unc104 interacts with DCVs to direct transport; however, it is possible that the active zone protein Liprin- α /SYD-2 serves as an adaptor protein for this process. In a colocalization and immunoprecipitation study, KIF1A was found to be associated with the vesicular membrane

Liprin- α (Shin et al., 2003). The same conclusion was obtained in a yeast-two hybrid study (Wagner et al., 2009). Live imaging in *C.elegans* using Unc-104 and SYD-2 as fluorescence resonance energy transfer (FRET) partners showed colocalized movements of these proteins (Wagner et al., 2009). *Drosophila liprin- α* mutants showed misaccumulation of synaptic vesicles and slower anterograde transport of Synaptobrevin-GFP transport in axons (Miller et al., 2005). Another study suggested that a Rab3 GDP/GTP exchange protein (Rab3-GEP), DENN/MADD, regulates cargo unloading through the direct interaction with the stalk domain of KIF1A. Rab3-carrying vesicles are more effectively transported in the GTP state (Niwa et al., 2008). Because Rab3 is a well known G protein involved in DCV exocytosis, it is possible that this DENN/MADD and KIF1A interaction is also involved in DCV transport.

At the terminal, retrograde DCV transport is also needed to maintain nerve function. It may serve to remove aged and unused materials from the nerve terminal for degradation at the soma. Antibody labeling of internalized native neuropeptides in rat sympathetic cervical ganglia revealed that incompletely released peptide contents are transported retrogradely back to the cell body (Li and Dahlstrom, 2007). Second, retrograde transport is also required to replenish neuropeptide stores at the terminal. Transiting retrograde DCVs were found to reload synaptic boutons immediately after activity-evoked release, a process termed activity-dependent capture (Shakiryanova et al., 2006b).

In the retrograde direction, it is believed that DCVs are transported by the universal minus-end directed motor, cytoplasmic dynein (Figure 3, right), although no data so far have proved the requirement of dynein in DCV transport. In the closest case, synaptic proteins were shown to misaccumulation at the ends of the neuronal processes in dynein mutant worms (Koushika et al., 2004). Most studies examining DCV retrograde transport showed the

involvement of the retrograde motor adaptor complex, Dynactin (Vaughan and Vallee, 1995); Figure 3). In one study, overexpression of p50/dynamitin and the first coiled-coil domain dominant negative mutant of p150^{Glued} (CC1) in cultured hippocampal neurons reduced axonal flux of DCVs in both anterograde and retrograde directions (Kwinter et al., 2009). Similarly, *Drosophila arpl* mutants displayed a reduced velocity and run length of amyloid precursor protein (APP) -carrying vesicles in both directions (Haghnia et al., 2007). Surprisingly, a study has shown that the actin-based motor myosin V may also play a role in retrograde axonal transport of DCVs: overexpressing a myosin dominant-negative myosin Va construct impaired both the flux and speed of retrograde DCVs in hippocampal neuron (Bittins et al., 2010).

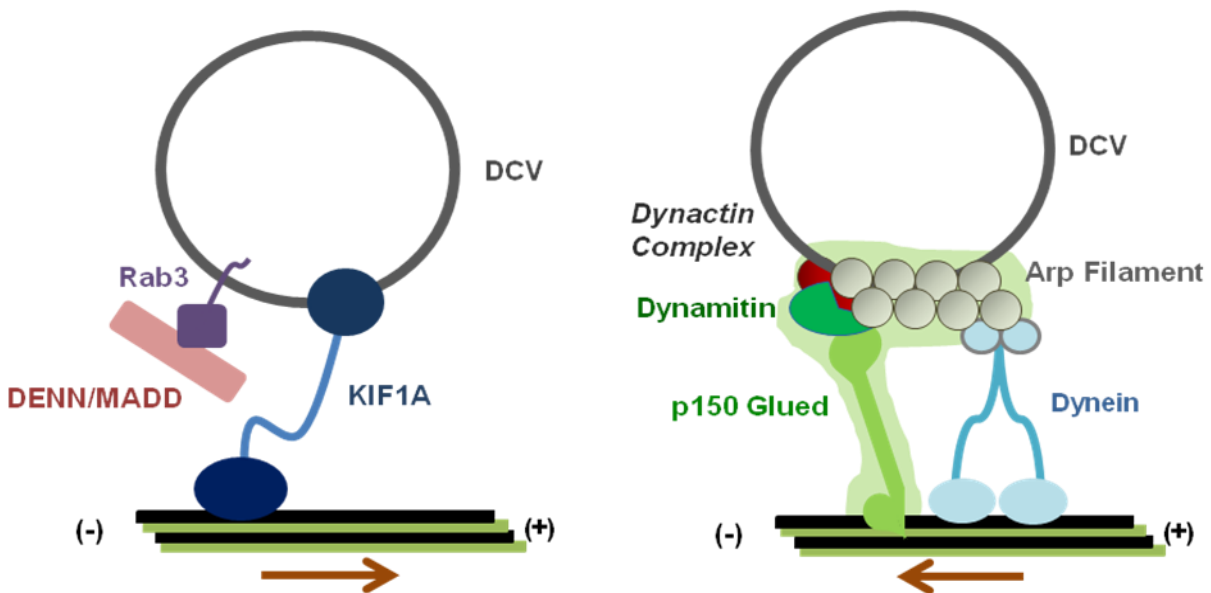


Figure 3 Anterograde and Retrograde motors for DCV transport

Left. DCVs are transported anterogradely by the KIF1A/Unc-104. No known adaptor has been reported for the cargo/motor association, but DENN/MADD/ Rab3 signaling may be involved in the loading/unloading of DCVs.

Right. Retrograde transport is driven by cytoplasmic dynein. It consists of a pair of dynein heavy chains, which carries the microtubule binding, ATPase motor domain (Pfister et al., 2006) and a pair of intermediate and light chains that links the motor to the cargo. The dynactin multisubunit complex serves as an adaptor molecule for cargo/motor association (Vaughan and Vallee, 1995). p150^{Glued} is the largest subunit and is involved in microtubule binding, cargo loading and retrograde transport initiation (Vaughan, 2005). Dynamitin serves as a scaffold for all the other subunits. Overexpression of dynamitin is commonly used as a tool to inhibit retrograde transport (Melkonian et al., 2007). The Actin- related protein (Arp) filament is involved in bidirectional coordination of the cargo (Haghnia et al., 2007). Note that the diagram is showing only the better characterized dynactin subunits.

1.2.4 Bidirectional DCV transport

Traditionally, it was believed that neuropeptides are transported exclusively in the anterograde direction to the nerve terminal, but it is now known that DCVs continuously moves bidirectionally along neuronal processes. Such bidirectional movement was first observed directly by time-lapse imaging of DCVs labeled with GFP-tagged phogrin in *C. elegans* axons (Zahn et al., 2004). Later, *in vivo* imaging of GFP tagged-atrial natriuretic factor (Anf-GFP) revealed that DCVs are transiting bidirectionally along axons and *en passant* boutons of resting motoneurons (Shakiryanova et al., 2006a). In cultured hippocampal neurons, neuropeptide Y (NPY) DCVs transit bidirectionally in the axon (Kwinter et al., 2009). Interestingly, a bimolecular fluorescence complementation (BiFC) assay in *C. elegans* found that Unc-104 is interacting directly with Syd-2(Liprin- α) and DCTN1 (p150^{Glued}) in a motor-adaptor complex. While Unc-104 was mostly associated with Syd-2 along the axon, it mainly associated with DCTN1 at the terminal, and the interaction slowed down anterograde and retrograde movements respectively (Hsu et al., 2011). These observations suggested that the bidirectional movement of DCVs may be regulated by the interaction of motor/adaptor complex with opposite directions in different compartments of the neuron.

Bidirectional transport coordination is a possible mechanism to regulate DCV loading and unloading on the microtubule, which may in turn, determine the specific site of DCV delivery. Nevertheless, DCV trafficking has mainly been studied in neuroendocrine cells which lack neuronal processes. Thus the mechanism by which bidirectional DCV movement is regulated remains unclear. Data thus far have suggested that neuronal activity can either inhibit or enhance DCV transport depending on the experimental system. At fly NMJs, activity reduces retrograde but not anterograde DCV flux across *en passant* boutons (Shakiryanova et al., 2006a),

allowing retrograde DCVs to be delivered to proximal boutons after release. In differentiated hippocampal neuron cultures, cell depolarization enhanced synaptic capture of intracellular neurotrophin transport vesicles (Frischknecht et al., 2008). In the trigeminal ganglion axon, activity-evoked depolarization increased anterograde DCV flux and decreased retrograde flux (Sobota et al., 2010). Anterograde transport velocity of peptidergic vesicles in neuroblastoma NS20Y was found to be increased by forskolin, the adenylyl cyclase activator (Washburn et al., 2002).

1.2.5 Axonal transport and neurodegenerative diseases

Axonal transport is crucial for the supply of newly synthesized materials and energy sources, such as DCVs, synaptic components and mitochondria, from the soma to the distal terminal to support nerve functions (Hollenbeck and Saxton, 2005). It is also important for the elimination of lysosomes and autophagosomes, which carry aged and damaged materials, from the axon and terminal to the soma for degradation (Chevalier-Larsen and Holzbaur, 2006). An increasing body of evidence suggests that axonal transport is also important in supporting retrograde signaling (Zweifel et al., 2005). For all the above reasons, defective axonal transport is believed to be a possible cause of neurodegeneration. Indeed, increasing lines of evidence shows that abnormal axonal transport is associated with many neurodegenerative diseases.

Pathologically, abnormal swelling and accumulation of protein aggregates in the axon is a hallmark in patients with neurodegeneration, suggesting that axonal transport is compromised in the neurons of these patients. Autopsy of a distal spinal and bulbar muscular atrophy (dsBMA) patient showed abnormal inclusions of dynactin and dynein in motor neurons (Puls et

al., 2005). Cytoskeleton abnormalities are also seen in the dystrophic neurites of Alzheimer disease patients (Praprotnik et al., 1996).

Human genetic studies have shown that mutations of motor/adaptor proteins cause many neurodegenerative diseases. A mutation of KIF1A was found in hereditary sensory and autonomic neuropathy type 2 (HSANII) (Riviere et al., 2011). Point mutations in the CAP-Gly domain of the dynactin p150^{Glued} subunit (*DCTN1* gene) were found in patients with two different forms of familial neurodegeneration (Puls et al., 2003), Perry syndrome (Farrer et al., 2009) and amyotrophic lateral sclerosis (ALS). Perry syndrome is an autosomal dominant disorder which consists of early-onset parkinsonism, depression, severe weight loss and hypoventilation (Farrer et al., 2009). ALS is the most common adult-onset motoneuron disease characterized by muscle weakness, muscle atrophy, and spasticity. Transgenic mice expressing the human p150^{Glued} protein mutated in ALS developed motoneuron diseases. Impaired vesicular transport in cell bodies, axonal swelling and axo-terminal were seen in the diseased motor neurons (Munch et al., 2004).

Indeed, multiple animal models of neurodegeneration were generated based on targeted mutations of the retrograde motor molecules. Legs at odd angles (*Loa*) mice express a mutant form of cytoplasmic dynein heavy chain. Heterozygous *Loa* mice exhibited impaired muscle function and motor coordination (Chen et al., 2007; Hafezparast et al., 2003). *In vivo* imaging of the dorsal root ganglion (DRG) neuron culture from *Loa*^{+/-} mice showed impaired retrograde transport of survival factors such as brain-derived neurotrophic factor (BDNF) and nerve growth factor (NGF) (Perlson et al., 2009). Another mouse model was generated by overexpressing the dynactin subunit dynamitin to disrupt dynein-dynactin complex interaction in postnatal motoneurons. These mice developed motoneuron degeneration characterized by muscle

weakness, and deficits in strength and endurance. In the motoneuron, neurofilament misaccumulation and the delay in retrograde neurotracer arrival at the cell body suggest an impairment of retrograde transport in these neurons (LaMonte et al., 2002).

1.3 ACTIVITY-DEPENDENT NEUROPEPTIDE RELEASE AT NERVE TERMINALS

Neuropeptides are released at the nerve terminal through the regulated secretory pathway. Upon action potential arrival, voltage gated Ca^{2+} channels (VGCCs) open and Ca^{2+} influx activate various Ca^{2+} sensors, eliciting a sequence of molecular events that trigger DCV exocytosis. Unlike SSVs, exocytosis of DCVs requires lower intracellular Ca^{2+} concentration (~ less than 1 μM) and the rise in Ca^{2+} concentration does not need to be focal (Ghijsen and Leenders, 2005). Rather, Ca^{2+} concentration at regions far away from the Ca^{2+} microdomain is produced by sustained action potential trains. It is believed that the long latency of DCV fusion after initial Ca^{2+} influx (3-50ms) is due to the slow Ca^{2+} concentration build up at the cytoplasmic region (Martin, 2003). The exact molecular mechanism by which the exocytosis of DCV and SSV are regulated remains unclear. Nevertheless, certain biophysical properties for DCV exocytosis are distinct from those for SSVs. In the following sections, some of these biophysical properties, such as their release probability and kinetics, will be described.

1.3.1 Releasability of DCVs

In many peptidergic neurons and neuroendocrine cells, only a fraction of DCVs stored at the terminal are release-competent (i.e., the readily releasable pool, RRP; (Thorn, 1966)). It has long been postulated that the RRP comprises DCVs that are immobilized, docked close to the plasma membrane and equipped with synaptic proteins for membrane fusion. Nevertheless, studies have revealed that DCV mobility is more crucial in determining releasability. Direct imaging of neuropeptide in growth cones of PC12 cells showed that rapidly moving DCVs near the plasma membrane are more releasable. In addition, mobile cytoplasmic DCVs can bypass the docking state to undergo exocytosis (Han et al., 1999; Ng et al., 2003). Similarly, in developing hippocampal neurons, exocytosis is favored by heterogeneously mobile DCVs, and fusion is often preceded by substantial DCV movement (Silverman et al., 2005). In the fly NMJ, activity-dependent mobilization of DCVs was found to facilitate post-tetanic potentiation (PTP) of neuropeptide release (Shakiryanoval et al., 2007; Shakiryanoval et al., 2005). Finally, DCV mobility is correlated with fusion probability, and that submicrometer motion is required for exocytosis (Degtyar et al., 2007).

The releasability of DCVs also depends on its age. The notion that newly synthesized hormone is preferentially released was first proposed many years ago. In a parathyroid hormone (PTH) radiolabelling experiment, pulse labeled PTH was found to be released faster than preexisting unlabelled PTH (MacGregor et al., 1975). With the advent of a timer fluorescent probe, DCVs of different ages could be selectively labeled with green (young) and red (old) using DsRed-E5. It was found that younger DCVs are distributed close to the cell membrane and are relatively immobile. On the other hand, older DCVs reside deeper inside the cell. Most importantly, membrane proximal, immobile and young DCVs preferentially release their

contents upon nicotine stimulation (Duncan et al., 2003; Wiegand et al., 2003). Recently, with the use of a newer fluorescent reporter, monomeric Kusabira Green Orange (mK-GO), which changes from green to red with a predictable time course ($t_{1/2} = 6h$), it was also found that younger DCVs undergo release exclusively in PC12 cells. Moreover, such age dependent preference of DCV exocytosis is regulated by the small GTPase Rab27A effectors, rabphilin and Slp4-a (Tsuboi et al., 2010)

1.3.2 Kiss and run exocytosis

Similar to SSVs, there are 2 possible consequences of DCVs after they fuse with the plasma membrane during exocytosis. DCVs may undergo full collapse fusion, which is classical mode of exocytosis. In this case, the entire vesicle collapses completely into the plasma membrane, allowing the instant release of all its contents. The vesicle membrane is later retrieved by clathrin-dependent endocytosis. The empty vesicle is then uncoated and recycled through the endosomal compartment (Heuser and Reese, 1973) (Figure 4, bottom). DCV may undergo transient fusion, a process now termed as kiss-and-run exocytosis or cavicapture (Ceccarelli et al., 1973; Fesce et al., 1994; Tsuboi et al., 2004). Kiss-and-run is a direct retrieval pathway in which vesicles fuse only transiently with the plasma membrane, maintaining their integrity and shape, and are endocytosed immediately without the need of clathrin. Vesicular contents are released only partially into the extracellular space by diffusion through the fusion pore opening. The fusion pore then closes and the same vesicle remains docked close to the plasma membrane, ready for another round of exocytosis (Figure 4, top). The choice for either type of exocytosis is associated with Ca^{2+} concentration (Ales et al., 1999). High frequency stimulation and hence low Ca^{2+} influx generally favor faster fusion events and full collapse of vesicles. On the other hand,

low frequency stimulation favors slower fusion and kiss-and-run exocytosis (Fulop and Smith, 2006).

Kiss-and-run is a very common mode of exocytosis for DCVs. It was first described in the 1990s with the use of amperometry and capacitance measurements. The flickering of membrane capacitance with concomitant release of serotonin suggested a fast, direct mode of DCV endocytosis right after exocytosis (Artalejo et al., 1995; Chow et al., 1992). Later, DCV fusion and content release could be monitored at a single vesicle level using fluorescence imaging. By imaging single DCVs labeled with Phogrin-GFP and the acridine orange cargo simultaneously, it was found that vesicles retained their integrity even after cargo release (Pouli et al., 1998). Kiss-and-run exocytosis of peptide containing DCVs was first revealed in pancreatic MIN6 beta cells, where neuropeptide Y(NPY)-Venus was found to be released from DCVs without full membrane fusion (Tsuboi and Rutter, 2003). It is now evident that DCVs in developing neurons can also undergo kiss-and-run exocytosis. Direct imaging of single DCV exocytosis in hippocampal neurons showed that more than half of the DCVs in the neurites exhibited prolonged and incomplete release (Xia et al., 2009).

1.3.3 Fusion pore and neuropeptide release kinetics

The narrow opening of fusion pore during kiss-and-run implies that the rate of release may be limited by the size of the neuropeptide. In PC12 cells, tissue plasminogen activator (tPA)-Venus is released 40 times slower than NPY-GFP, which is three times smaller. Nevertheless, NPY-GFP-GFP, which has an intermediate size, releases the slowest, arguing that factors other than relative size of the cargo and fusion pore can affect the speed of fusion (Felmy, 2007). For example, biochemical interaction between the peptide and the luminal matrix may affect the

cargo diffusion rate. Indeed, Semaphorin3A (Sema3A) and BDNF were found to be released as a stable deposit. The released deposit stays on the extracellular membrane for a prolonged period (~2 min) and diffuses gradually. Such events were not correlated with the size of the cargo, rather they depend on the specific cargo and their interactions with the luminal matrix (de Wit 2009).

The duration and size of fusion pore opening determine how much content can be released. The current model suggests that the GTPase scission protein, dynamin I, is a key regulator for fusion pore opening (Chan et al., 2010). Overexpression of GTPase defective mutant increases the dwell time of fusion while overexpression of the PH domain mutant induces full fusion of vesicles (Tsuboi et al., 2004). The activity of dynamin I depends on the dephosphorylation by calcineurin (Cousin et al., 2001). Recent studies suggested that fusion pore constriction by Ca^{2+} -dependent amphiphysin is a key step before dynamin scission (Llobet et al., 2008). Contrasting data were found regarding the role of myosin II in fusion pore regulation. While increased expression and phosphorylation levels of myosin II accelerates fusion pore dilation thus increasing the amount of hormone release, inhibition of myosin II phosphorylation stabilizes fusion pore dilation (Aoki et al., 2010; Berberian et al., 2009; Neco et al., 2008). The actin network is another regulator for DCV fusion pore constriction, mainly by stabilizing the membrane invagination during exocytosis. Overexpression of β -actin and treatment with the actin destabilizer cytochalasin slowed the release of a large neuropeptide, tissue plasminogen activator (tPA), during kiss and run (Felmy, 2007).

1.3.4 Role of kiss and run exocytosis is controlling release

Kiss-and-run exocytosis plays an important role in controlling neuropeptide secretion. The slow and partial release of neuropeptides prevents store deprivation under repetitive firing. The rapid retrieval of DCVs without undergoing clathrin-dependent endocytosis allows efficient reuse of resources. The narrow fusion pore during exocytosis serves as a filter to select transmitters to be released based on their size. The fusion pore size is in turn regulated by electrical activity and other molecular regulators. Such a size-exclusion mechanism is important because DCVs often contain with multiple subclasses of transmitters (e.g. peptides vs biogenic amines) (Elhamdani et al., 2006; Zhang et al., 2009). Peptide cargo release was also found to be prevented from release through the small fusion pore under spontaneous activity (Vardjan et al., 2007) (Figure 4).

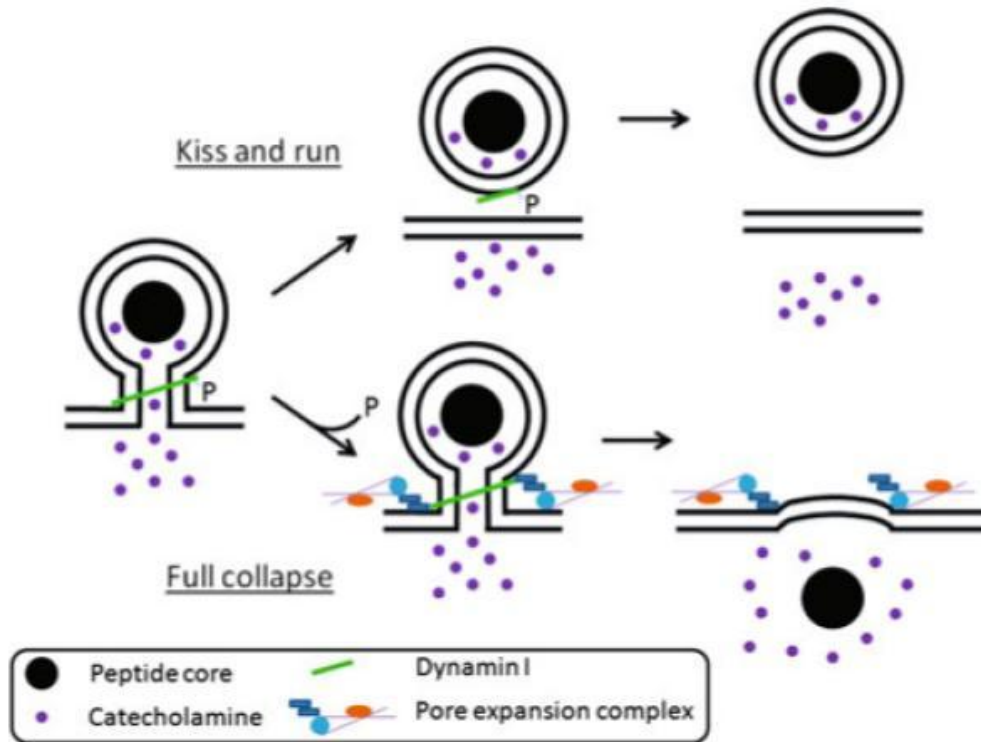


Figure 4 Kiss-and-run versus full collapse fusion

Top path. In kiss-and-run exocytosis, vesicular contents are released incompletely before the fusion pore constricts and retrieves the vesicle again. The transient fusion pore formed may serve as a size filter to prevent high molecular weight contents, eg. peptides, from releasing. **Bottom path,** vesicle is collapsed completely into the plasma membrane and all the vesicular contents are discharged. The fusion pore size is regulated by both the activity of dynamin and the pore expansion complex. Adapted from (Chan et al., 2010).

1.4 THE EXPERIMENTAL SYSTEM : *IN VIVO* DCV IMAGING IN NEURONS

1.4.1 Tools to study DCV transport and exocytosis

Axonal transport was originally studied by localizing organelles using electron microscopy after nerve ligation treatment (Brauckmann, 2004). Later, a new technique was invented to pulse chase newly synthesized radiolabeled proteins along the axon of a dorsal root ganglion cell. By analyzing the composition of the radioactive proteins at different regions of the axon at different time points, the rate of protein transport could be determined (Tobias and Koenig, 1975). With the development of immunocytochemistry, the transport properties of specific proteins of interest could be examined with the use of mutants and nerve ligation (Dahlstrom, 2010). Nevertheless, these strategies are limited to steady state imaging of fixed preparations. Many dynamic transport processes are not resolved and artifacts are often introduced into fixed preparations.

DCV exocytosis is often studied by patch clamp capacitance measurements (Neher and Marty, 1982). The change in capacitance is correlated with the change surface area. Therefore, fusion and endocytic events of single vesicles to the plasma membrane are reflected as discrete steps of capacitance increase and decrease, respectively (Kanno et al., 2004). The magnitude of the capacitance steps can be used to estimate the diameter of the single vesicle and thus differentiating DCVs and SSVs (also termed as microvesicles) (Figure 5A). In the 90s, amperometry was invented to measure the quantal release of readily oxidizable transmitters from DCVs with the use of electrodes placed close by the release site (MacDonald and Rorsman, 2007) (Figure 5B). Nevertheless, capacitance or amperometry measurements provide only membrane fusion or content release kinetics, unless both techniques are used simultaneously. In addition, no spatial information about the vesicle (e.g. localization and mobility) is obtained with

these methods. More importantly, neuropeptides are not easily oxidizable and therefore such studies have been limited to release of monoamine neurotransmitters.

The advent of fluorescent proteins in the 90s resolved many of the above issues in studying DCV transport and exocytosis. By labeling DCVs using fluorescent proteins, DCV distribution, motion and exocytosis, as well as the release of neuropeptides can be monitored in real-time from a live preparation using a conventional fluorescent microscope. Fluorescence recovery after photobleaching (FRAP) can also be used to track the motion of labeled vesicles in a region that is normally filled by too many DCVs for visualization (Levitan et al., 2007). Furthermore, DCVs can be labeled with timer proteins that change their excitation/emission spectra with time, so that DCVs of different ages are selectively labeled with different colors. The distribution of DCVs with different colors at different cellular compartments allows one to track DCVs according to their age. Examples of these probes include DsRed-E5 and mK-GO (Brigadski et al., 2005; Tsuboi et al., 2010). Finally, with the use of photoconvertible fluorescent proteins that change fluorescent color upon laser activation, DCVs can be pulse-chased even more precisely with no dependence on vesicle age. Photoactivation can be used to acutely label a small population of DCVs at a specific region, and the translocation of these labeled DCVs can be followed to other cellular locations. Commonly used photoactivatable fluorescent proteins include: Kaede and Eos-FP (Lukyanov et al., 2005).

Neuropeptide release can be measured by labeling DCVs with fluorescent protein tagged neuropeptides. The decrease in fluorescence after activity represents the amount of release. Membrane fusion during exocytosis can be monitored by pH sensitive fluorescent proteins (Figure 5). In mammalian cells, the vesicle lumen normally has an acidic pH ($\text{pH} < 6$), while the physiological extracellular medium is alkaline ($\text{pH} > 7$). Therefore, by tagging a pH-sensitive

fluorescent protein to the luminal domain of any integral vesicle protein, (e.g. vesicle-associated membrane protein (VAMP)/ synaptobrevin, or phogrin), fusion events can be detected as an increase of fluorescent signal due to the neutralization of the surrounding medium.

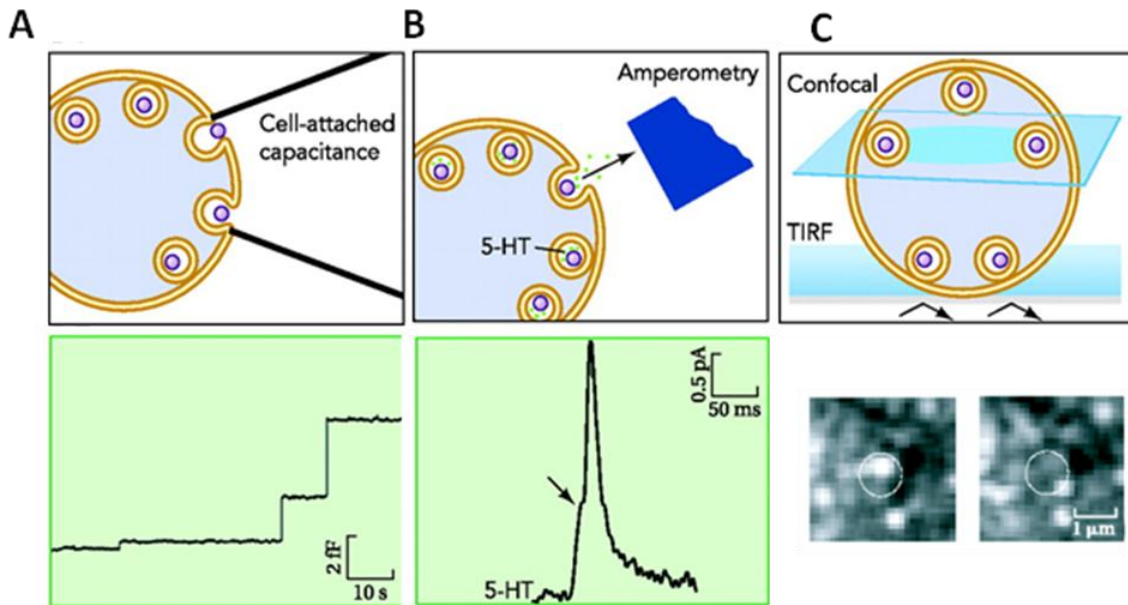


Figure 5 Common tools to study DCV exocytosis

A. Cell attached capacitance measurements monitor the change in surface area of a small patch of cell membrane. Single vesicle exocytosis is detected as a step-wise increase in capacitance. **B.** Amperometry measures the release of oxidizable transmitters, such as 5-HT. An electrode is placed close to the membrane and the release of a single vesicle can be detected as an amperometry spike. **C.** Fluorescence imaging can be done by total internal reflection fluorescence (TIRF) or confocal microscopy, both of which can limit the number of visible vesicles by focusing on a thin focal plane. Single vesicle release events can be detected by the change in fluorescent intensity of a punctum. Lateral movement of the vesicle can also be monitored. Adapted from (MacDonald and Rorsman, 2007)

1.4.2 Animal models and experimental systems:

Research of DCV biology has mainly been based on tissue culture systems. Primary endocrine cell cultures including pancreatic or medullary chromaffin cells are the most commonly used

systems. The pheochromocytoma (PC12) cell line is another well-established system because it is robust and easy to culture. More importantly, PC12 cells can be induced by nerve growth factors to differentiate into sympathetic neurons, which exhibit extended processes and growth cone structures. Although native DCVs in PC12 cells contain mainly dopamine and sometimes noradrenaline, fluorescent protein tagged neuropeptides can be ectopically expressed by transfection. This allows DCV trafficking and release to be directly monitored. Nevertheless, differentiated PC12 cells still lack typical neuron morphology, such as branches and *en passant* boutons, meaning that their use to study axonal transport is limited. In addition, it has been argued that PC12 cells have a tumorigenic lineage and the secretory pathway may be altered. Thus, findings from PC12 cells may not represent normal physiological characteristics.

Many limitations of the PC12 system can be overcome by using *Drosophila* larval NMJ. In this model, third instar larvae are dissected dorsally and the NMJ located on the surface of exposed abdominal muscles can be imaged using conventional upright microscopy (Brent et al., 2009) (Figure 1-3). With careful dissection and correct bathing medium (hemolymph-like saline), the preparation can stay alive for hours without additional temperature and gas control, thus allowing simple imaging and electrophysiological studies at the NMJ (Imlach and McCabe, 2009). Compared to vertebrate models, the fly larva has a simpler and more identifiable neuronal system. Axon bundles projecting from the ventral ganglion allows easy electrical manipulation of NMJ in a specific muscle segment (Figure 6). A huge number of fly genetic mutants have been identified and are publicly available; besides, ectopic gene expression also allows simple genetic manipulation of proteins of interest with high spatial/ temporal specificity (Duffy, 2002). Proteins of interest tagged with different fluorescent proteins can be expressed in specific tissues, and protein expression levels, localization and cellular dynamics can be

monitored *in vivo* with ease (Levitan et al., 2007; Schmid and Sigrist, 2008; Smith and Taylor, 2011). In addition, transgenic UAS constructs for mutant, dominant negative or constitutive active proteins, and RNA interference (RNAi) can be overexpressed timely to specific tissues of wild-type or mutant organisms for different genetic perturbation or rescue experiments (McGuire et al., 2004).

In a 3rd instar larva, there are 32 motoneurons innervating 30 post-synaptic muscle cells in each abdominal hemisegment. Conventionally, these motoneurons are classified into three classes based on their bouton morphology. Type I boutons are the best characterized NMJ. They form predominantly excitatory glutamatergic synapses with the partnering muscle. Their morphology (e.g. branch points, bouton number and size) is stereotypical. They are further classified into type-Ib (b: big) with a diameter of 3-5 μm , or type-Is (s: small) with a diameter of 1-1.5 μm (Prokop, 2006). Ultrastructural analysis from electron micrographs, showed that about 200 DCVs are present in a type Ib bouton (Atwood et al., 1993). Proctolin and PACAP38-like peptides are the only two neuropeptides that have been identified in type I boutons (Anderson et al., 1988b; Zhong and Pena, 1995). Type III boutons are more elongated (2-5 μm), and DCVs are more densely packed (50 fold) in these boutons (Jia et al., 1993). The majority of fly neuropeptides, such as leukokinin-like and the insulin-like peptide, are expressed in the peptidergic type III motoneurons (Gorczyca et al., 1993; Landgraf et al., 2003).

About 10 years ago, our group generated a transgenic fly that expresses Emerald GFP-tagged atrial natriuretic factor (Anf-GFP), a mammalian neuropeptide that stimulates diuresis and vasodilation (Inagami, 1989), in neurons (*elav-Gal4 UAS-preproANF-EMD*)(Rao et al., 2001a). *In vivo* imaging showed that Anf-GFP labeled DCVs transport bidirectionally along resting axons and NMJs. Upon stimulation, Anf-GFP is released and the amount could be

quantified from the drop in fluorescence (Levitan et al., 2007; Rao et al., 2001a; Shakiryanova et al., 2005; Shakiryanova et al., 2006a).

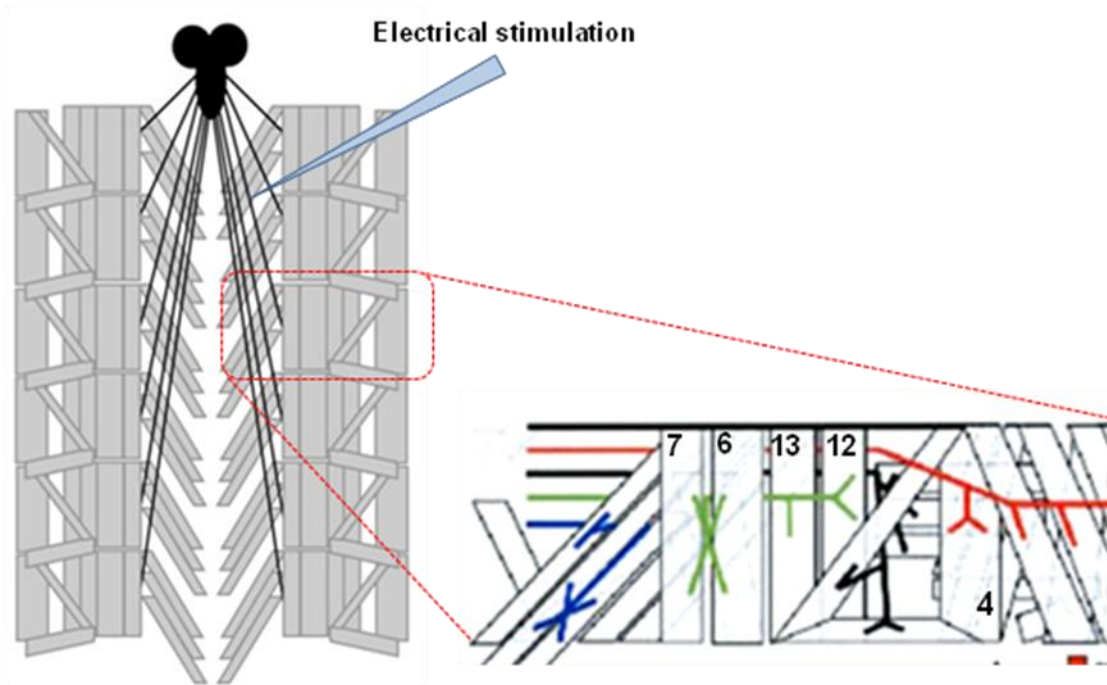


Figure 6 A dissected fly larval preparation

1.5 THESIS GOAL

Neurons undergo repetitive firing for neurotransmission and transmitters in the terminal are subjected to continuous depletion. Therefore, accurate and timely delivery of DCVs to the nerve terminal, as well as the tight regulation of neuropeptide release should be ensured. However, the supply logistics and exocytosis properties of DCVs within a fully differentiated nerve terminal still remain unknown. To address the above issues, this thesis attempts to answer the following questions by imaging GFP-tagged neuropeptides at the fly NMJ *in vivo*: 1) How are

bidirectionally transiting DCVs delivered to branches and *en passant* boutons? 2) What are the release properties (e.g. mobility, releasability and exocytosis kinetics) of DCVs in a live, differentiated nerve terminal? 3) What is the signaling pathway involved in the replenishment of the neuropeptide store after activity?

Chapter 2 has been published as “Neuropeptide delivery to synapses by long-range vesicle circulation and sporadic capture” in *Cell* (Wong et al., 2012). It will describe how a novel circulation route taken by DCVs to deliver neuropeptides bidirectionally via sporadic capture. It will present the use of a newly developed optical technique, simultaneous photobleaching and imaging (SPAIM), to track single DCVs. In Chapter 3, I will use SPAIM to examine the exocytosis properties of single DCVs upon electrical stimulation. It will show newly arrived DCVs undergo exocytosis exclusively by kiss-and-run exocytosis, and can undergo multiple rounds of exocytosis to further discharge their contents. Chapter 4 has been published as “Presynaptic ryanodine receptor-CamKII signaling is required for activity-dependent capture of transiting vesicles” in *Journal of Molecular Neuroscience* (Wong et al., 2009). It will examine the requirement of ryanodine receptor -CamKII signaling in activity-dependent DCV capture. In the end, I will summarize the major findings of the thesis and discuss the implication and future directions of the studies.

2.0 NEUROPEPTIDE DELIVERY TO SYNAPSES BY LONG RANGE VESICLE CIRCULATION AND SPORADIC CAPTURE

2.1 ABSTRACT

Neurotransmission requires anterograde axonal transport of dense-core vesicles (DCVs) containing neuropeptides and active zone components from the soma to nerve terminals. However, it is puzzling how one-way traffic could uniformly supply sequential release sites called *en passant* boutons. Here *Drosophila* neuropeptide-containing DCVs are tracked *in vivo* for minutes with a new method called simultaneous photobleaching and imaging (SPAIM). Surprisingly, anterograde DCVs typically bypass proximal boutons to accumulate initially in the most distal bouton. Then excess distal DCVs undergo dynactin-dependent retrograde transport back through proximal boutons into the axon. Just before reentering the soma, DCVs again reverse for another round of anterograde axonal transport. While circulating over long distances, both anterograde and retrograde DCVs are captured sporadically in *en passant* boutons. Therefore, vesicle circulation, which includes long range retrograde transport and inefficient bidirectional capture, overcomes the limitations of one-way anterograde transport to uniformly supply release sites with DCVs.

2.2 INTRODUCTION

Neurotransmission relies on axonal transport of neuropeptides and active zone components packaged in dense-core vesicles (DCVs) to the nerve terminal (Ahmari et al., 2000; Zupanc, 1996). Many terminals feature sequential varicose sites called *en passant* boutons, which release neuropeptides to regulate neuronal circuits or large postsynaptic targets, such as muscle cells. In *en passant* boutons, neuropeptide stores are typically uniform reflecting equivalent accumulation of DCVs that reside in each bouton for many hours (Shakiryanova et al., 2006a). The kinesin responsible for anterograde axonal transport of DCVs has been identified (Barkus et al., 2008; Jacob and Kaplan, 2003). However, it is not known how anterograde transport equivalently supplies DCVs to *en passant* boutons to ensure that neurotransmission is robust.

The difficulty in distributing DCVs generated in the soma among *en passant* boutons is evident when possible models based on one-way anterograde transport are considered. For example, if boutons were filled in order, then the most proximal bouton would be supplied first and distal boutons might be starved for resources. Even with stochastic delivery, this problem persists: with a fixed probability of delivering anterograde DCVs to each bouton, delivery would still be highest for the most proximal bouton and decrement for each subsequent bouton. In principle, this issue could be overcome by routing cargoes specifically to each *en passant* bouton, but there is no known address system for directing delivery of DCVs from the soma to a potentially large and dynamically changing number of boutons. Therefore, although *en passant* boutons are common throughout the nervous system, the mechanism for uniformly maintaining their DCV pools by anterograde transport is unknown.

Here the “rules of the road” for neuronal DCVs are determined by combining *Drosophila* genetic methods with a technique that enables tracking of neuropeptide-containing

DCVs in native nerve terminals for minutes. Anterograde axonal transport, which had been thought to fully account for delivery to the terminal, is shown to be just the first step in a surprising, but elegant, routing strategy that produces uniform presynaptic neuropeptide stores.

This chapter was largely written and edited by my advisor Dr. Edwin Levitan in the format of a research article. It has been published as “Neuropeptide delivery to synapses by long-range vesicle circulation and sporadic capture” in *Cell* in March 2012 (Wong et al., 2012). All the experimental design, data collection and data quantification were performed by me with advice from Dr. Dinara Shakiryanova. It also has contribution by Drs. Chaoming Zhou, David Deitcher and Thomas Lloyd for the generation of genetic mutants that were used in many experiments.

2.3 RESULTS

2.3.1 Preferential anterograde transport of DCVs to the most distal bouton

To determine how the uniform neuropeptide stores in *Drosophila* motoneuron type Ib boutons (Anderson et al., 1988a) are supplied, the Geneswitch (GS) system (Nicholson et al., 2008) was used to induce expression of Emerald GFP-tagged Atrial Natriuretic Factor (Anf-GFP), a reporter of native neuropeptide packaging and release in *Drosophila* larvae (Heifetz and Wolfner, 2004; Husain and Ewer, 2004; Kula et al., 2006; Loveall and Deitcher, 2010; Rao et al., 2001b; Shakiryanova et al., 2006a). Independent of Anf-GFP labeling, boutons were detected with a TRITC-conjugated anti-horseradish peroxidase antibody (TRITC-HRP) and numbered from distal to proximal (Figure 7A). Surprisingly, neuropeptide accumulated initially in the

most distal bouton (#1) and only later was distributed uniformly among *en passant* boutons #1-4 (Figure 7A,B). Similar results were obtained with heat shock induction of GFP-tagged *Drosophila* proinsulin-like peptide 2 (Dilp2-GFP, Figure 7C,D). Therefore, the initial distal accumulation cannot be attributed to a particular neuropeptide or induction mechanism. Finally, when neuropeptide release was inhibited by removing extracellular Ca^{2+} , fluorescence recovery after photobleaching (FRAP) of constitutively expressed Anf-GFP (i.e., driven by *elav-GALA*) also revealed preferential neuropeptide accumulation in the most distal bouton (Figure 7E,F, Movie S1). This finding independently verifies the polarized neuropeptide accumulation detected with pulse labeling and furthermore proves that this pattern cannot be explained by differential release by *en passant* boutons.

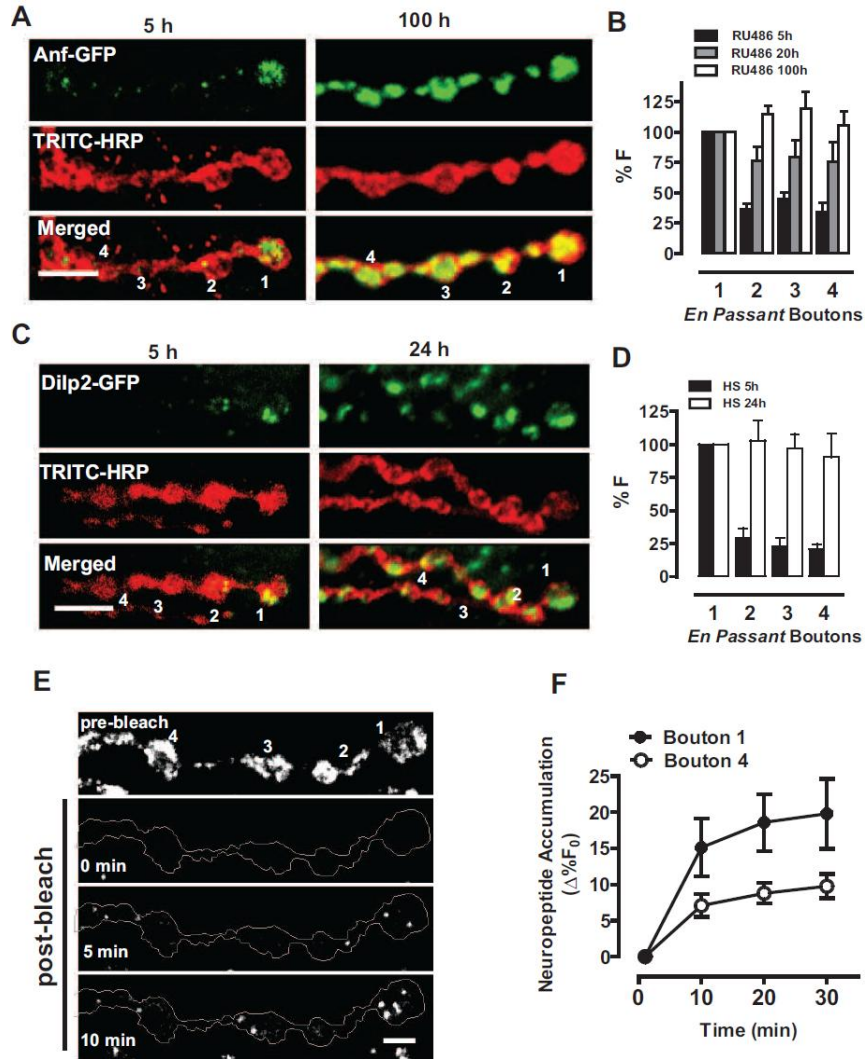


Figure 7 Neuropeptide accumulates initially in the most distal bouton

A. Nerve terminal Anf-GFP fluorescence images after RU486 induction for 5 and 100 hours. TRITC-conjugated HRP labeling localized the neuronal membrane. *En passant* boutons are numbered from the most distal (#1) to proximal (Scale bar, 5 μ m). **B.** Quantification of fluorescence relative to the most distal bouton (%F) after RU486 (5 h, n=11; 20 h, n=10; 100 h, n=12). Note that data are displayed from most distal bouton #1 to proximal bouton #4. **C.** Nerve terminal Dilp2-GFP images after heat shock induction for 5 or 24 hours. Scale bar, 5 μ m. **D.** Quantification of Dilp2-GFP fluorescence after heat shock induction for 5 h (n=8) and 24 h, n=5). Note that data are displayed from most distal bouton #1 to proximal bouton #4. **E.** Time-lapse images before and after photobleaching (Scale bar, 2.5 μ m). Contrast was adjusted to visualize DCV puncta. **F.** FRAP quantified in the most distal bouton (#1) and a proximal bouton (#4) (n=12). In all figures, error bars are standard error of the mean. See also Movie S1.

The above experiments exclude many potential models for maintaining neuropeptide stores in *en passant* boutons including delivery in order, stochastic delivery and parallel address-based delivery. Instead, there must be a routing mechanism that preferentially produces DCV accumulation in the most distal bouton at first, but eventually results in evenly distributed DCVs. To gain insight into this mechanism, DCVs were tracked as they populated the nerve terminal with a new approach called simultaneous photobleaching and imaging (SPAIM). In initial SPAIM experiments the distal region of the nerve terminal was photobleached. Then after a punctum likely corresponding to a single DCV (Shakiryanova et al., 2006a) entered the photobleached region, a laser beam was positioned to photobleach subsequent newcomers. Finally, while continually photobleaching newcomers, a second independent scanning beam was used to simultaneously image the unbleached DCV for minutes (Figure 8A). This allowed the initial unbleached bright DCV to be distinguished from the nearly completely photobleached newcomers (Movie S2).

SPAIM revealed complex anterograde DCV routing within the nerve terminal. For example, an individual trajectory from a proximal bouton to the most distal bouton contained multiple pauses, a transient change in direction and looping exploration of boutons before coming to rest (Figure 8B, Movie S2). Bouton visits fell into 3 kinetic classes: (1) DCVs moving $0.75 \pm 0.03 \mu\text{m/s}$ ($n=62$) bypassed a bouton within 5 s in 45% of cases, (2) visited boutons transiently (5-120 s) or (3) stayed longer than 5-10 minute time-lapse experiments (Figure 8C,D), which were classified as capture. Because proximal capture was infrequent (Figure 8D, open bars), anterograde flux dropped at each proximal bouton by ~10% (Figure 8E). This result has two implications: first, there is nearly uniform accumulation of anterograde DCVs in each proximal bouton because there is modest depletion of DCV flux at each bouton,

and second, capture in proximal boutons is inefficient so that excess DCVs remain to accumulate in the most distal bouton (Figure 8D filled bars, E). These experiments show that DCVs do not move directly to their ultimate destinations, but instead can pause and make detours along the way. Furthermore, the initially polarized accumulation of neuropeptide is caused by the sporadic proximal capture of anterograde DCVs as they make their complex journey through the terminal.

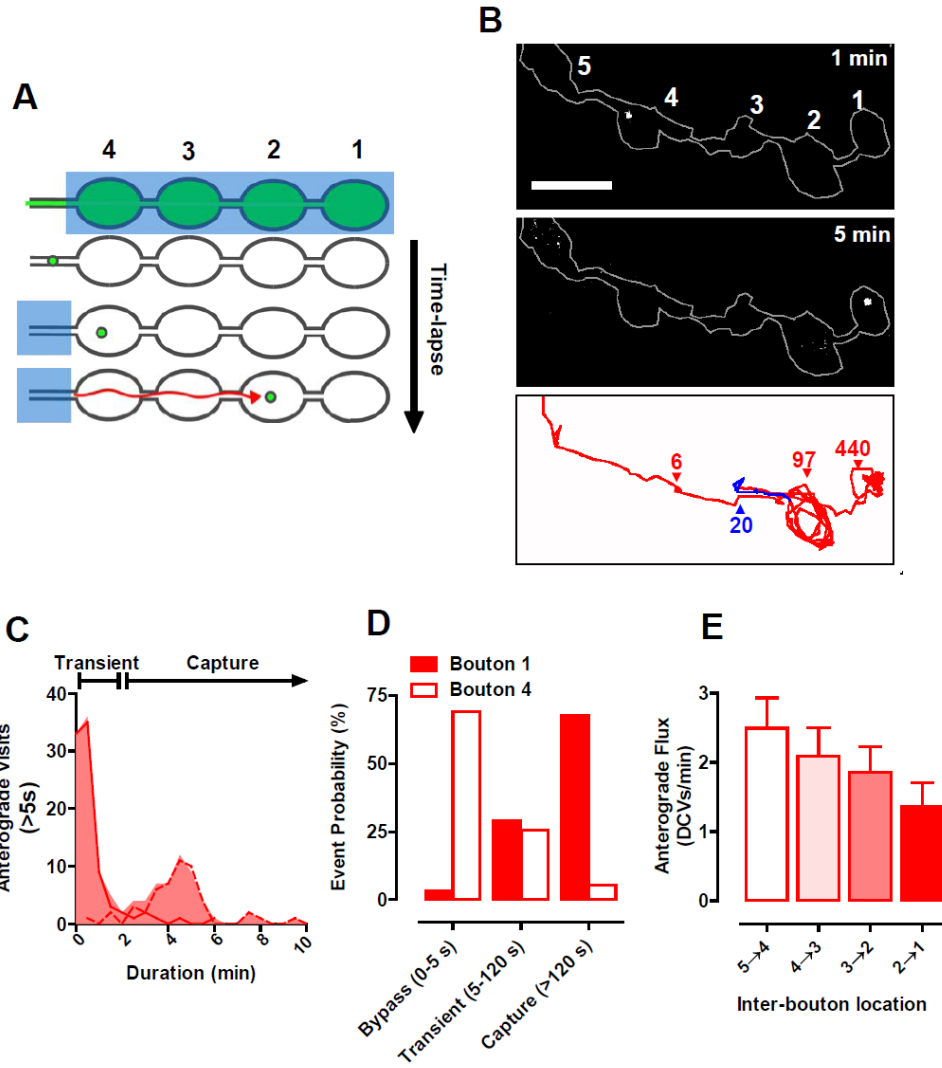


Figure 8 Complex anterograde DCV traffic in the terminal

A. SPAIM experimental design. Blue boxes, photobleaching regions; Red arrow, possible trajectory of the newcomer DCV. At least 4 boutons were examined in each experiment. **B.** Anterograde DCV images (upper and middle) and trajectory (bottom). Red, anterograde; Blue, retrograde. Colored numbers indicate pause durations in seconds. Scale bar, 5 μ m. **C.** Frequency distribution of visits >5 s ($n=138$ from 62 tracked DCVs in 17 animals, 30 s binning) at *en passant* boutons, which comprise 55% of total events. Dashed line indicates events that were interrupted by the end of time-lapse data acquisition. **D.** Probability of DCVs to bypass (duration 0-5 s), transiently visit (duration 5-120 s) or be captured (duration >120 s) at boutons #1 and #4 ($n=86$ events from 14 DCVs in 14 animals). **E.** Anterograde DCV flux between boutons in 5 minutes after photobleaching ($n=15$). See also Movie S2.

2.3.2 Retrograde DCV transport delivers neuropeptide to proximal boutons

Given that anterograde transport is biased to the most distal bouton, how is uniform neuropeptide storage eventually accomplished? The above SPAIM experiments showed that changes in transport direction were rare and transient in proximal boutons. However, in 10 of 62 initially anterograde trajectories acquired, DCVs converted to retrograde transport in the most distal bouton. Analysis of these events showed that their number was limited because conversion to retrograde transport was slow (i.e. comparable to the time scale of these experiments). Thus, retrograde flux had not yet reached values found at steady state. Nevertheless, this result raised two new questions. First, if newcomer anterograde DCVs can leave the distal bouton, might retrograde transport dissipate the initial distal gradient in neuropeptide accumulation? Second, what is the fate of DCVs that leave the distal bouton by retrograde transport?

To address these questions, SPAIM experiments were designed to detect retrograde traffic of DCVs that had already accumulated in the most distal bouton. In this case, proximal boutons were photobleached, but the most distal bouton was spared. Then anterograde newcomers were continually photobleached by a laser beam located upstream of the region of interest while simultaneously imaging DCVs leaving the most distal bouton with the second scanner (Figure 9A top). For comparison, SPAIM was also used to detect traffic out of a proximal bouton (Figure 9A bottom). These experiments showed that retrograde DCV flux from the distal bouton was far greater than DCV flux from a proximal bouton (Figure 9B, Movie S3 and Movie S4), suggesting that retrograde DCV transport out of the most distal bouton removes excess DCVs supplied by anterograde transport.

Consistent with this conclusion, inhibition of retrograde transport resulted in excess neuropeptide accumulation in the most distal bouton. Because retrograde transport depends on

activation of the motor dynein by the dynactin multisubunit complex, it can be inhibited by genetically affecting dynactin subunits (e.g. by driving expression of dominant negative p150 Glued ($Gl^{\Delta 96}$) (Allen et al., 1999) or dynamitin (Dmn) overexpression (Burkhardt et al., 1997)). Transgenic expression of $Gl^{\Delta 96}$ or Dmn resulted in excess Anf-GFP accumulation in the most distal bouton (Figure 9C, D). The effect of inhibiting retrograde transport was not limited to Anf-GFP because, in the absence of any GFP construct expression, $Gl^{\Delta 96}$ also promoted distal accumulation of the native neuropeptide proproctolin (Figure 9E, F). Therefore, dynactin-dependent retrograde DCV transport is required to dissipate the neuropeptide gradient produced by anterograde transport.

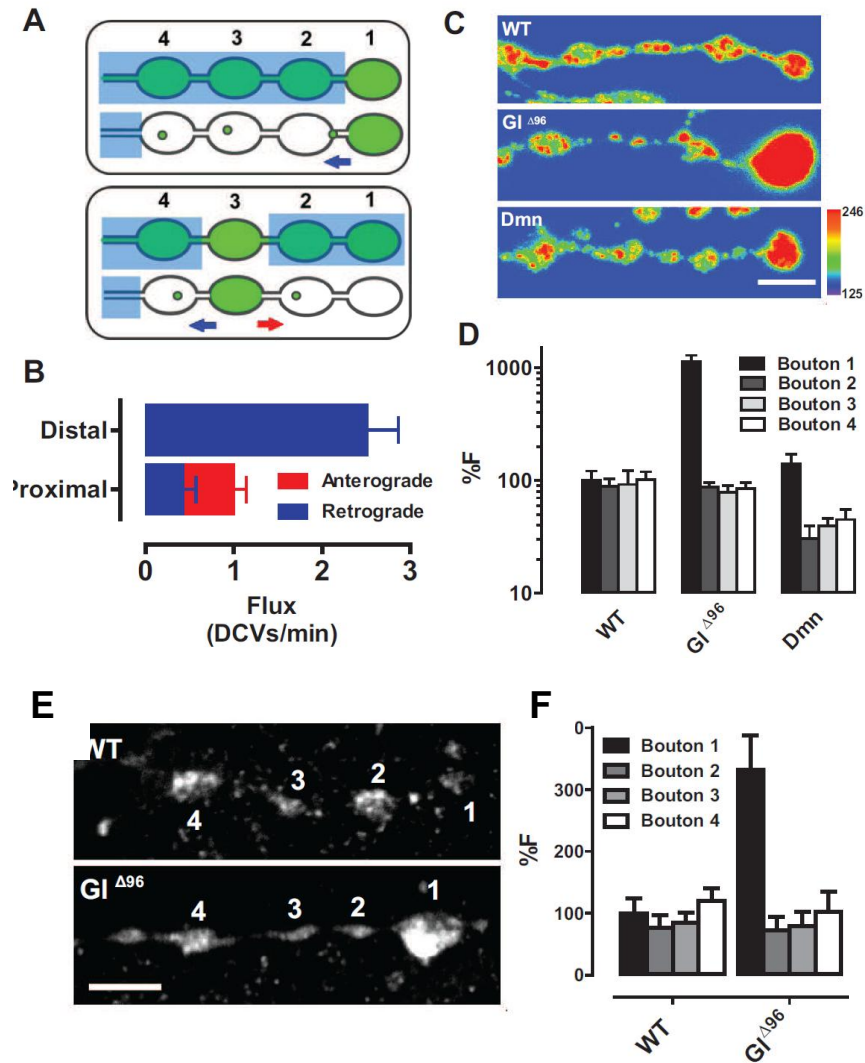


Figure 9 Retrograde transport of excess DCVs out of the distal bouton

A. SPAIM strategies for detecting DCV efflux from distal (Top) and proximal (bottom) boutons in 5 minutes after photobleaching large blue rectangles. The green boutons were spared from photobleaching and then anterograde newcomers were blocked by the beam positioned at the location of the small blue squares. Flux was measured at the position of the arrows (Red, anterograde; Blue, retrograde). **B.** Quantification of DCV flux from proximal (n=10) and distal (n=13) boutons. **C.** Pseudo-color images showing distal Anf-GFP accumulation after inhibiting dynactin with $GI^{\Delta 96}$ or Dmn. Scale bar, 5 μ m. Warmer colors represent higher fluorescence. **D.** Anf-GFP intensity relative to the wild type control (WT) distal bouton (%F) (WT, n=18; $GI^{\Delta 96}$, n=20; Dmn, n=7). See also Figure S1 and Movies S3 and S4. **E.** Immunofluorescence signal for proproctolin in muscle 4 boutons of wild type (WT) and $GI^{\Delta 96}$ animals. Bar, 5 μ m. **F.** Quantification of proproctolin fluorescence levels in *en passant* boutons (n=7).

Interestingly, SPAIM showed that retrograde transport in the terminal shares many features found with anterograde transport. First, retrograde DCVs moving $0.73 \pm 0.03 \mu\text{m/s}$ (n=63) often (i.e. 56% of events) bypassed proximal boutons (Figure 10A). Second, trajectories featured both transient visits and capture in proximal boutons, as well as rare transient reversals in direction (Figure 10A, B). Third, capture was inefficient and uniform among proximal boutons so that flux dropped by ~10% per bouton (Figure 10C). This similarity to anterograde capture ensures that any subtle proximal-distal gradient produced on the way toward the distal bouton is counterbalanced by a symmetric gradient in capture on way back from the distal bouton. Most importantly, inefficient sporadic capture of retrograde DCVs contributes to neuropeptide accumulation in proximal boutons.

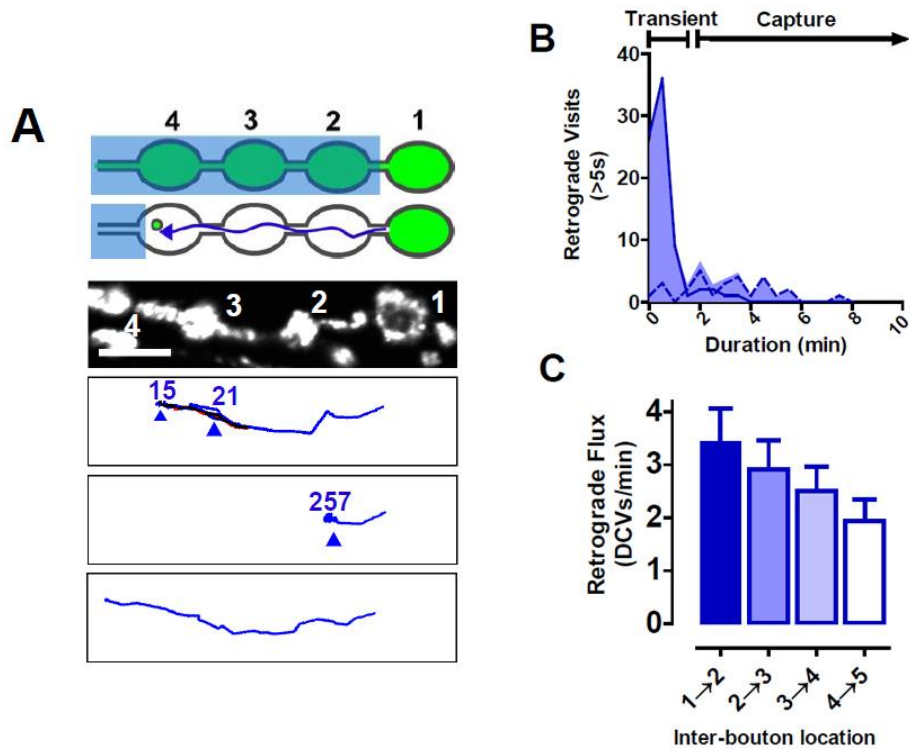


Figure 10 Retrograde DCV traffic and capture in the terminal

A. Top two panels, SPAIM strategy for detecting retrograde DCVs leaving the most distal bouton. Third panel, image of boutons prior to photobleaching. Bottom three panels, sample retrograde trajectories. The first shows transient visits and an anterograde reversal. The second shows capture. The third shows bypasses to exit region of interest. Blue, retrograde; Red, anterograde; Overlapping anterograde and retrograde, black; Scale bar, 5 μ m. **B.** Frequency distribution of retrograde visits >5 s (n=106 events in 63 tracked DCVs in 20 animals), which comprise 57% of total events. Dashed line indicates events that were interrupted by the end of time-lapse data acquisition. **C.** Retrograde flux of DCVs from bouton #1 in 5 minutes after photobleaching (n=7).

2.3.3 Uncaptured retrograde DCVs stop just before reentering the soma

Another consequence of inefficient capture was that some retrograde DCVs were not captured in any of the proximal boutons. Because *Drosophila* motoneuron terminals are branched structures (Figure 11A), retrograde DCVs must therefore either change direction to reenter the same or a neighboring terminal branch or continue on into the axon (Figure 11B). SPAIM was used to distinguish between these possibilities: after photobleaching a branch point, retrograde traffic was imaged while simultaneously photobleaching anterograde newcomers (Figure 11C). Time-lapse imaging showed that retrograde DCVs never turned to enter another terminal branch, only rarely reversed direction to return to the same branch and usually continued on into the axon (Figure 11D, Movie S5). Therefore, uncaptured retrograde DCVs are not typically retained in the terminal, but instead proceed toward the soma.

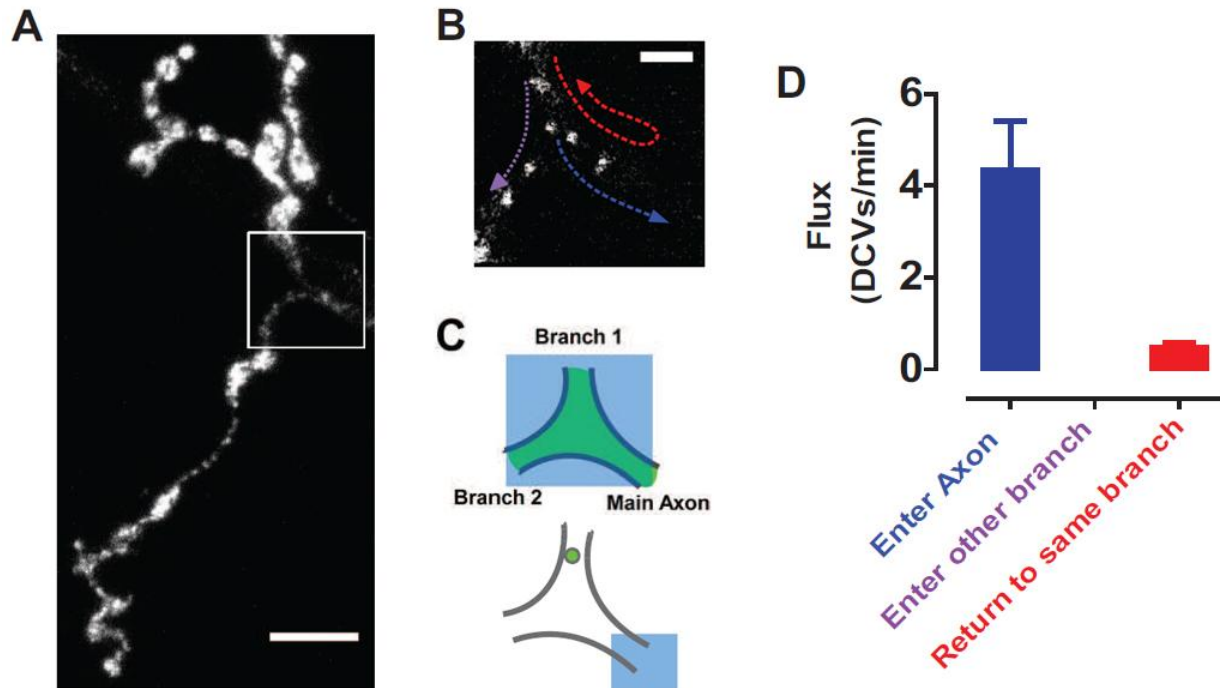


Figure 11 Uncaptured retrograde DCVs leave the terminal to enter the axon

A. Projection stack showing Anf-GFP in a muscle 4 terminal with photobleached branch point indicated with a box. Scale bar, 10 μm . **B.** Single image of the photobleached region showing DCVs and possible retrograde trajectories (colored arrows). Scale bar, 2.5 μm . **C.** SPAIM strategy for viewing retrograde DCVs entering branch point. Following photobleaching of the branch point (large blue box), anterograde newcomers are photobleached (small blue box) while simultaneously imaging retrograde DCVs. **D.** Quantification of retrograde DCV flux at the branch point ($n=7$). Note that the preferential traffic into the axon was also seen at muscle 6/7 terminals. See also Movie S5.

There is extensive retrograde transport of neuropeptidergic DCVs in the axon (Alonso and Assenmacher, 1983). A conventional hypothesis would be that retrograde DCVs return to the soma to be degraded. However, SPAIM demonstrated that many DCVs contribute to retrograde transport simply because they were not captured on the way to and from the most distal bouton. Therefore, transport back through the proximal axon into the soma was imaged to determine the fate of retrograde DCVs. Unfortunately, resolving this traffic in motoneurons was not feasible for three reasons. First, the soma and axon are often not in a single plane of focus, which is needed for continual imaging of transport. Second, available motoneuron drivers label multiple clustered somata, which makes it difficult to discriminate individual axon-soma pairs. Finally, because motoneuron somata are located in the central nervous system (i.e. the ventral ganglion), light scattering by the surrounding tissue degrades the confocal signal from individual DCVs and interferes with photobleaching. Because of these limitations, retrograde DCV traffic was studied in an optically accessible neuron that is amenable to imaging traffic back through the proximal axon to the soma.

Specifically, we focused on the lateral td neuron, which has its soma located on the surface of the body wall near muscle 8 and produces an anterior projecting dendrite and a posterior projecting axon (Bodmer, 1987). In the larva, the lateral td neuron expresses Anf-GFP in response to the peptidergic cell driver *386A-GAL4* (Figure 12A). Importantly, the soma, proximal processes and the first axonal branch of lateral td neurons can be imaged in a single plane of focus (Figure 12A). Little DCV traffic entered the proximal dendrite, as expected for a presynaptic cargo (Rolls, 2011). Therefore, we determined the fate of retrograde DCVs moving from the segmental nerve and peripheral axons toward the td neuron soma, which is distinguished from the proximal axon by morphology and the reciprocal distributions of the

microtubule associated protein futsch and the Golgi marker mannosidase II-egfp (ManII-GFP; (Ye et al., 2007) (Figure 12B). Surprisingly, in 5 minute FRAP experiments, retrograde DCVs accumulated in the proximal axon (i.e. the region between the soma and the first axonal branch) far more than in the soma (Figure 12C, Movie S6). Time-lapse experiments showed that this occurred because flux into the soma was ~ 7.5 -fold less than into the proximal axon (Figure 12D). Thus, only a small fraction of retrograde DCVs traverse the proximal axon to enter the soma.

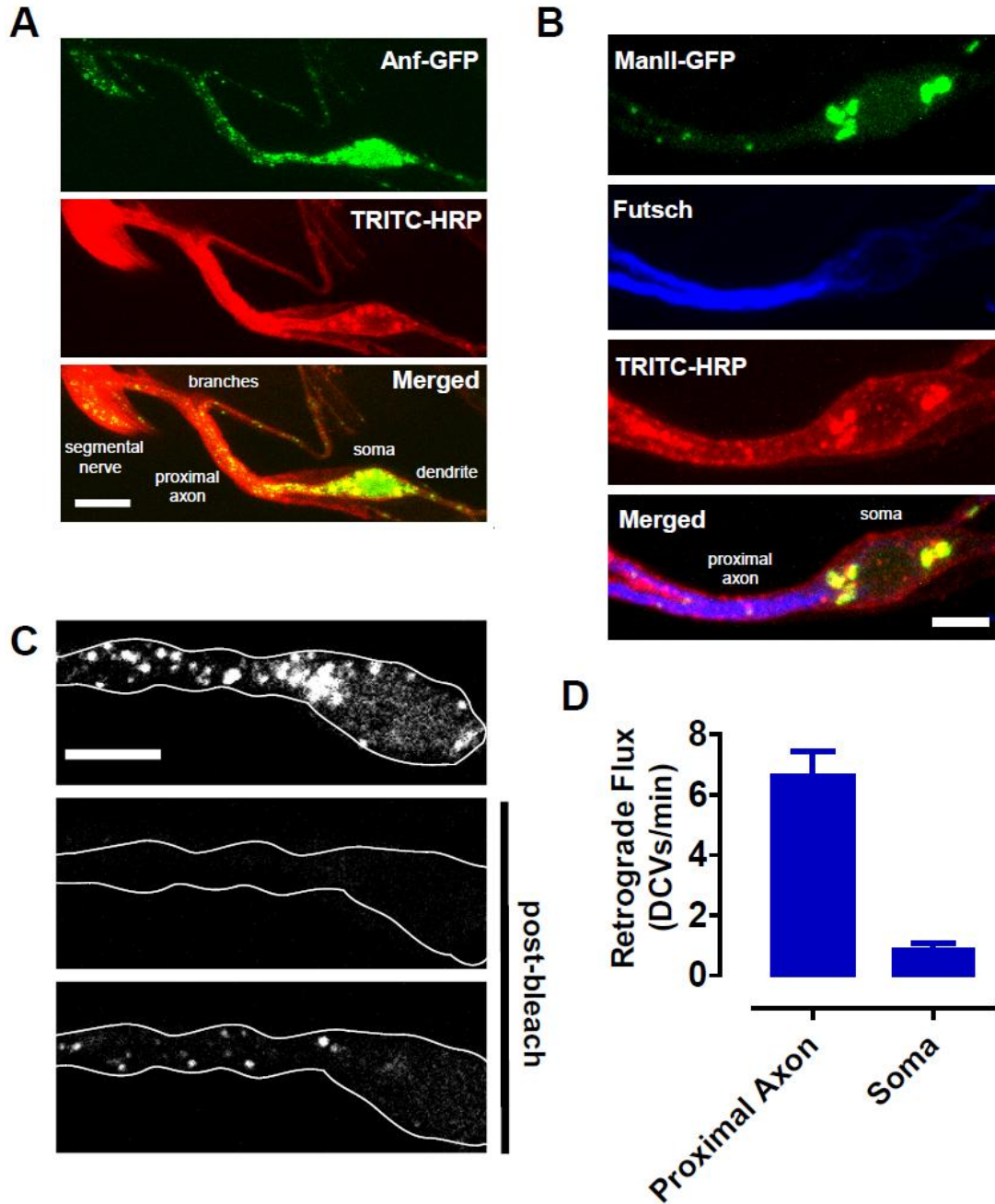


Figure 12 Accumulation of retrograde DCVs in the proximal axon

A. Anf-GFP (Top) expressed in a lateral td neuron. Neuronal membrane was labeled with TRITC-HRP antibody. Scale bar, 10 μ m. **B.** Localization of the Golgi marker (Man II-GFP, green) and the microtubule associated protein futsch detected by immunofluorescence (blue). Scale bar, 5 μ m. **C.** Representative images of the lateral td neuron soma and proximal axon before and after photobleaching. Scale bar, 5 μ m. **D.** Quantification of retrograde DCV flux into the proximal axon and soma (n=10). See also Movie S6.

2.3.4 Retrograde DCVs circulate back into the axon

Three independent lines of experimentation demonstrated that DCVs switch from retrograde to anterograde transport in the proximal axon. First, the soma and proximal axon were photobleached. SPAIM was then used to detect nascent anterograde DCVs in the absence of retrograde newcomers. As expected, the flux of nascent DCVs, which originated only from the soma, was very low in the 5 minutes after photobleaching (Figure 13A, Soma, B). Yet, anterograde flux out of the proximal axon measured in this time period was easily detected when retrograde DCVs were not photobleached (Figure 13A, proximal axon open bar, Movie S6). Therefore, anterograde DCVs exiting the proximal axon must have been former retrograde newcomers. Second, the effect of photobleaching retrograde newcomers from the axon on anterograde flux out of the proximal axon was determined. When the supply of retrograde DCVs from the axon was cut off, anterograde exit of DCVs from the proximal axon was nearly eliminated (Figure 13A, proximal axon open and filled bars). Again, this result is consistent with reversal of retrograde DCVs in the proximal axon. Finally, in 5 minute trajectories detected by SPAIM (Figure 13C), ~30% of retrograde DCVs reversed and left the proximal axon by anterograde transport (Figure 13D, Movie S7). In contrast, reversals in the soma only occurred in ~2% of trajectories, showing that the proximal axon is the major turnaround site for retrograde DCVs. Interestingly, after converting to anterograde transport, DCVs left either by the branch they used to approach the soma or the other possible axonal branch. Therefore, retrograde axonal transport provides DCVs that circulate back from the proximal axon to generate anterograde transport toward all release sites, where DCVs can be captured while traveling to and from the most distal boutons.

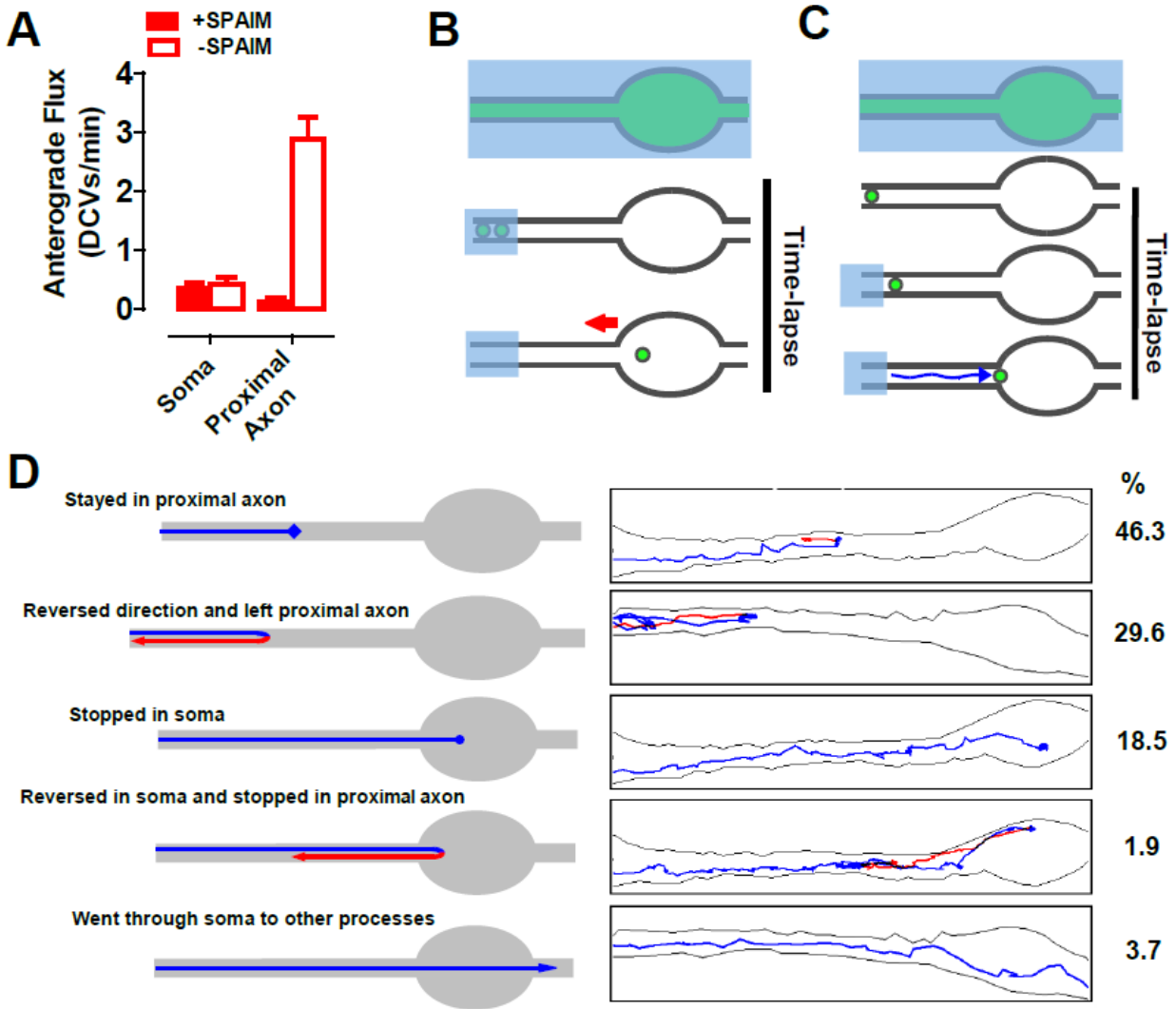


Figure 13 Retrograde DCVs reverse in the proximal axon to reenter the axon

A. Anterograde flux from the proximal axon and soma in 5 minutes after photobleaching. +SPAIM indicates that retrograde newcomers were photobleached. **B.** SPAIM experimental design to prevent retrograde newcomers from the axon entering the large photobleached region so flux from nascent DCVs moving out of the soma (red arrow) can be quantified. **C.** SPAIM experimental design to determine trajectories of retrograde DCVs entering the proximal axon. Note that photobleaching of retrograde newcomers began only after a one DCV entered the proximal axon from the axon. **D.** 5 minute trajectories of retrograde DCVs after returning to the proximal axon. Left images describe trajectory classes. Right images show representative data. Percentage of tracked DCVs (n=54) for each class is presented on the right. Blue lines, retrograde; Red lines, anterograde.

2.4 DISCUSSION

2.4.1 Supplying *en passant* boutons by vesicle circulation

One-way anterograde transport of DCVs was believed to fully explain neuropeptide delivery to nerve terminals. However, SPAIM in different neuronal compartments (i.e. *en passant* boutons, axonal branches, the proximal axon, and the soma) showed that neuropeptide accumulation in nerve terminal release sites is mediated by sporadic anterograde and retrograde capture of DCVs circulating between the proximal axon and distal boutons (Figure 14). These findings cannot be attributed to phototoxicity as they are supported by SPAIM-independent induction and mutant experiments, the match between flux measured without photobleaching (Shakiryanova et al., 2006a), the consistency of DCV behavior after multiple bouts of photobleaching, and the detection of release from single DCVs (See Chapter 4), which demonstrates viability and function.

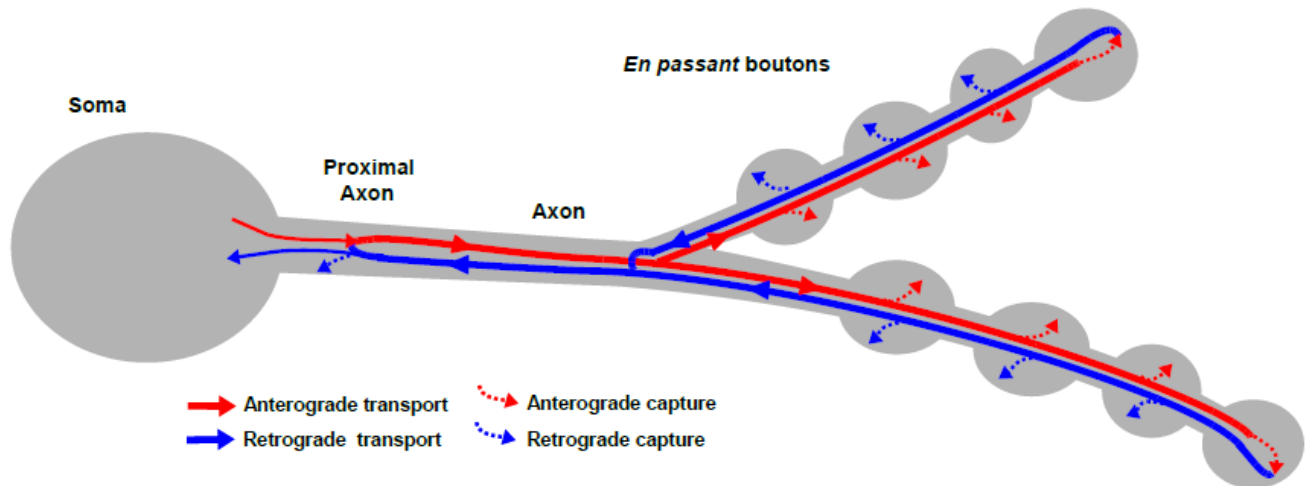


Figure 14 Vesicle circulation model for synaptic neuropeptide delivery

Vesicle circulation model for synaptic neuropeptide delivery. Anterograde DCVs are routed from the soma toward the most distal bouton in each branch. After reversing, dynactin-mediated retrograde transport routes DCVs past branch points into the axon. Once arriving in the proximal axon, many retrograde DCVs reverse to journey toward release sites again, thus avoiding degradation in the soma. While undergoing long-distance circulation, there is a low probability of being captured at each proximal bouton. This produces initial accumulation in the most distal bouton. However, because capture is slow compared to vesicle flux, neuropeptide stores in *en passant* boutons eventually fill equally despite differences in distance from the soma. See also Movies S6 and S7.

It was surprising that DCVs travel such far distances and that their presynaptic capture is inefficient, but this elegantly overcomes the limitations of relying solely on one-way transport (see Introduction) to produce the uniform neuropeptide accumulation that characterizes *en passant* boutons. Indeed, the conundrum of how to ensure that all potential release sites can function effectively regardless of distance from the soma or presence on different branches, which is critical for neurons, is resolved by vesicle circulation. Vesicle circulation also accounts for the long known, but mysterious, abundance of retrograde DCVs in axons (Alonso and Assenmacher, 1983) and ensures that DCVs do not readily return to the soma to be degraded. Furthermore, vesicle circulation provides a novel explanation for the finding that perturbing

retrograde DCV transport in neurons affects anterograde transport (Kwintar et al., 2009): interrupting retrograde transport prevents circulating retrograde DCVs from contributing to anterograde flux and so would reduce total anterograde transport. Finally, because the same kinesin motor transports neuropeptides and many other presynaptic proteins (Barkus et al., 2008; Hall and Hedgecock, 1991; Jacob and Kaplan, 2003; Okada et al., 1995; Pack-Chung et al., 2007a), vesicle circulation could be a general strategy for maintaining the synaptic function of *en passant* boutons. In this light, it is interesting that retrograde transport is compromised in neurodegenerative diseases (Strom et al., 2008); (Perlson et al., 2010). A previously unconsidered contributing factor to the early onset loss of synaptic function could be that diseases that affect dynactin-dependent retrograde transport perturb vesicle circulation that normally maintains the terminal. Therefore, vesicle circulation may be significant under physiological and pathological conditions.

2.4.2 SPAIM: a new tool for studying traffic

SPAIM detects DCVs in a native synapse for many minutes. In contrast, we found that photoactivation-based approaches using PA-GFP, tdEosFP and mOrange did not work well with *Drosophila* DCVs. This may be due to suboptimal targeting, difficulty in inducing photoactivation in the mildly acidic (Sturman et al., 2006) and oxidizing lumen of *Drosophila* DCVs, and the lower brightness and poorer folding of many photoactivatable proteins compared to emerald GFP. Given the availability of bright, well characterized GFP constructs, SPAIM represents a tenable method for tracking DCVs in native *Drosophila* neurons. In addition to detecting vesicle circulation, SPAIM could be used to study how presynaptic DCV mobilization is induced by activity in a native synapse and how DCV traffic changes with synaptic

development and plasticity. Furthermore, as noted above, SPAIM can detect release from single DCVs induced by nerve stimulation, which opens the possibility of studying peptidergic transmission at the level of individual vesicles in a native synapse. Therefore, SPAIM could answer many questions concerning neuronal DCVs.

In principle, SPAIM could be applied to any fluorescent organelle. However, a dual scanner confocal microscope, which was used here, might not be ideal for detecting very dim signals. When optical sectioning is not required, this limitation could be overcome by using a single scanner system for initially photobleaching a region of interest and then for continually photobleaching newcomers while simultaneously imaging individual organelles with a sensitive camera. In fact, performing SPAIM experiments by coupling a camera with a common single scanner confocal microscope may be an attractive option to overcome both the insensitivity and the expense of dual scanner systems. With the appropriate setup, SPAIM could be used to study traffic in terminals, dendrites, cilia, and filopodia.

2.5 MATERIALS AND METHODS

2.5.1 *Drosophila*

Emerald GFP was inserted at the EcoRV cut site in the preproDilp2 C-peptide sequence (kindly provided by E. Rulifson) and the resultant Dilp2-GFP fragment was cloned into the pUAST vector at the EcoRI and NotI sites for generation of transgenic UAS-Dilp2-GFP/CyO flies.

The following lines were maintained as double homozygotes for both transgenes, with female larvae selected for imaging experiments: *elav>Anf-GFP* (*elav-Gal4C155 UAS-preproAnf-EMD*), *386A>Anf-GFP* (*w, UAS-preproAnf-EMD;386A-Gal4*), *HS>Dilp2-GFP* (*w; UAS-Dilp2-GFP/CyO; Hsp70-Gal4*) and *GS>Anf-GFP* (*GS 3550-2, UAS-preproAnf-EMD*). To study the role of dynactin, male wild type (Canton S), *UAS-GlΔ96* and *UAS-Dmn* flies were crossed with female *GS>Anf-GFP* flies and F1 male larvae were selected for imaging. To localize the Golgi in lateral td neurons, *UAS-ManII-GFP* (Ye *et al.*, 2007; kindly provided by Y.N. Jan) males were crossed with female *386A-Gal4* flies and F1 larvae were used for imaging.

All animals were raised at 25°C, except in heat shock induction experiments in which larvae grown at 18°C were incubated at 37°C for 2 h and then maintained at 29°C. For RU486 induction, *GS>Anf-GFP* larvae were transferred to food containing 100 µg/ml RU486, which was made from a stock ethanol solution containing 100 mg/ml RU486 (Mifepristone; Sigma) mixed into freshly cooked Jazzmix food (Fisher Scientific) that had been cooled down to 60°C. In induction experiments, 3rd instar larvae, selected at specific time points after heat shock or RU486 exposure, were filleted and incubated with TRITC-conjugated anti-HRP (1:100, Jackson Immunoresearch) for 20-30 minutes on ice to stain neuronal membranes prior to GFP imaging.

2.5.2 Immunocytochemistry and Antibodies

Filleted larvae were fixed in 4% paraformaldehyde with 7% picric acid for 1 hour followed by permeabilization with 0.3% Triton X-100. For futsch labeling, the following antibodies were used: anti-Futsch/22C10 (1:100, Developmental Studies Hybridoma Bank) and Alexa 350-conjugated goat anti-mouse IgG (1:1000, Invitrogen). For proctolin precursor labeling, preparations were incubated in polyclonal anti-proctolin precursor serum (1:1000; Taylor *et al.*, 2004; kindly provided by D.R. Nässel) at 4°C for 2 days followed by Dylight 488-conjugated goat anti-rabbit IgG (1:1000, Jackson ImmunoResearch).

2.5.3 Imaging

Transport was quantified in muscle 6/7 type Ib boutons, muscle 4 motoneuron branches (although consistent results were obtained in muscle 6/7 branches) and lateral td neurons. In all cases, wandering 3rd instar larvae were filleted and imaged (Levitan *et al.*, 2007) in Ca²⁺-free HL3 solution (in mM: 70 NaCl, 5 KCl, 0.5 Na₃EGTA, 20 MgCl₂, 10 NaHCO₃, 5 trehalose, 115 sucrose, and 5 HEPES, pH 7.2) with an upright Olympus Fluoview FV1000 confocal laser scanning microscope equipped with an 80/20 beamsplitter in the laser combiner, a second “SIM” scanner, a dichroic mirror to recombine the SIM and main scanner beams, and a Olympus LUMFL 60X (NA 1.1) water immersion objective. GFP and TRITC were imaged using 488 nm and 559 nm excitation lasers, respectively. All prebleached images and images taken for quantification purpose were acquired at a minimum resolution 17 pixels/μm at laser power and detection settings that did not generate saturated signals or produce significant photobleaching.

When time-lapse was not required, fluorescence intensity for each *en passant* bouton was measured in Z stacks (29 images at 0.35 μm steps) taken of type Ib terminals on muscle 6/7. For td neurons, single images were acquired, with the trachea left intact. Photobleaching was performed using 100% 488 nm laser power from the SIM scanner in the line scanning mode. Time-lapse images were taken at 1 frame/s at a single plane of focus. To enable detection of single DCVs in flux and tracking experiments, time-lapse images were taken with a 5-fold increase in 488 nm main scanning laser power compared to prebleach images.

In SPAIM experiments, initial photobleaching was performed using 488 nm SIM scanning at speed of 40-100 $\mu\text{m}/\text{pixel}$ and 100% SIM laser power. Then the SIM scanner setting was reduced to 20%-30% power (i.e., 110 μW below the objective) for simultaneous photobleaching while acquiring images with the main scanner using ~ 4 μW of power below the objective scanning at 4 $\mu\text{m}/\text{pixel}$. All SPAIM experiments lasted at least 5 minutes or until the DCV reversed direction and left the region of interest in tracking experiments.

2.5.4 Image Analysis

Images were analyzed using ImageJ (NIH) software. For intensity measurements, stacks were first transformed into averaged Z projections. A region of interest was drawn around each bouton and background subtracted GFP fluorescence was measured as the mean grey value unless otherwise specified. In pulse-labeling experiments, boutons were identified with HRP labeling. FRAP ($\Delta\%F_0$) of each bouton was calculated as relative fluorescence to the corresponding prebleached bouton subtracted by the residual fluorescence immediately after photobleaching. In dynactin perturbation experiments, fluorescence was measured as total grey value from the averaged Z projection. Flux was determined by manually counting DCVs moving through a ROI

over a period of minutes. Single DCVs were tracked and trajectories were plotted using the Manual Tracking plugin in ImageJ.

3.0 CHARACTERIZATION OF DCV EXOCYTOSIS AT NERVE TERMINALS

3.1 ABSTRACT

Neuropeptides, which control emotion, behavior and body homeostasis, are released at nerve terminals through the exocytosis of dense-core vesicles (DCVs). Because the neuropeptide store at nerve terminals relies exclusively on the supply of nascent DCVs from the distant soma, tight regulation of neuropeptide release should be ensured to prevent the deprivation of releasable DCVs after activity. Although DCV exocytosis has been extensively studied, most findings were based on endocrine cell cultures that lack special polarized and differentiated features of neurons. Here, we use simultaneous photobleaching and imaging (SPAIM) to study exocytosis of single DCVs *in vivo* at the *Drosophila* larval neuromuscular junction (NMJ). Results show that release-competent DCVs supply neuropeptides to the terminal constantly, independent of their transport direction, location and mobility. These DCVs release exclusively by kiss-and-run exocytosis, and neuropeptides are dissipated slowly. More interestingly, these partially emptied DCVs can undergo multiple rounds of exocytosis to further discharge their contents. Overall, the study suggests that terminals are supported by the constant supply and recycling of releasable DCVs. At the same time, neuropeptide stores are utilized only progressively through partial release, thus preventing the deprivation of resources during repetitive firing.

3.2 INTRODUCTION

After neuropeptides are synthesized and packaged at the soma, neuropeptide-containing DCVs are delivered to release sites, where they await action potentials to trigger exocytosis. Because neuropeptides cannot be synthesized at the periphery or recycled after release, efficient neuropeptide transmission relies on the supply of DCVs from the soma. Of equal importance, the amount of release must be tightly controlled to prevent deprivation of neuropeptides at the terminal. Despite the abundance of DCVs at the terminal, only a small fraction of them are capable to undergo exocytosis. It is now believed that releasability of DCVs is associated with multiple biophysical properties.

Releasability depends on the mobility and age of DCVs. Direct imaging in differentiated PC12 cells and hippocampal neurons revealed that a fraction of DCVs are highly mobile. Unlike small synaptic vesicles (SSVs), DCVs do not need to be immobilized closed to the plasma membrane before exocytosis. Instead, exocytosis is favored by membrane-distal DCVs that move towards the plasma membrane upon stimulation (Han et al., 1999; Ng et al., 2003; Silverman et al., 2005). Indeed, mobility of DCVs promotes DCV releasability. First, DCV mobility is correlated with fusion probability, and that molecular-scale motion is required before fusion (Degtyar et al., 2007). In addition, it was found that activity-dependent mobilization of DCVs facilitates post-tetanic potentiation (PTP) of neuropeptide release (Shakiryanova et al., 2005). Releasability is also favored by younger vesicles. With the use of timer fluorescent proteins, such as DsRedE5 and monomeric Kusabira Green Orange (mK-GO), DCVs were labeled with different colors depending on their age. It was found that younger vesicles undergo exocytosis more frequently (Duncan et al., 2003; Tsuboi et al., 2010; Wiegand et al., 2003).

Releasable DCVs may fully collapse into the plasma membrane after exocytosis, discharging all their neuropeptides at once. The vesicle membrane is then recycled by clathrin-dependent endocytosis. More frequently, they undergo kiss-and-run exocytosis, in which DCVs are fused only transiently with the plasma membrane, and neuropeptides are released partially through the fusion pore before DCVs are rapidly endocytosed. The transient fusion pore formation limits the time and extent of neuropeptide release during exocytosis. At the same time, both the size and biochemical properties of the neuropeptide contribute to its diffusion rate.

DCV exocytosis was classically studied by membrane capacitance and amperometry measurements. Thus far, the most popular experimental model has been endocrine cell culture (e.g. chromaffin and PC12 cells). Because neuronal processes or well-differentiated nerve terminals are absent in these models, no information can be obtained about exocytosis properties of DCVs in relation to their specific transport direction and bouton location. Even with the use of the neuronal culture, such as developing hippocampal neurons, synaptic boutons are too small to resolve the movement of DCVs. In addition, *in vitro* models are always less desirable systems because they may not reflect the true property of neurons that have a post-synaptic partner.

Here, we use the *Drosophila* larval neuromuscular junction (NMJ) as an *in vivo* model to study DCV exocytosis at the nerve terminal. By labeling DCVs with GFP-tagged neuropeptides, together with the use of a newly developed imaging strategy, simultaneous photobleaching and imaging (SPAIM), the movement and exocytosis of individual DCVs within *en passant* boutons are imaged upon electrical stimulation. Specifically, we address whether DCVs are more releasable when they are 1) captured in the anterograde or retrograde directions; 2) captured at a particular *en passant* bouton location; 3) captured or just transiently visiting the bouton; 4) mobile or immobile. We also examine the release kinetics of neuropeptides from single DCVs

during exocytosis. Results show that release-competent DCVs supply neuropeptides to the terminal constantly, independent of their transport direction, location and mobility. These DCVs release exclusively by kiss-and-run exocytosis, and neuropeptides are released slowly. More interestingly, these partially emptied DCVs can undergo multiple rounds of exocytosis to further discharge their contents.

3.3 RESULTS

3.3.1 Single DCVs exocytosis at the nerve terminal by SPAIM tracking

Electrical stimulation (1 min 70 Hz) was applied while single DCVs labeled with GFP tagged-atrial natriuretic factor (Anf-GFP) were tracked in the nerve terminal by SPAIM (see Chapter 2 for detailed description of the method). Upon stimulation, fluorescence decreases were seen in some of these DCVs, suggesting neuropeptide release (Figure 15A, B). To ensure that the fluorescence decrease is Ca^{2+} influx-dependent, SPAIM experiments were performed under Ca^{2+} -free conditions. Here, the acute release of neuropeptide during stimulation was abolished, although a slow and small fluorescence decrease (~15-20%) was seen 30 s after the onset of action potentials (Figure 15C), suggesting that a small portion of neuropeptides may be released through a Na^+ -dependent, Ca^{2+} influx-independent pathway. Releasable and unreleasable DCVs were sorted based on the amount of neuropeptide release after 1 min stimulation: the frequency distribution in Figure 15D shows two distinct populations of releasable vesicles. One of these, with about 70% DCVs, released more than 18% neuropeptide content, and represents the Ca^{2+}

releasable pool. The population with less release represents Ca^{2+} influx-independent events and are classified as unreleasable for our study (Figure 15D).

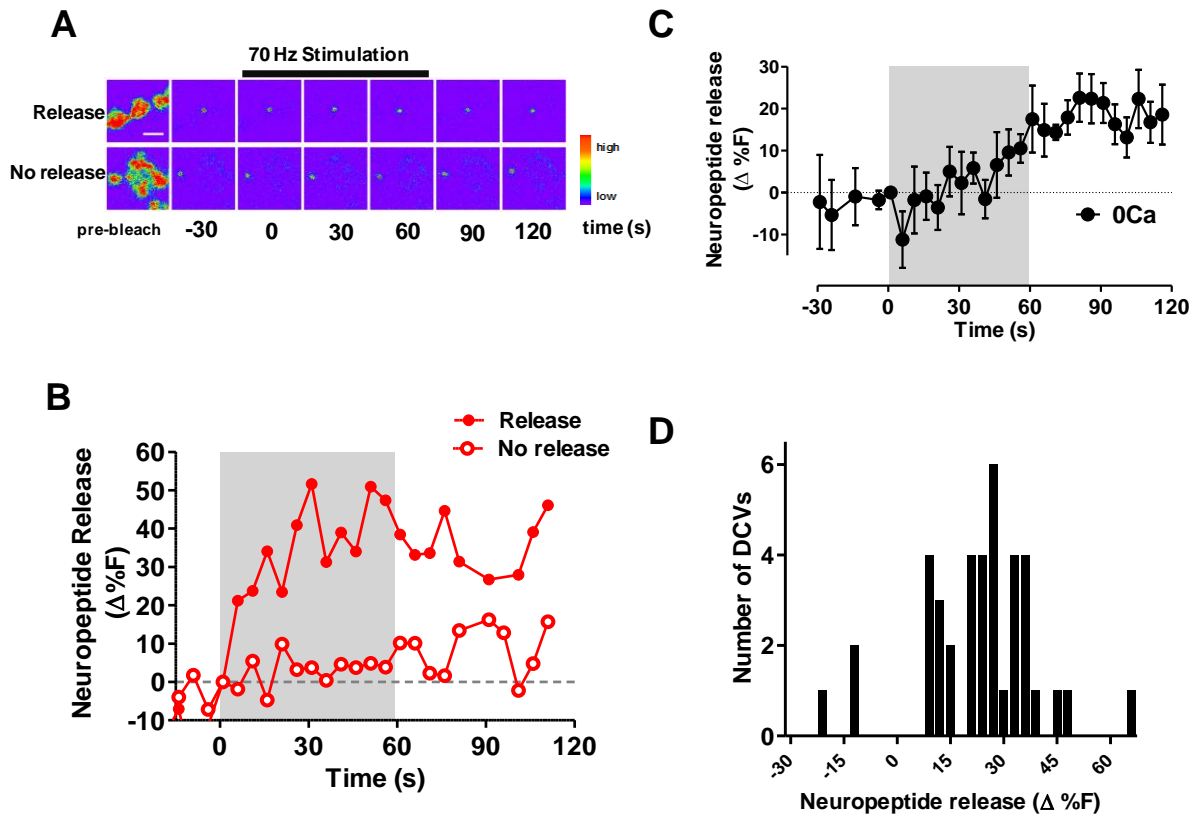


Figure 15 Measuring neuropeptide release from single DCVs by SPAIM

A. Representative pseudocolored time-course images of a releasable (Top), and an unreleasable (Bottom) single DCV before and after 1 min 70 Hz stimulation. Scale bar= $2\mu\text{m}$. **B.** Representative neuropeptide release time course of a releasable and an unreleasable DCV. Neuropeptide release was quantified as the percentage change of percentage fluorescence prior to stimulation ($\%F$). **C.** Average time course of neuropeptide release from DCVs stimulated in Ca^{2+} free medium. Note the delay neuropeptide release after 30s. **D.** Frequency distribution of neuropeptide release from all the DCVs under study ($n=39$). Here, neuropeptide release was calculated by averaging $\Delta\%F$ from $t=60-120\text{s}$ after stimulation, when release has usually plateaued. Error bars represent SEM.

3.3.2 Releasability of DCVs as measured by probability and size of release

As described previously, newly arrived DCVs from either the anterograde or retrograde direction can bypass boutons quickly (<5 s), stay inside a bouton for a transient visit (5-120 s), or be captured for a prolonged period (>120 s) (see Chapter 2). To test if directionality and capture affect release probability, electrical stimulation was applied while DCVs were visiting transiently or captured in a bouton. In these experiments, captured DCVs were defined as those that stayed within the same bouton for at least 2 mins before stimulation, while visiting DCVs were defined as those that stayed within the same bouton for less than 1 min. (Figure 16A, top). Anterograde or retrograde DCVs that were captured or visiting a bouton also underwent exocytosis with similar probability (50-75%) (Figure 16A, Bottom). Although trajectories of DCVs show that DCVs may stay immobile, jitter, or loop around a bouton during visits or captures (Figure 16B, top, also see Chapter 2), the mobility preceding activity did not affect releasability (Figure 16B, Bottom). Finally, release probabilities of DCVs was also independent of their respective bouton location (Figure 16C).

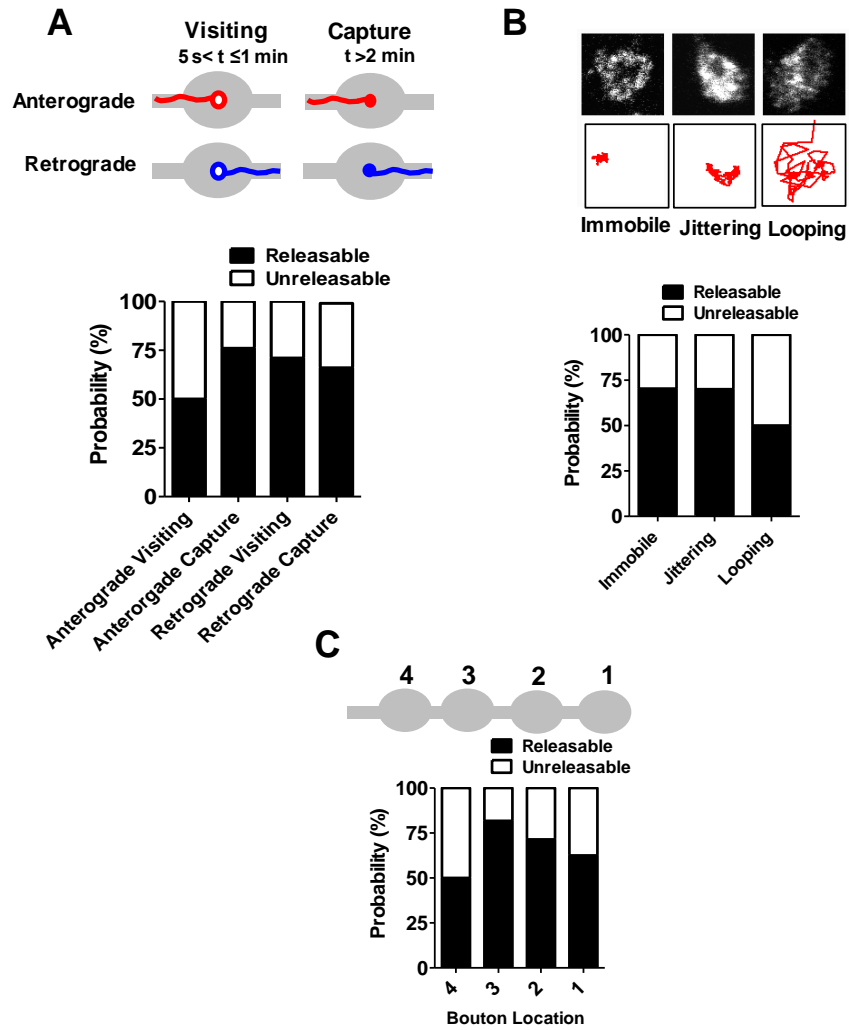


Figure 16 Releasability of DCVs in relation to their transport directions, time of residence, mobility and bouton locations

A. Top panel: Upon arrival at a bouton from either direction, DCVs may visit transiently or be captured (See Chapter 2). DCVs were induced to undergo exocytosis after specific time periods as shown. Bottom: Exocytosis probability of anterograde and retrograde DCVs that were visiting or captured (Anterograde visit, n=6 Anterograde capture, n=17; Retrograde visit, n=7; Retrograde capture, n=9) **B.** Top panel: Possible trajectories of DCVs when visiting or captured in the respective bouton. Bottom: Probability of exocytosis after DCVs have displayed specific behavior (Immobile, n=25; Jittering, n=12; Looping, n=2). **C.** Top panel: *En passant* bouton location with specific numbering. Bottom: Probability of exocytosis at different bouton locations (Bouton 1, n=8; Bouton 2, n=14; Bouton 3, n=11; Bouton 4, n=6)

To further examine releasability, we also monitored the time course and extent of neuropeptide release from releasable DCVs. DCVs captured at either the proximal or distal boutons share the same release kinetics: ~25% neuropeptide is released and the release is slow (i.e. $t_{1/2} \sim 10$ s) (Figure 17A). Anterograde or retrograde DCVs that were visiting or captured both showed similar release kinetics (Figure 17B, C). No differences in release kinetics were seen between anterograde and retrograde vesicles (Figure 17D). Together, these results suggest that newly arrived DCVs that are visiting or captured at the distal or proximal boutons, from anterograde or retrograde directions, mobile or stationary, all undergo exocytosis with the same probability and release kinetics.

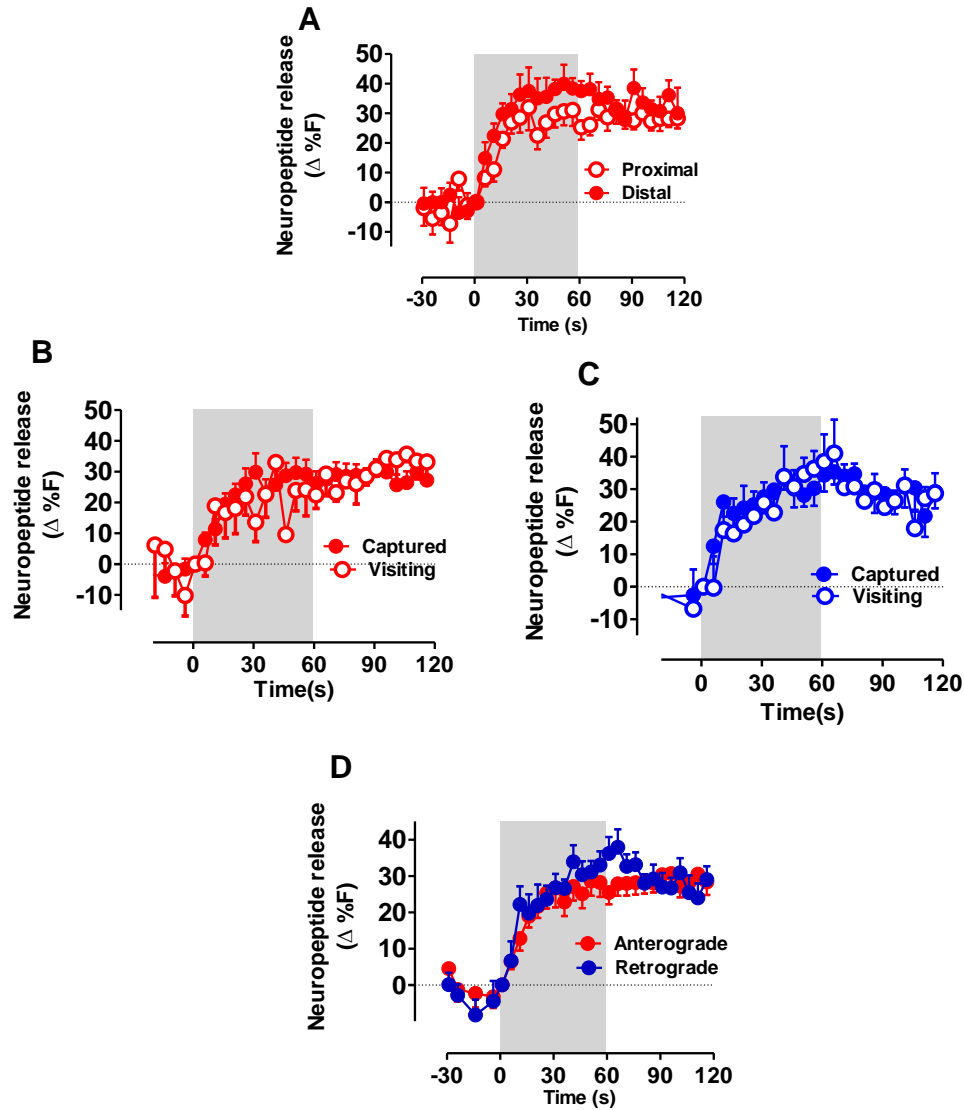


Figure 17 Neuropeptides are released partially and slowly independent of DCV transport directions and bouton locations

a) Average time-course of neuropeptide release from releasable anterograde DCVs captured at a proximal (n=8) or distal bouton (n=5) for >2 min.. **B.** Average time-course of release for releasable captured (n=13) or visiting (Residence time : 5s-1 min, n=3) vesicles. **C.** Average time-course of release for retrograde DCVs, Capture, n=6 ; Visiting, n= 5. **D.** Average time-course of neuropeptide release from releasable anterograde (n=13) and retrograde (n=6) DCVs. All images were acquired at 1 s/ frame. Data points are averaged from 5 consecutive time points. Values are means \pm S.E.M .Shaded area, 1 min 70 Hz stimulation.

3.3.3 Release kinetics of neuropeptides

To determine whether the slow release kinetics was caused by the extended stimulation protocol, a shorter stimulation protocol (10 s) was applied to induce release. Unexpectedly, release continued for another 30s after stimulation stopped, implying that either the fusion pore opening persisted after stimulation or that neuropeptides were released as a stable deposit that diffuses away slowly from the membrane surface (Figure 18A). By applying multiple 10 s 70 Hz stimulations at 1 min intervals, we found that the same DCV can undergo multiple rounds of exocytosis, although the amount of release decreases with increasing number of stimulations (Figure 18B and C). The difference in release amount after repetitive stimulation excluded the possibility that exocytosis was detected from a packet of multiple DCVs in the SPAIM experiment. Rather, release is from the same DCVs.

To test if such prolonged release from single DCVs is the result of kiss-and-run exocytosis, some preliminary release experiments were done with inhibition of endocytosis using Dynasore, a dynamin-specific inhibitor (Kirchhausen et al., 2008; Macia et al., 2006). In these experiments, neuropeptide released from a individual bouton with many DCVs upon 1 min 70 Hz stimulation was measured after 30 min incubation with 100 μ M Dynasore. Unexpectedly, exocytosis was nearly completely abolished in 2/3 of the experiments, while the rest showed a two-fold increase in neuropeptide release as compared to the DMSO-treated control. Activity-dependent capture was also abolished upon Dynasore treatment. (Figure 18D). Future experiments using dyngo-4 (Harper et al., 2011), a newer version of Dynasore with higher dynamin I specificity, or overexpression of a temperature sensitive dynamin mutant, UAS-Shibire-TS (Chen et al., 1991; Kitamoto, 2001), will be needed to further explain the release property of single DCVs.

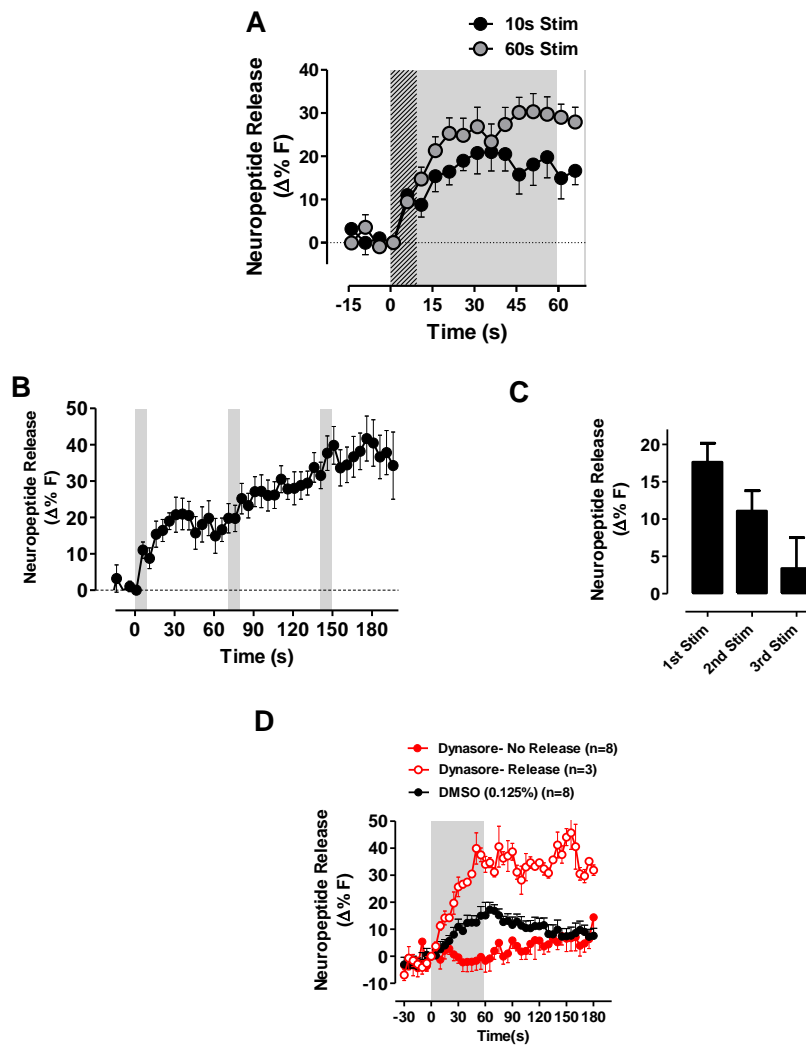


Figure 18 DCVs can undergo multiple rounds of exocytosis with release persisted long after stimulation

a) Average time-course of neuropeptide release from anterogradely captured DCV upon 10s (n=12) or 60s (n=17) 70 Hz stimulation. Striped area, 10s stimulation period. Shaded area, 60s stimulation period. **b)** Average time-course of neuropeptide release from anterogradely captured DCV upon multiple 10s 70 Hz stimulation. Shaded area, 10s stimulation period. **c)** Amount of release after consecutive stimulations. Values were obtained by averaging the release amount at each time point from t=40-70 s after stimulation. **d)** Average time-course of neuropeptide release from individual bouton after 30 min 100uM Dynasore (n=12) or 0.125% DMSO treatment (n=8). All images were acquired at 1 s/ frame. Data points are averaged from 5 consecutive time points. Values are means ±S.E.M.

3.4 DISCUSSION

3.4.1 Releasability is independent of transport direction age and mobility

These data suggest that DCVs that are constantly delivered to the nerve terminal through bidirectional sporadic capture (see Chapter 3 for the circulation strategy) are release-competent (~70% release probability), but release only partially. If we assume that most anterograde DCVs are young vesicles that are recently synthesized from the soma and retrograde DCVs are older vesicles that have resided in the terminal for a longer time, these findings may indicate that young and old DCVs are similar in terms of releasability. The fact that anterograde DCVs undergo exocytosis during their brief visits also suggests that DCVs are primed for release before they enter a bouton. One would expect that mobility facilitates release (Shakiryanova et al., 2005, Shakiryanova et al., 2007), but our data do not support such a bias. Transiting DCVs are not able to exocytose (data not shown), indicating that interbouton movement (likely driven by microtubule-based transport) does not favor release. Intrabouton motions such as jittering and looping allow for exocytosis but do not enhance releasability. These are distinct exocytosis properties of DCVs in the nerve terminal that are different from what were found in endocrine or neuronal cell cultures previously (see Introduction).

3.4.2 Kiss and run exocytosis as the predominant role of release

Releasable DCVs released only ~25% of their content even when strong and prolonged stimulation was applied, indicating that kiss-and-run is the predominant mode of exocytosis for DCVs. These data are in strong agreement with the finding from the neurite of developing

hippocampal neurons, in which only ~30% of Anf-GFP is released from single DCVs in each exocytic event upon high potassium-evoked depolarization (Xia et al., 2009). Nevertheless, contrasting findings were found in PC-12 cells, where fast, complete release of Anf-GFP was seen upon stimulation by Ba^{2+} or 500ms depolarization. This indicates that cell types and stimulation protocol may affect the efficiency of release (Barg et al., 2002; Han et al., 1999). At the same time, preselection by SPAIM for newly arrived DCVs may also be a cause for such discrepancy. It is possible that resident DCVs, which were not examined in the study are more likely to undergo full collapse fusion.

We found that partially emptied vesicles are capable to undergo multiple rounds of kiss-and-run exocytosis to release neuropeptide gradually. DCV recycling may serve as a mechanism utilized by the neuron to minimize the depletion of DCVs at nerve terminals upon repetitive firings, which would require the delivery of new DCVs from the remote synthesis/packaging site. In fact, repetitive kiss-and-run exocytosis has been reported previously upon single nerve stimulation, but those events are more rapid and are most likely due to the formation of flickering fusion pores (Staal et al., 2004; Xia et al., 2009). It is possible that DCVs in the fly NMJ also flicker, but the high signal noise and low temporal resolution of the SPAIM imaging have prevented us from detecting such events.

The requirement for vesicle scission during kiss-and run was examined by dynamin inhibition. However, preliminary experiments using Dynasore to inhibit dynamin-mediated endocytosis showed varying results: either release was inhibited or more release was seen. Therefore, future SPAIM experiment using dyngo-4 (Harper et al., 2011), a newer version of Dynasore with higher dynamin I specificity, or overexpression of the temperature sensitive

dynamamin mutant, UAS-Shibire-TS (Chen et al., 1991; Kitamoto, 2001), will be needed to further explain the release properties of single DCVs.

3.4.3 Imaging single DCV exocytosis at a live nerve terminal

SPAIM is a powerful technique to trace single DCV movement and to measure DCV flux at specific regions of the neuron by limiting newcomer DCVs from entering the imaging region of interest (Chapter 2). By combining SPAIM and electrical stimulation, the release of neuropeptides from single DCVs upon repeated stimulations was measured for the first time at live synaptic terminals.

The key for single particle tracking is to limit the number of visible particles during imaging. In conventional TIRF imaging, particle number can be limited by visualizing only the in-focus DCVs close to the membrane. In this setting, much information about the 3D movement of DCVs is lost once they move out of focus. In addition, although DCVs can be resolved to a single vesicle level, a large number of DCVs are still present in the ROI, therefore most DCV can only be monitored for one round of exocytosis, making it difficult to study DCV kinetics after multiple stimulations. In SPAIM, the number of visible particles in the ROI can be minimized down to one single DCV by simultaneous photobleaching. In addition, because imaging can be done by conventional confocal or widefield microscopy, the focal plane can be adjusted while imaging, and the lateral movement of DCVs away from the release sites can also be traced. This allows the same vesicle to be tracked before and after multiple rounds of stimulation. Lastly, SPAIM is a particularly valuable tool to study DCV exocytosis in *Drosophila* larval preparation. Because fly boutons are much smaller than a whole endocrine cell, and because they are embedded inside the muscle, patch clamping is difficult and thus

capacitance measurements of DCV fusion are not feasible. Due to the unique anatomic orientation of the NMJ after dissection, it is impossible to place a coverslip on the preparation, and thus TIRF imaging is also impossible.

Despite all the advantages of the SPAIM strategy, there are some limitations for its use to study DCV dynamics and kinetics. First, due to the nature of the photobleaching experiment, SPAIM preselects for DCV new comers. Therefore the data may not be representative of all DCVs because it does not include resident population. Second, image acquisition is labor-intensive and data can be very noisy because DCVs are constantly moving in a 3-dimensional space that requires constant re-focusing. For the same reason, brighter and more stationary DCVs may be preselected for imaging. Therefore, further advancement of the imaging system will be needed to improve the strategy.

3.5 MATERIALS AND METHODS

The *Drosophila* line, *elav>Anf-GFP* (*elav-Gal4C155 UAS-preproAnf-EMD*) was maintained as double homozygotes for both transgenes, with female larvae selected for imaging experiments. All animals were raised at 25°C and fed on Jazzmix food (Fisher Scientific).

Wandering 3rd instar larvae were filleted and imaged (Levitan *et al.*, 2007) in Ca²⁺-free HL3 solution (in mM: 70 NaCl, 5 KCl, 0.5 Na₃EGTA, 20 MgCl₂, 10 NaHCO₃, 5 trehalose, 115 sucrose, and 5 HEPES, pH 7.2) .

Imaging was performed with an upright Olympus Fluoview FV1000 confocal laser scanning microscope equipped with an 80/20 beamsplitter in the laser combiner, a second “SIM” scanner, a dichroic mirror to recombine the SIM and main scanner beams, and a Olympus

LUMFL 60X (NA 1.1) water immersion objective. GFP was imaged using 488 nm excitation lasers, respectively at a frame rate of 1 Hz. In SPAIM experiments, initial photobleaching was performed using 488 nm SIM scanning at speed of 100 $\mu\text{m}/\text{pixel}$ and 100% SIM laser power. Then the SIM scanner setting was reduced to 20%-30% power for simultaneous photobleaching while acquiring images with the main scanner. After a DCV was seen to have resided at a bouton for a specific period, motor nerves were stimulated with suction electrodes at 70 Hz for either 1 minute or 10 s.

Drugs were bath applied after dissection. Dynasore was obtained from Sigma-Aldrich (St. Louis, MO), and was dissolved in DMSO as stocks (80 mM) and subsequently diluted to yield a final concentration of 0.125% DMSO.

Images were analyzed using ImageJ software (NIH). For intensity measurements, a region of interest was drawn around each DCV at each time point and background subtracted. GFP fluorescence was measured as the mean grey value unless otherwise specified. Neuropeptide release was quantified as the change of percent fluorescence prior to stimulation ($\Delta\%F$) unless otherwise specified. Data points were binned every 5 time points to reduce data noise. Single DCVs were tracked and trajectories were plotted using the Manual Tracking plugin in ImageJ.

4.0 PRESYNAPTIC RYANODINE RECEPTOR-CAMKII SIGNALING IS REQUIRED FOR ACTIVITY-DEPENDENT CAPTURE OF TRANSITING VESICLES.

4.1 ABSTRACT

Activity elicits capture of dense-core vesicles (DCVs) that transit through resting *Drosophila* synaptic boutons to produce a rebound in presynaptic neuropeptide content following release. The onset of capture overlaps with an increase in the mobility of DCVs already present in synaptic boutons. Vesicle mobilization requires Ca^{2+} -induced Ca^{2+} release by presynaptic endoplasmic reticulum (ER) ryanodine receptors (RyRs) that in turn stimulates Ca^{2+} /calmodulin-dependent kinase II (CamKII). Here we show that the same signaling is required for activity-dependent capture of transiting DCVs. Specifically, the CamKII inhibitor KN-93, but not its inactive analog KN-92, eliminated the rebound replacement of neuropeptidergic DCVs in synaptic boutons. Furthermore, pharmacologically or genetically inhibiting neuronal sarco-endoplasmic reticulum calcium ATPase to deplete presynaptic ER Ca^{2+} stores or directly inhibiting RyRs prevented the capture response. These results show that the presynaptic RyR-CamKII pathway, which triggers mobilization of resident synaptic DCVs to facilitate exocytosis, also mediates activity-dependent capture of transiting DCVs to replenish neuropeptide stores.

4.2 INTRODUCTION

The function of nerve terminals depends on vesicular delivery of proteins synthesized in the soma to synaptic boutons. Transport vesicles are known to contain channels, active zone constituents and neuropeptides (Ziv and Garner, 2004; Zupanc, 1996). In contrast to synaptic membrane proteins and classical transmitters that are recycled following exocytosis, neuropeptide release is irreversible. Thus, peptidergic transmission depends on the replacement of neuropeptide-containing dense-core vesicles (DCVs). This is potentially a very slow process because delivery of vesicles synthesized in the soma to nerve terminals by fast axonal transport can take days. However, a cell biological strategy has been discovered that bypasses such delays. Activity-dependent capture of transiting vesicles utilizes a pool of DCVs that rapidly pass through the resting nerve terminal, but that are captured in response to a burst of activity (Shakiryanova et al., 2006a). The onset of this capture, which is evident as decreased DCV efflux and increased neuropeptide content in synaptic boutons, occurs over a period of minutes instead of the hours that would be required for conventional steady state DCV replacement. Essentially, the nerve terminal can tap into the transiting DCV pool to rapidly replenish neuropeptide stores without any direct involvement of the soma. Hence, activity-dependent capture of transiting DCVs eliminates the delay in delivering nascent DCVs, apportions resources based on activity and places control of synaptic neuropeptide storage at sites of release instead of the site of synthesis (i.e. the soma) (Shakiryanova et al., 2006a). A similar recruitment process also occurs with neurotrypsin-containing vesicles, which were concluded to rapidly undergo exocytosis following stimulated capture (Frischknecht et al., 2008). Likewise, vesicle capture appears to be involved in release of presynaptic Wnt/Wingless protein (Ataman et al.,

2008). Therefore, activity-dependent capture of transiting vesicles supports synaptic neuropeptide, enzyme and developmental peptide release.

The signaling required for activity-dependent capture of transiting DCVs is unknown. The long duration of this response in *Drosophila* motor neurons (i.e., for ~0.5 hour) coupled with the requirement for electrical activity suggests a potential involvement of Ca²⁺-induced phosphorylation. In fact, recent experiments have shown that such signaling increases the mobility of resident DCVs in synaptic boutons. Mobilization, which is triggered by Ca²⁺ influx and persists for ~10 minutes (Shakiryanova et al., 2005), requires Ca²⁺-induced Ca²⁺ release from presynaptic endoplasmic reticulum (ER) via ryanodine receptors (RyRs) (Shakiryanova et al., 2007). Subsequently, Ca²⁺/calmodulin-dependent protein kinase II (CamKII) is activated as a necessary step for DCV mobilization (Shakiryanova et al., 2007). The overlapping onset of the capture and mobilization responses in the first minutes following a brief tetanus stimulated us to investigate whether the RyR-CamKII pathway participates in activity-dependent capture of transiting vesicles.

Here a GFP (Green Fluorescent Protein)-tagged neuropeptide is imaged at the intact *Drosophila* neuromuscular junction. We report that the rebound in synaptic neuropeptide stores following activity-evoked release, which is caused by capture of transiting vesicles (Shakiryanova et al., 2006a), requires RyR-mediated Ca²⁺ efflux from presynaptic ER and activation of CamKII. Therefore, RyR-CamKII signaling initiates both mobilization of resident DCVs within synaptic boutons and capture of DCVs from the rapidly transiting pool.

This chapter has been published as “Presynaptic Ryanodine Receptor-CamKII Signaling is Required for Activity-dependent Capture of Transiting Vesicles” in *Journal of Molecular Neuroscience* in January 2009 (Wong et al., 2009). The work was contributed by my advisor Dr.

Edwin Levitan for the preparation of the manuscript. It was also contributed by Drs. Dinara Shakiryanova, Chaoming Zhou, David Deitcher for experimental advice and the generation of genetic mutants.

4.3 RESULTS

Drosophila type Ib boutons were electrically stimulated to induce release and subsequent capture of transiting DCVs. Prior to stimulation, the signal from the GFP-tagged neuropeptide was stable within a bouton. However, 70 Hz motor nerve stimulation for a minute induced a rapid release of ~20% of the neuropeptide (i.e., fluorescence dropped to ~80% of the resting value). This was followed by a rebound in the following 4 minutes to reach ~90% of the baseline content (Figure 20), which is mediated by capture of transiting DCVs (Shakiryanova et al., 2006a). Hence, capture of transiting DCVs resulted in rapid replacement of ~50% of the neuropeptide release by synaptic boutons.

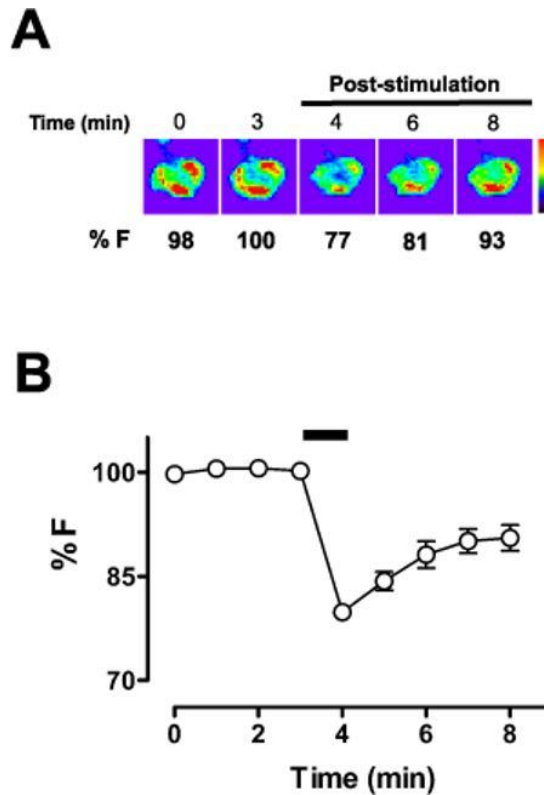


Figure 19 Activity-dependent neuropeptide capture following electrical stimulation

A. Pseudo-color images of GFP-tagged neuropeptide fluorescence in a type Ib bouton before and after 70 Hz electrical stimulation for 1 minute. The relative amount of peptide content was quantified as percentage fluorescence prior to stimulation (%F). **B.** Time course of neuropeptide content (n=12). Black bar indicates stimulation. Each experimental point was from one bouton in an independent preparation. Error bars represent standard error of the mean (SEM). Note the rebound in neuropeptide content following release, which is caused by activity-dependent capture of transiting DCVs (Shakiryanova et al., 2007).

To determine whether CamKII activity is required for activity-dependent DCV capture, we examined the effect of CamKII inhibition on the response to the above electrical stimulation. Specifically, the effect of the CamKII inhibitor KN-93 was compared to its inactive analog KN-92. Both compounds slightly increased acute release (i.e. the rapid drop in GFP fluorescence immediately following stimulation) (Figure 20). This minor response, which was not seen with a

different stimulation protocol (Shakiryanova et al., 2007), must not involve CamKII because it was produced by both analogs. However, a concentration of KN-93 that abolishes activity-evoked DCV mobilization (Shakiryanova et al., 2007) eliminated the subsequent rebound of neuropeptide content, while the capture response remained detectable with KN-92 (Figure 20). To normalize for potential differences in release, capture was quantified as the percent of released neuropeptide that was replaced in 4 minutes after the cessation of electrical stimulation. Based on this analysis, KN-93 and KN-92 produced statistically different results (Figure 21, left). Hence, although the KN compounds may have had a shared minor nonspecific effect on release, the KN-93-specific inhibition of the rebound in neuropeptide content implies that CamKII activity is required for activity-dependent capture of transiting DCVs.

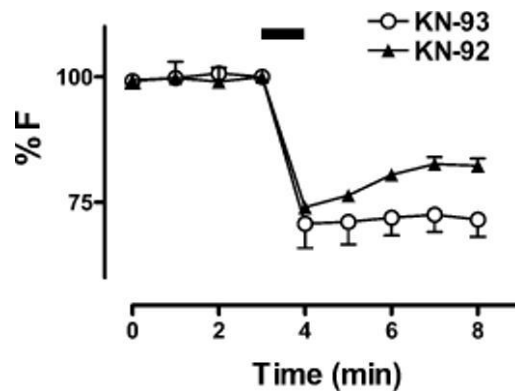


Figure 20 CamKII inhibition abolishes activity-dependent DCV capture

CamKII inhibition abolishes activity-dependent DCV capture. Neuropeptide content time course following 15-minute pretreatment with 10 μ M KN-92 (filled triangles, n=4) or KN-93 (open circles, n=6). Black bar indicates 70Hz electrical stimulation. Error bars represent SEM.

Because activation of CamKII for DCV mobilization requires ER Ca^{2+} release mediated by RyRs (Shakiryanova et al., 2007), the role of RyRs in activity-dependent DCV capture was studied. Pretreatment with an inhibitory concentration of ryanodine eliminated capture (i.e. the replacement of released neuropeptide was not significantly different from zero) (Figure 21). To independently verify that ER Ca^{2+} release was required, ER Ca^{2+} stores were depleted by inhibiting the Sarco/Endoplasmic Reticulum Ca^{2+} -ATPase (SERCA) with Thapsigargin (Tg) in Ca^{2+} -free medium for 20 minutes. The preparation was then returned to normal Ca^{2+} -containing solution and electrically stimulated. This protocol dramatically reduced the capture response, while a vehicle control had no effect (Figure 21). Thus, release of ER Ca^{2+} by RyRs is required for activity-dependent capture of transiting DCVs.

The pharmacologic agents used thus far were bath applied and so acted on both the presynaptic neuron and the postsynaptic muscle. To ensure activity-dependent DCV capture is not caused by retrograde RyR-induced signaling, presynaptic ER Ca^{2+} stores were targeted genetically by expressing a temperature-sensitive dominant negative SERCA subunit (Kum170, (Sanyal et al., 2005) specifically in neurons. At a permissive temperature, the capture response in Kum170-expressing boutons was intact. However, replacement of released neuropeptide was inhibited after shifting the animals to the restrictive temperature for 8 minutes (Figure 21, right). In contrast, this treatment did not affect capture in control animals subjected to the restrictive temperature (data not shown). Therefore, presynaptic ER Ca^{2+} release by RyRs is essential for CamKII-mediated capture of transiting DCVs.

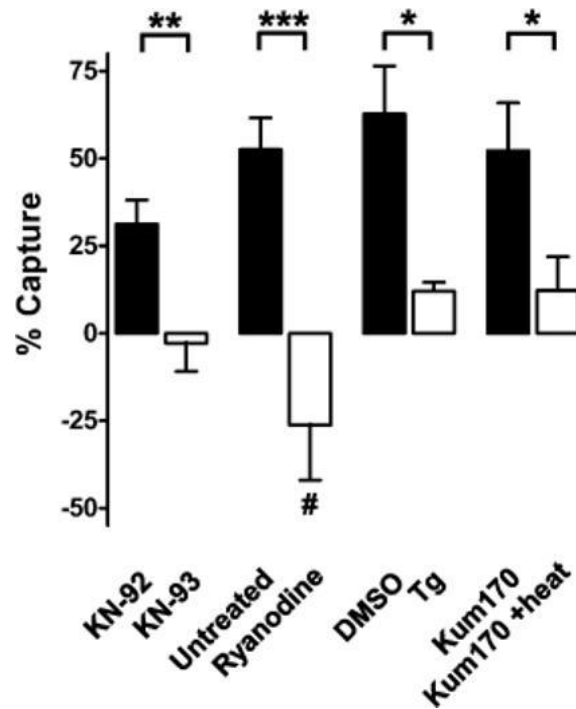


Figure 21 CamKII and presynaptic Ca²⁺ release by ER RyRs are required for activity-dependent DCV capture

Comparison of capture after inhibiting CamKII with KN-93 (n=6) or treating with an inactive analog KN-92 (n=4), inhibiting RyRs with 100 μ M ryanodine (n=6) for 15 minutes versus untreated controls (n= 12), and ER Ca²⁺ store depletion by the SERCA pump inhibitor Tg (20 μ M, n=5) for 20 minutes versus its vehicle control (n=6). Finally, the requirement for presynaptic ER Ca²⁺ release was tested in animals expressing temperature-sensitive dominant negative SERCA pre-exposed for 8 minutes to 22°C (Kum170, n=6) or 40°C (Kum170 + heat, n=10). Unpaired t-test results: *P < 0.05, **P < 0.01 , ***P < 0.001. # indicates no significant difference from zero by one sample t-test. Error bars represent SEM.

4.4 DISCUSSION

In vivo imaging has shown that a brief bout of activity elicits prolonged DCV mobilization and capture. These processes are independent because capture requires axonal transport while

mobilization does not (Shakiryanova et al., 2005; Shakiryanova et al., 2006a). Nevertheless, the onsets of mobilization of resident DCVs and capture of transiting DCVs overlap (i.e. both develop over minutes following seconds of activity). This observation stimulated us to test the hypothesis that these two mechanisms are initiated by the same signaling. Previous studies had established that Ca^{2+} influx triggers DCV mobilization by activating RyR-mediated Ca^{2+} release from presynaptic ER that in turn stimulates CamKII (Shakiryanova et al., 2007). The pharmacological and genetic experiments presented here establish that RyR-CamKII signaling is also required for activity-dependent capture of transiting DCVs.

This finding raises the issue of how a single signaling pathway produces responses with different durations: after seconds of activity, DCV mobilization lasts ~10 minutes, while the capture response lasts ~40 minutes (Shakiryanova et al., 2005; Shakiryanova et al., 2006a). One possible consideration is that these kinetic differences could originate in the processes responsible for reversal of mobilization and capture. Specifically, RyR-CamKII signaling could initiate the two processes in parallel, but dephosphorylation of distinct CamKII substrates might occur at different rates, possibly because of the involvement of different phosphatases. This potential explanation suggests that identifying the CamKII substrates that mediate mobilization and capture will be important for understanding the diversity in long-lasting responses initiated by activity-triggered presynaptic RyR-CamKII signaling. Recently, CamKII-dependent phosphorylation of kinesin superfamily protein 17 (KIF17) was found to be essential for unloading NMDA receptor-carrying cargoes from microtubules near the postsynaptic density (Guillaud et al., 2008). Therefore, CamKII might induce capture by triggering dissociation of transiting DCVs from their molecular motor dynactin complex, which would contain both a kinesin-3 family member UNC-104/Kif1 (Barkus et al., 2008; Pack-Chung et al., 2007b) and a

dynein retrograde motor, while mobilization might depend on another CamKII substrate. Alternatively, some process downstream of dephosphorylation might be rate determining for reversal of capture. For example, once captured vesicles are committed to return to the transiting pool, they might need to recruit an unoccupied motor complex to support rapid transiting. If such complexes are rare, then recovery from capture would be very slow. In contrast, recovery from mobilization, which does not require exiting from the bouton, would not be limited in the same way. Regardless of the specific basis for the diverse time courses of mobilization and capture, the use of the same signaling pathway to induce both of these effects is an elegant means to ensure that facilitation of release is coupled to replacement of depleted synaptic neuropeptide stores.

4.5 MATERIALS AND METHODS

Drosophila melanogaster expressing Emerald GFP-tagged atrial natriuretic factor in neurons (*elav-Gal4 UAS-preproANF-EMD*) were used as previously described (Levitan et al., 2007; Rao et al., 2001a; Shakiryanova et al., 2006a). *elav-GAL4 UAS-preproANF-EMD; UAS-Kum170/CyO, Act-GFP* animals express the temperature-sensitive dominant negative SERCA Kum170 mutant in neurons (Sanyal et al., 2005; Shakiryanova et al., 2006a). SERCA was inactivated by incubating these animals in Ca²⁺-free HL3 saline (70 mM NaCl, 5 mM KCl, 20 mM MgCl₂, 115 mM sucrose, 5 mM trehalose, 5 mM HEPES, 10 mM NaHCO₃, 0.5 mM EGTA, pH 7.25) at 40°C for 8 minutes.

Female third instar wandering larvae were filleted in Ca²⁺-free HL3 saline. The ventral ganglion was severed to eliminate central input to the motor neurons that induces muscle

contraction. During live imaging and electrical stimulation, animals were bathed in HL3 saline (70 mM NaCl, 5 mM KCl, 1.5 mM CaCl₂, 20 mM MgCl₂, 115 mM sucrose, 5 mM trehalose, 5 mM HEPES, 10 mM NaHCO₃, pH 7.25) supplemented with 10 mM L-glutamate (HL3-Glut). L-glutamate was included to desensitize postsynaptic glutamate receptors and minimize muscle contraction during imaging experiments. Type Ib synaptic boutons located on muscles 6 and 7 in segments A3 to A6 were imaged using a cooled CCD camera on an upright wide-field epifluorescence microscope with 40× or 60× water-immersion objectives. Motor nerves were stimulated with suction electrodes at 70 Hz for 1 minute. Capture was calculated as the percent of recovery of peptide fluorescence four minutes after the cessation of stimulation normalized to release (i.e., the initial drop in fluorescence immediately after electrical stimulation).

Drugs were bath applied after dissection. Ryanodine (high purity, water soluble), KN-92 and KN-93 were obtained from Calbiochem, La Jolla, CA. KN-92 and thapsigargin (Alamone labs, Jerusalem, Israel) were dissolved in DMSO as stocks and subsequently diluted to yield a final concentration of 0.05% DMSO.

5.0 DISCUSSION

5.1 SUMMARY AND SIGNIFICANCE OF FINDINGS

Because protein synthesis and packaging machinery are not present at the nerve terminal, neuropeptides are made and packaged into dense core vesicles (DCVs) exclusively at the remote cell body. For this reason, accurate and timely delivery of DCVs from the cell body to the nerve terminal is crucial to constantly replenish released neuropeptides. At the same time, because neurons undergo repetitive firing, neuropeptide release at the nerve terminal must be tightly regulated to avoid storage depletion. Therefore, it is important to understand how neuropeptides are supplied and released at the nerve terminal at steady state to maintain nerve function.

Traditionally, it was believed that DCVs are delivered to the nerve terminal exclusively through anterograde fast axonal transport. However, it is now known that DCVs are continuously transiting bidirectionally along the axon and at resting nerve terminal. In addition, nerve terminals have very complex architecture. They are highly branched with release sites located in *en passant* boutons. It is unclear how DCVs can be delivered to these diverse sites evenly at the nerve terminal. Although DCV exocytosis and neuropeptide release have been extensively studied and much is known about the neuropeptide releasability, such studies were performed in endocrine cell cultures in which special polarized and differentiated features of neurons are absent. Therefore, the native mechanism used by DCVs to release neuropeptide at the synaptic

terminal was not known. For these reasons, it is essential to use a differentiated neuron system to further our understanding on DCV trafficking and exocytosis. In this thesis, GFP-tagged neuropeptides (Anf-GFP) were expressed and imaged *in vivo* at the fly larval NMJ to study DCV transport and exocytosis.

Chapter 2 examined how neuropeptides are delivered to the nerve terminal via bidirectional DCV transport. We first used inducible gene expression systems to pulse-label DCVs at the NMJ. It was found that newly synthesized DCVs preferentially accumulate at the most distal bouton. Next, FRAP was performed at terminals constitutively expressing Anf-GFP. DCVs were found to recover the fastest at the most distal bouton even under calcium-free conditions, suggesting that the DCV gradient seen was not due to differential release at proximal boutons. High-frequency timelapse imaging after photobleaching showed that most newly arrived anterograde DCVs bypass proximal boutons and accumulate at the most distal bouton, suggesting that DCVs are preferentially delivered to the most distal bouton. A novel optical technique called SPAIM was developed to track single DCV movement. In this experiment, a nerve terminal is first photobleached and allowed for recovery. Immediately after the first labeled DCV arrives at the nerve terminal, a second laser scanner is used to photobleach all the newcomers at the proximal end of the terminal while the main scanner continues to simultaneously image the movement of the first vesicle. Vesicle trajectories showed that DCVs take a complex journey (pausing, looping, direction reversal) to arrive at their destinations. They also revealed 3 classes of kinetic events upon arrival at a bouton. DCV may be visiting for a short time (residence time <2 min), captured for a prolonged period (≥ 2 min), or bypass the bouton (<5 s). Capture events were most frequent at the most distal bouton. These results suggest that the initially polarized accumulation of neuropeptide is caused by the sporadic proximal

capture of anterograde DCVs as they make their complex journey through the terminal. Disrupting retrograde transport by overexpression of dynactin mutant subunits caused accumulation of neuropeptides at the most distal boutons. These retrograde DCVs are also captured sporadically at proximal boutons, as shown from their SPAIM trajectories. The routes taken by these retrograde DCVs were also examined at the branch point of nerve terminals. Retrograde DCVs mostly return to the main axon and never enter neighboring branches for delivery. SPAIM experiments revealed that, upon entering the proximal axon, returning DCVs can reverse direction and reenter the axon, possibly for another round of delivery. Together, the study shows that neuropeptide delivery in nerve terminal release sites is mediated by sporadic anterograde and retrograde capture of DCVs circulating between the proximal axon and distal boutons

In Chapter 3, DCV exocytosis properties were examined at a single vesicle level in the fly NMJ using different SPAIM paradigms. It was found that DCVs that are 1) delivered from the anterograde or retrograde directions, 2) captured or just visited for a brief period, and 3) delivered to proximal or distal boutons are all capable of supporting release. Furthermore, labeled DCVs retained a significant fraction of fluorescence upon stimulation, indicating that neuropeptides are released incompletely and that kiss-and-run exocytosis predominates. In addition, neuropeptides are released very slowly (i.e., release may last for up to 30s), suggesting that diffusion of neuropeptides from DCVs may be limited by the size of the fusion pore during kiss-and-run exocytosis. By tracking the same DCVs for extended period while stimulating the nerve multiple times, it was found that partially emptied DCVs can undergo multiple rounds of exocytosis. Overall, the study suggests that neuropeptide stored at the terminal is utilized

progressively through partial release and local recycling of DCVs, thus minimizing the supply of newly synthesized DCVs from the remote cell body.

Chapter 4 examined the signaling pathway involved in activity-dependent capture of DCVs. By measuring intensity changes of GFP labeled DCVs at the NMJ bouton before and after electrical stimulation, the amounts of neuropeptide release and activity-dependent capture were determined. The CamKII inhibitor KN-93, but not its inactive analog KN-92, abolished the replenishment of neuropeptidergic DCVs in synaptic boutons after release. Furthermore, pharmacologically or genetically inhibiting neuronal SERCA pump to deplete presynaptic ER Ca^{2+} stores or directly inhibiting RyRs prevented the capture response. These results suggest that presynaptic RyR-CamKII pathway is shared by two different cellular processes to mobilize DCVs and capture transiting DCVs after activity.

The studies presented in the thesis demonstrate elegant mechanisms utilized by the neuron to maintain efficient neuropeptide secretion. By keeping a constant supply through bidirectional capture and minimizing the overuse of DCVs at the nerve terminal, the neuropeptide store is not depleted under repetitive firing. The circulation strategy used by DCVs to deliver neuropeptides explains why defects in retrograde transport may contribute to neurodegenerations. The work also developed a novel strategy to track single DCVs in nerve terminals for a prolonged period, which can be applied to study trafficking and dynamics of other organelles. Overall, this dissertation provides new insight into the macroscopic and biophysical properties of DCVs on trafficking and exocytosis at the nerve terminal. These will facilitate future research to identify molecular players for neuropeptide transmission and possible drug targets to combat related diseases.

5.2 EFFECTIVE SUPPLY OF NEUROPEPTIDES THROUGH A CELLULAR CONVEYOR SYSTEM

Considering that protein synthesis and motor driven transport are both energy-demanding processes, it is surprising that neuropeptide delivery operates by making and transporting excess DCVs to the most distal bouton first. Nevertheless, it may be the most optimal mechanism to distribute DCVs evenly to *en passant* boutons. Given that there is no known addressing system to target cargoes to a specific bouton along the dynamic terminal, DCVs may have been randomly distributed at each *en passant* bouton with equal probability. However, in this case, proximal boutons would always gain earliest access to anterograde DCVs and the most distal bouton would be loaded with fewer DCVs. Therefore, by constantly transporting excess DCVs to the most distal end, all proximal boutons are given an equal chance to encounter vesicles and capture some of them for storage. Excess DCVs accumulate at the most distal bouton can then be removed by retrograde transport and given another chance to explore proximal boutons for delivery. More importantly, this circulation strategy allows every bouton to be replenished upon activity-evoked exocytosis by capturing transiting DCVs (Shakiryanova et al., 2006a). Uncaptured DCVs, however, can return to the proximal axon, reverse direction and reenter the terminal again for another round of delivery. An analogy to this circulation route would be the conveyor system, which is widely used in industries as the most efficient and economical system to distribute products to diverse downstream processing units. Here, DCVs are analogous to products on a conveyor belt waiting to be removed somewhere along the line. In this system, production can be controlled by sampling the rate of product return. It is possible that a molecular sensor is present at the proximal axon to assess the returning DCV flux and adjust protein synthesis and degradation thereafter.

Sporadic capture may have other physiological significance. It is now known that vesicles that carry important active zone precursors, piccolo-bassoon transport vesicles (PTVs), share the same anterograde motor as DCVs, suggesting that active zone proteins and other synaptic proteins (Hall and Hedgecock, 1991; Jacob and Kaplan, 2003; Okada et al., 1995) in addition to neuropeptides, are also delivered to *en passant* boutons using the same strategy (Goldstein et al., 2008; Pack-Chung et al., 2007b). Our data also suggest that the most distal bouton, which plays distinct roles in neurotransmission and neurodevelopment, is allowed to access newer/younger protein first. Despite the even distribution of the active zone protein (Bruchpilot, Brp) in the fly NMJ (Kittel et al., 2006; Wagh et al., 2006), several studies have shown that synaptic strength changes across *en passant* boutons. As measured by Ca^{2+} influx at the post-synapse, a steep gradient of synaptic strength was seen across *en passant* bouton, with the most distal bouton having the strongest presynaptic release (Guerrero et al., 2005). The single action potential Ca^{2+} transient also decreases from the distal to the proximal bouton (Lnenicka et al., 2006). It is also known that the most distal bouton is more dynamic and plastic (Dent et al., 1999; Hummel et al., 2000; Roos et al., 2000).

5.3 CONSERVED NEUROPEPTIDE USE VIA PROGRESSIVE KISS-AND-RUN EXOCYTOSIS

Kiss-and-run is the exclusive mode of exocytosis for newly arrived DCVs at the fly NMJ. This is in strong agreement with previous findings based on endocrine and neuronal cultures as the model system (Ceridono et al., 2011; Ferraro et al., 2005; Xia et al., 2009). In fact, kiss-and-run is a more desirable mode of exocytosis for DCV for many reasons. First, the progressive release

will prevent the depletion of DCVs under repetitive firing of the neuron, as the supply of DCV is limited by the synthesis and delivery from the soma. The ability of DCVs to undergo multiple rounds of exocytosis allows local recycling of resources, thus minimizing the demand of DCV supply. Secondly, it provides an additional strategy for the nerve terminal to regulate amount of neuropeptide release locally. Unlike SSVs, in which quantal content is determined locally through the regulation of vesicular transporters and quantal size can be controlled instantly at the nerve terminal. For DCVs, neuropeptide content is determined by expression levels and packaging efficiency at the site of synthesis in the soma. In this case, quantal size is regulated at a remote site with a long time delay. One may argue that neuropeptides can be packaged in more vesicles of smaller quantal size and so release can be regulated by quantal contents. However, this is an undesirable strategy because many more cellular resources will be needed to sort and deliver neuropeptides. Therefore, by utilizing kiss-and-run exocytosis, DCVs can control the amount of neuropeptide release by regulating other parameters locally, such as size of the fusion pore and duration of the open state. Lastly, the fusion pore in kiss-and-run can also serve as a size-dependent filter to select the type neurotransmitters (e.g. neuropeptides versus classical neurotransmitters) to be released (Fulop et al., 2005).

5.4 POTENTIAL MECHANISM FOR CONSTITUTIVE AND ACTIVITY-DEPENDENT CAPTURE

Although the current study does not identify any molecular players mediating preferential transport, some speculation on the underlying mechanism can be made based on the structural organization of synaptic boutons. Because microtubule tracks in fly NMJ mostly extend to the

most distal bouton (Conde and Caceres, 2009), it is likely that DCVs are constitutively transported anterogradely by kinesin until they reach the end of microtubules and fall off. Interestingly, it is now known that the retrograde adaptor protein p150^{Glued}, which is also required for retrograde transport initiation at the microtubule plus-end (Vaughan et al., 2002), is localized most abundantly at the most distal bouton of fly NMJ (personal communication with *Lloyd. T et al*). Therefore the most distal bouton may serve as a hot spot for DCVs to be equipped with retrograde motor and reverse direction, facilitating vesicle circulation. It is tempting to think that dynamic microtubule plus-ends, which are responsible for the “search-and-capture” retrograde transport initiation (Mimori-Kiyosue and Tsukita, 2003), are also more abundant at the most distal bouton. Nevertheless, by expressing the RFP-tagged microtubule plus-end binding protein (EB1-RFP) to examine the dynamic behavior of microtubule plus-ends (Mattie et al., 2010) (Figure A1, Movie S 8), it was found that dynamic plus-ends are evenly distributed across *en passant* boutons. These results may argue that in the nerve terminal, the search-and-capture mechanism is critical for retrograde transport.

RyR-CamKII mediated activity-dependent capture was found to capture retrograde DCVs from the transiting pool (Shakiryanova et al., 2006). Apparently, such capture involves the unloading of retrograde DCVs from the microtubule track, either by disrupting the motor-microtubule, or motor-vesicle interactions. Increasing evidence has shown that CamKII is involved in the regulation of motor-cargo interactions. At the post-synaptic density, CamKII phosphorylates the kinesin superfamily protein 17 (KIF17) and induces the dissociation of Mint1, a scaffolding protein complex, from NMDA receptor-containing cargoes (Guillaud et al., 2008). CamKII also acts as a molecular switch to inhibit the interaction between myosin V and melanosomes in *Xenopus* melanophores through the phosphorylation of the myosin tail (Karcher

et al., 2001). Although myosin V has long been known to be an actin-based motor that also participates in short-range transport, a few studies have shown that myosin V is involved in the retrograde transport of DCVs and tetanus toxin-containing vesicles (Bittins et al., 2010; Lalli et al., 2003). The activity of KIF1A, the anterograde motor involved in DCV trafficking, may also be regulated by CamKII. A study has shown that CamKII phosphorylates the KIF1A/cargo adaptor protein, Liprin α . This causes the degradation of Liprin α through the ubiquitin-proteasome system, and the dissociation of KIF1A from the cargo, leukocyte common antigen-related (LAR) family receptor protein tyrosine phosphatases (Dunah et al., 2005; Hoogenraad et al., 2007; Shin et al., 2003). Although activity-dependent capture involves the unloading of retrograde transiting DCVs, and KIF1A is an anterograde motor, many lines of evidence suggest that KIF1A cooperates with dynein to coordinate bidirectional transport such that perturbing anterograde motors disrupts retrograde transport (Barkus et al., 2008; Lo et al., 2011). Therefore, it is possible that the phosphorylation of Liprin α by CamKII plays a role in unloading the retrograde DCV from kinesin motors.

Interestingly, the same signaling pathway is shared with another axonal transport-independent activity-dependent process, vesicle mobilization, which is more acute (~10 mins). This suggests to that CamKII may initiate vesicle mobilization by phosphorylating an independent substrate. Alternatively, the rate of dephosphorylation of CamKII substrates for capture and mobilization may be different. Regardless of the specific basis for the diverse time courses of mobilization and capture, the use of the same signaling pathway to induce both of these effects is an elegant means to ensure that facilitation of release is coupled to replacement of depleted synaptic neuropeptide stores.

5.5 SIGNIFICANCE OF THE STUDY

5.5.1 New insight into neurodegenerative diseases

Conventional models suggest that impaired retrograde transport leads to misaccumulation of toxic materials at the periphery (Chevalier-Larsen and Holzbaaur, 2006), and perturbs retrograde long-distance signaling from the nerve terminal (Ilieva et al., 2009; Perlson et al., 2009), which further induces loss of synaptic function and finally cell death. This study suggests that defective retrograde transport also affects delivery of neuropeptides, which may contribute to the development of neurodegeneration. Thus far, studies regarding microtubule-based transport have mainly been focused on measuring the flux, velocity and pause-time of different cargoes along the axon (Bilsland et al., 2010) but not at the terminal, where loading and unloading of cargoes mainly takes place. Here, by understanding the trafficking pattern of DCV along *en passant* boutons, our study also provides new insight into how disrupted microtubule-based transport affects neuronal function at the subsynaptic level, which will eventually be helpful in understanding how molecular motors function.

5.5.2 Technology Advancement

The use of SPAIM has facilitated several important novel observations in native synapses. These include: 1) tracking single DCV movement; 2) measurement of DCV flux in a single direction in spite of their bidirectional movement; and 3) monitoring single DCV exocytosis at the terminal. Unlike the use of conventional TIRF, SPAIM allows DCVs to be tracked on different focal planes. Another advantage of SPAIM tracking is that experiments can be repeated simply by

rebleaching the same terminal and waiting for the next DCV to enter the region of interest, thus allowing pair-wise comparisons on the trajectory, mobility, and exocytosis properties of different vesicle from the same terminal. SPAIM also overcomes the difficulties associated with the use of photoactivatable proteins, which are usually more pH sensitive, dimmer and require critical environmental conditions for photoactivation. In principle, the technique can also be applied to other fluorescent organelles, such as receptor-carrying vesicles, mitochondria, and lysosomes to study traffic in diverse polarized cell structures.

5.6 FUTURE DIRECTIONS

More experiments will be needed to further characterize the properties of neuropeptide release. Release should be measured upon multiple rounds of short-duration (5 s) stimulation with longer recovery period. This set of experiment should better resolve the time course of peptide release between stimulations. We are also interested to see if DCVs can eventually be emptied after multiple rounds of stimulation. To further examine the role of dynamin and kiss-and-run exocytosis of DCVs, Dyngo-4a, a dynasore analogue with higher affinity to dynamin I, could be used to inhibit dynamin activity. Alternatively, a temperature sensitive dynamin mutant, *shibire*, can be used.

Although the *in vivo* imaging technique applied in our studies is very powerful and has allowed many novel observations of DCV trafficking, there are limitations of the current technique. First, all the imaging experiments were based on ectopic overexpression of exogenous neuropeptides in motoneurons that do not normally release large amount of neuropeptide. Although we were able to show that the DCV circulation strategy is utilized by neurons to

deliver the native neuropeptide proctolin (Figure 9), suggesting that the trafficking mechanism reported is not an artifact from the neuropeptide overexpression, findings from the neuropeptide release studies may be artificial because the amount of neuropeptide in each DCV may be higher than the endogenous level. To understand the native release mechanism, a valuable approach could be to use an inducible-gene expression system to limit the neuropeptide expression level. Alternatively, it may be desirable to knock-in a GFP-tagged native fly neuropeptide that is expressed endogenously in the type III peptidergic neuron.

With the new SPAIM technique, we can look further into the DCV transport properties within a bouton, such as activity-dependent vesicle mobilization. In addition, the delivery pattern of other organelles and vesicle cargoes, such as mitochondria, active zones and receptor molecules, can also be studied. Further work needs to be done to elucidate local traffick properties. For example, how do acute changes in the morphology of branches and *en passant* boutons affect DCV transport? This can be studied by ablating specific neuronal regions with the use of a two-photon laser. Since the work presented in this thesis focuses only on the biophysical and macroscopic properties of DCV trafficking and exocytosis, follow-up studies to identify signaling pathways and proteins that are involved in these processes will also be of great importance.

APPENDIX A

SUPPLEMENTAL INFORMATION

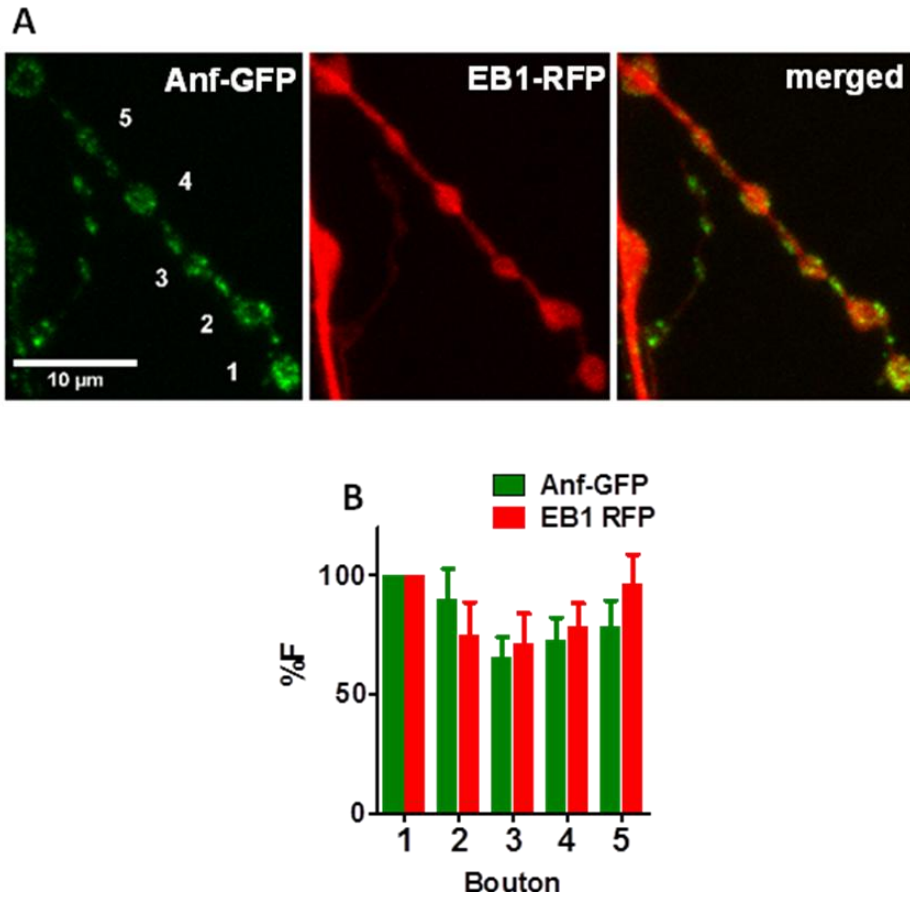


Figure A1 Localization of EB1 across en passant boutons

A. Representative Z-stack images of a terminal co-expressed with EB1-RFP and Anf-GFP. *En passant* boutons are numbered from the most distal (#1) to proximal. **B.** Quantification of fluorescence relative to the most distal bouton (%F) (n=7). Error bars represent S.E.M.

Movie S1. FRAP experiment showing preferential traffic to the distal bouton. Timestamp shows time after photobleaching in minutes and seconds. Scale bar, 2.5 μm .

Movie S2. SPAIM experiment showing complex DCV movement to the distal bouton. Scale bar, 5 μm .

Movie S3. SPAIM experiment showing DCV efflux from the distal bouton. Scale bar, 5 μm .

Movie S4. SPAIM experiment showing DCV efflux from a proximal bouton. Scale bar, 5 μm .

Movie S5. SPAIM experiment showing retrograde flux at a branch point. Scale bar, 5 μm .

Movie S6. SPAIM experiment showing DCV flux at a proximal axon. Top, SPAIM experiment showing lack of generation of nascent DCVs following photobleaching of the soma and the AIS. Bottom, subsequently the preparation was photobleached and imaged without photobleaching retrograde newcomers. Note the accumulation and reversal of DCVs in the AIS.

Movie S7. SPAIM experiment showing the arrival and reversal of a retrograde DCV in the boxed region of the AIS.

Movie S 8. Microtubule plus-end dynamic across en passant boutons.

BIBLIOGRAPHY

Agnati, L.F., Zoli, M., Stromberg, I., and Fuxe, K. (1995). Intercellular communication in the brain: wiring versus volume transmission. *Neuroscience* 69, 711-726.

Ahmari, S.E., Buchanan, J., and Smith, S.J. (2000). Assembly of presynaptic active zones from cytoplasmic transport packets. *Nature neuroscience* 3, 445-451.

Ales, E., Tabares, L., Poyato, J.M., Valero, V., Lindau, M., and Alvarez de Toledo, G. (1999). High calcium concentrations shift the mode of exocytosis to the kiss-and-run mechanism. *Nat Cell Biol* 1, 40-44.

Allen, M.J., Shan, X., Caruccio, P., Froggett, S.J., Moffat, K.G., and Murphey, R.K. (1999). Targeted expression of truncated glued disrupts giant fiber synapse formation in *Drosophila*. *The Journal of neuroscience : the official journal of the Society for Neuroscience* 19, 9374-9384.

Alonso, G., and Assenmacher, I. (1983). Retrograde axoplasmic transport of neurosecretory material. An immunocytochemical and electron-microscopic study of transected axons in normal and colchicine-treated rats. *Cell Tissue Res* 233, 183-196.

Anderson, M.S., Halpern, M.E., and Keshishian, H. (1988a). Identification of the neuropeptide transmitter proctolin in *Drosophila* larvae: characterization of muscle fiber-specific neuromuscular endings. *The Journal of neuroscience : the official journal of the Society for Neuroscience* 8, 242-255.

Anderson, M.S., Halpern, M.E., and Keshishian, H. (1988b). Identification of the neuropeptide transmitter proctolin in *Drosophila* larvae: characterization of muscle fiber-specific neuromuscular endings. *J Neurosci* 8, 242-255.

Aoki, R., Kitaguchi, T., Oya, M., Yanagihara, Y., Sato, M., Miyawaki, A., and Tsuboi, T. (2010). Duration of fusion pore opening and the amount of hormone released are regulated by myosin II during kiss-and-run exocytosis. *Biochem J* 429, 497-504.

Artalejo, C.R., Henley, J.R., McNiven, M.A., and Palfrey, H.C. (1995). Rapid endocytosis coupled to exocytosis in adrenal chromaffin cells involves Ca²⁺, GTP, and dynamin but not clathrin. *Proc Natl Acad Sci U S A* 92, 8328-8332.

Ataman, B., Ashley, J., Gorczyca, M., Ramachandran, P., Fouquet, W., Sigrist, S.J., and Budnik, V. (2008). Rapid activity-dependent modifications in synaptic structure and function require bidirectional Wnt signaling. *Neuron* 57, 705-718.

Atwood, H.L., Govind, C.K., and Wu, C.F. (1993). Differential ultrastructure of synaptic terminals on ventral longitudinal abdominal muscles in *Drosophila* larvae. *J Neurobiol* 24, 1008-1024.

- Barg, S., Olofsson, C.S., Schriever-Abeln, J., Wendt, A., Gebre-Medhin, S., Renstrom, E., and Rorsman, P. (2002). Delay between fusion pore opening and peptide release from large dense-core vesicles in neuroendocrine cells. *Neuron* 33, 287-299.
- Barkus, R.V., Klyachko, O., Horiuchi, D., Dickson, B.J., and Saxton, W.M. (2008). Identification of an axonal kinesin-3 motor for fast anterograde vesicle transport that facilitates retrograde transport of neuropeptides. *Mol Biol Cell* 19, 274-283.
- Berberian, K., Torres, A.J., Fang, Q., Kisler, K., and Lindau, M. (2009). F-actin and myosin II accelerate catecholamine release from chromaffin granules. *J Neurosci* 29, 863-870.
- Bilsland, L.G., Sahai, E., Kelly, G., Golding, M., Greensmith, L., and Schiavo, G. (2010). Deficits in axonal transport precede ALS symptoms in vivo. *Proc Natl Acad Sci U S A* 107, 20523-20528.
- Bittins, C.M., Eichler, T.W., Hammer, J.A., 3rd, and Gerdes, H.H. (2010). Dominant-negative myosin Va impairs retrograde but not anterograde axonal transport of large dense core vesicles. *Cell Mol Neurobiol* 30, 369-379.
- Bodmer, R., and Jan, Y.N. (1987). Morphological differentiation of the embryonic peripheral neurons in *Drosophila*. *Roux's Arch Dev Biol* 196, 69-77.
- Brauckmann, S. (2004). The virtue of being too early: Paul A. Weiss and 'axonal transport'. *Hist Philos Life Sci* 26, 333-353.
- Brent, J.R., Werner, K.M., and McCabe, B.D. (2009). *Drosophila* larval NMJ dissection. *J Vis Exp*.
- Brigadski, T., Hartmann, M., and Lessmann, V. (2005). Differential vesicular targeting and time course of synaptic secretion of the mammalian neurotrophins. *J Neurosci* 25, 7601-7614.
- Burkhardt, J.K., Echeverri, C.J., Nilsson, T., and Vallee, R.B. (1997). Overexpression of the dynamitin (p50) subunit of the dynactin complex disrupts dynein-dependent maintenance of membrane organelle distribution. *J Cell Biol* 139, 469-484.
- Cauli, B., Tong, X.K., Rancillac, A., Serluca, N., Lambolez, B., Rossier, J., and Hamel, E. (2004). Cortical GABA interneurons in neurovascular coupling: relays for subcortical vasoactive pathways. *J Neurosci* 24, 8940-8949.
- Ceccarelli, B., Hurlbut, W.P., and Mauro, A. (1973). Turnover of transmitter and synaptic vesicles at the frog neuromuscular junction. *J Cell Biol* 57, 499-524.
- Ceridono, M., Ory, S., Momboisse, F., Chasserot-Golaz, S., Houy, S., Calco, V., Haeberle, A.M., Demais, V., Bailly, Y., Bader, M.F., *et al.* (2011). Selective recapture of secretory granule components after full collapse exocytosis in neuroendocrine chromaffin cells. *Traffic* 12, 72-88.
- Chan, S.A., Doreian, B., and Smith, C. (2010). Dynamin and myosin regulate differential exocytosis from mouse adrenal chromaffin cells. *Cell Mol Neurobiol* 30, 1351-1357.

- Chen, M.S., Obar, R.A., Schroeder, C.C., Austin, T.W., Poodry, C.A., Wadsworth, S.C., and Vallee, R.B. (1991). Multiple forms of dynamin are encoded by shibire, a *Drosophila* gene involved in endocytosis. *Nature* *351*, 583-586.
- Chen, X.J., Levedakou, E.N., Millen, K.J., Wollmann, R.L., Soliven, B., and Popko, B. (2007). Proprioceptive sensory neuropathy in mice with a mutation in the cytoplasmic Dynein heavy chain 1 gene. *J Neurosci* *27*, 14515-14524.
- Chevalier-Larsen, E., and Holzbaur, E.L. (2006). Axonal transport and neurodegenerative disease. *Biochim Biophys Acta* *1762*, 1094-1108.
- Chow, R.H., von Ruden, L., and Neher, E. (1992). Delay in vesicle fusion revealed by electrochemical monitoring of single secretory events in adrenal chromaffin cells. *Nature* *356*, 60-63.
- Conde, C., and Caceres, A. (2009). Microtubule assembly, organization and dynamics in axons and dendrites. *Nat Rev Neurosci* *10*, 319-332.
- Cousin, M.A., Tan, T.C., and Robinson, P.J. (2001). Protein phosphorylation is required for endocytosis in nerve terminals: potential role for the dephosphins dynamin I and synaptojanin, but not AP180 or amphiphysin. *J Neurochem* *76*, 105-116.
- Dahlstrom, A.B. (2010). Fast intra-axonal transport: Beginning, development and post-genome advances. *Prog Neurobiol* *90*, 119-145.
- Degtyar, V.E., Allersma, M.W., Axelrod, D., and Holz, R.W. (2007). Increased motion and travel, rather than stable docking, characterize the last moments before secretory granule fusion. *Proc Natl Acad Sci U S A* *104*, 15929-15934.
- Dent, E.W., Callaway, J.L., Szebenyi, G., Baas, P.W., and Kalil, K. (1999). Reorganization and movement of microtubules in axonal growth cones and developing interstitial branches. *J Neurosci* *19*, 8894-8908.
- Duffy, J.B. (2002). GAL4 system in *Drosophila*: a fly geneticist's Swiss army knife. *Genesis* *34*, 1-15.
- Dunah, A.W., Hueske, E., Wyszynski, M., Hoogenraad, C.C., Jaworski, J., Pak, D.T., Simonetta, A., Liu, G., and Sheng, M. (2005). LAR receptor protein tyrosine phosphatases in the development and maintenance of excitatory synapses. *Nat Neurosci* *8*, 458-467.
- Duncan, R.R., Greaves, J., Wiegand, U.K., Matskevich, I., Bodammer, G., Apps, D.K., Shipston, M.J., and Chow, R.H. (2003). Functional and spatial segregation of secretory vesicle pools according to vesicle age. *Nature* *422*, 176-180.
- Eichler, T.W., Kogel, T., Bukoreshtliev, N.V., and Gerdes, H.H. (2006). The role of myosin Va in secretory granule trafficking and exocytosis. *Biochem Soc Trans* *34*, 671-674.

- Elhamdani, A., Azizi, F., and Artalejo, C.R. (2006). Double patch clamp reveals that transient fusion (kiss-and-run) is a major mechanism of secretion in calf adrenal chromaffin cells: high calcium shifts the mechanism from kiss-and-run to complete fusion. *J Neurosci* 26, 3030-3036.
- Farrer, M.J., Hulihan, M.M., Kachergus, J.M., Dachsel, J.C., Stoessl, A.J., Grantier, L.L., Calne, S., Calne, D.B., Lechevalier, B., Chapon, F., *et al.* (2009). DCTN1 mutations in Perry syndrome. *Nat Genet* 41, 163-165.
- Felmy, F. (2007). Modulation of cargo release from dense core granules by size and actin network. *Traffic* 8, 983-997.
- Ferraro, F., Eipper, B.A., and Mains, R.E. (2005). Retrieval and reuse of pituitary secretory granule proteins. *The Journal of biological chemistry* 280, 25424-25435.
- Fesce, R., Grohovaz, F., Valtorta, F., and Meldolesi, J. (1994). Neurotransmitter release: fusion or 'kiss-and-run'? *Trends Cell Biol* 4, 1-4.
- Frischknecht, R., Fejtova, A., Viesti, M., Stephan, A., and Sonderegger, P. (2008). Activity-induced synaptic capture and exocytosis of the neuronal serine protease neurotrypsin. *The Journal of neuroscience : the official journal of the Society for Neuroscience* 28, 1568-1579.
- Fulop, T., Radabaugh, S., and Smith, C. (2005). Activity-dependent differential transmitter release in mouse adrenal chromaffin cells. *J Neurosci* 25, 7324-7332.
- Fulop, T., and Smith, C. (2006). Physiological stimulation regulates the exocytic mode through calcium activation of protein kinase C in mouse chromaffin cells. *Biochem J* 399, 111-119.
- Ghijssen, W.E., and Leenders, A.G. (2005). Differential signaling in presynaptic neurotransmitter release. *Cell Mol Life Sci* 62, 937-954.
- Goldstein, A.Y., Wang, X., and Schwarz, T.L. (2008). Axonal transport and the delivery of pre-synaptic components. *Curr Opin Neurobiol* 18, 495-503.
- Goldstein, L.S., and Yang, Z. (2000). Microtubule-based transport systems in neurons: the roles of kinesins and dyneins. *Annu Rev Neurosci* 23, 39-71.
- Gorczyca, M., Augart, C., and Budnik, V. (1993). Insulin-like receptor and insulin-like peptide are localized at neuromuscular junctions in *Drosophila*. *J Neurosci* 13, 3692-3704.
- Guerrero, G., Reiff, D.F., Agarwal, G., Ball, R.W., Borst, A., Goodman, C.S., and Isacoff, E.Y. (2005). Heterogeneity in synaptic transmission along a *Drosophila* larval motor axon. *Nat Neurosci* 8, 1188-1196.
- Guillaud, L., Wong, R., and Hirokawa, N. (2008). Disruption of KIF17-Mint1 interaction by CaMKII-dependent phosphorylation: a molecular model of kinesin-cargo release. *Nature cell biology* 10, 19-29.

- Hafezparast, M., Klocke, R., Ruhrberg, C., Marquardt, A., Ahmad-Annuar, A., Bowen, S., Lalli, G., Witherden, A.S., Hummerich, H., Nicholson, S., *et al.* (2003). Mutations in dynein link motor neuron degeneration to defects in retrograde transport. *Science* *300*, 808-812.
- Haghnia, M., Cavalli, V., Shah, S.B., Schimmelpfeng, K., Bruschi, R., Yang, G., Herrera, C., Pilling, A., and Goldstein, L.S. (2007). Dynactin is required for coordinated bidirectional motility, but not for dynein membrane attachment. *Mol Biol Cell* *18*, 2081-2089.
- Hall, D.H., and Hedgecock, E.M. (1991). Kinesin-related gene *unc-104* is required for axonal transport of synaptic vesicles in *C. elegans*. *Cell* *65*, 837-847.
- Han, W., Ng, Y.K., Axelrod, D., and Levitan, E.S. (1999). Neuropeptide release by efficient recruitment of diffusing cytoplasmic secretory vesicles. *Proc Natl Acad Sci U S A* *96*, 14577-14582.
- Harper, C.B., Martin, S., Nguyen, T.H., Daniels, S.J., Lavidis, N.A., Popoff, M.R., Hadzic, G., Mariana, A., Chau, N., McCluskey, A., *et al.* (2011). Dynamin inhibition blocks botulinum neurotoxin type A endocytosis in neurons and delays botulism. *J Biol Chem* *286*, 35966-35976.
- Heifetz, Y., and Wolfner, M.F. (2004). Mating, seminal fluid components, and sperm cause changes in vesicle release in the *Drosophila* female reproductive tract. *Proc Natl Acad Sci U S A* *101*, 6261-6266.
- Heuser, J.E., and Reese, T.S. (1973). Evidence for recycling of synaptic vesicle membrane during transmitter release at the frog neuromuscular junction. *J Cell Biol* *57*, 315-344.
- Hollenbeck, P.J., and Saxton, W.M. (2005). The axonal transport of mitochondria. *J Cell Sci* *118*, 5411-5419.
- Hoogenraad, C.C., Feliu-Mojer, M.I., Spangler, S.A., Milstein, A.D., Dunah, A.W., Hung, A.Y., and Sheng, M. (2007). Liprin- α degradation by calcium/calmodulin-dependent protein kinase II regulates LAR receptor tyrosine phosphatase distribution and dendrite development. *Dev Cell* *12*, 587-602.
- Hsu, C.C., Moncaleano, J.D., and Wagner, O.I. (2011). Sub-cellular distribution of UNC-104(KIF1A) upon binding to adaptors as UNC-16(JIP3), DNC-1(DCTN1/Glued) and SYD-2(Liprin- α) in *C. elegans* neurons. *Neuroscience* *176*, 39-52.
- Huang, J.D., Brady, S.T., Richards, B.W., Stenolen, D., Resau, J.H., Copeland, N.G., and Jenkins, N.A. (1999). Direct interaction of microtubule- and actin-based transport motors. *Nature* *397*, 267-270.
- Hummel, T., Krukkert, K., Roos, J., Davis, G., and Klambt, C. (2000). *Drosophila* Futsch/22C10 is a MAP1B-like protein required for dendritic and axonal development. *Neuron* *26*, 357-370.
- Husain, Q.M., and Ewer, J. (2004). Use of targetable GFP-tagged neuropeptide for visualizing neuropeptide release following execution of a behavior. *J Neurobiol* *59*, 181-191.

- Ilieva, H., Polymenidou, M., and Cleveland, D.W. (2009). Non-cell autonomous toxicity in neurodegenerative disorders: ALS and beyond. *J Cell Biol* 187, 761-772.
- Imlach, W., and McCabe, B.D. (2009). Electrophysiological methods for recording synaptic potentials from the NMJ of *Drosophila* larvae. *J Vis Exp*.
- Inagami, T. (1989). Atrial natriuretic factor. *J Biol Chem* 264, 3043-3046.
- Jacob, T.C., and Kaplan, J.M. (2003). The EGL-21 carboxypeptidase E facilitates acetylcholine release at *Caenorhabditis elegans* neuromuscular junctions. *J Neurosci* 23, 2122-2130.
- Jia, X.X., Gorczyca, M., and Budnik, V. (1993). Ultrastructure of neuromuscular junctions in *Drosophila*: comparison of wild type and mutants with increased excitability. *J Neurobiol* 24, 1025-1044.
- Kanno, T., Ma, X., Barg, S., Eliasson, L., Galvanovskis, J., Gopel, S., Larsson, M., Renstrom, E., and Rorsman, P. (2004). Large dense-core vesicle exocytosis in pancreatic beta-cells monitored by capacitance measurements. *Methods* 33, 302-311.
- Karcher, R.L., Roland, J.T., Zappacosta, F., Huddleston, M.J., Annan, R.S., Carr, S.A., and Gelfand, V.I. (2001). Cell cycle regulation of myosin-V by calcium/calmodulin-dependent protein kinase II. *Science* 293, 1317-1320.
- Kirchhausen, T., Macia, E., and Pelish, H.E. (2008). Use of dynasore, the small molecule inhibitor of dynamin, in the regulation of endocytosis. *Methods Enzymol* 438, 77-93.
- Kitamoto, T. (2001). Conditional modification of behavior in *Drosophila* by targeted expression of a temperature-sensitive shibire allele in defined neurons. *J Neurobiol* 47, 81-92.
- Kittel, R.J., Wichmann, C., Rasse, T.M., Fouquet, W., Schmidt, M., Schmid, A., Wagh, D.A., Pawlu, C., Kellner, R.R., Willig, K.I., *et al.* (2006). Bruchpilot promotes active zone assembly, Ca²⁺ channel clustering, and vesicle release. *Science* 312, 1051-1054.
- Kole, M.H., Ilschner, S.U., Kampa, B.M., Williams, S.R., Ruben, P.C., and Stuart, G.J. (2008). Action potential generation requires a high sodium channel density in the axon initial segment. *Nat Neurosci* 11, 178-186.
- Koushika, S.P., Schaefer, A.M., Vincent, R., Willis, J.H., Bowerman, B., and Nonet, M.L. (2004). Mutations in *Caenorhabditis elegans* cytoplasmic dynein components reveal specificity of neuronal retrograde cargo. *J Neurosci* 24, 3907-3916.
- Kula, E., Levitan, E.S., Pyza, E., and Rosbash, M. (2006). PDF cycling in the dorsal protocerebrum of the *Drosophila* brain is not necessary for circadian clock function. *J Biol Rhythms* 21, 104-117.
- Kwintner, D.M., Lo, K., Mafi, P., and Silverman, M.A. (2009). Dynactin regulates bidirectional transport of dense-core vesicles in the axon and dendrites of cultured hippocampal neurons. *Neuroscience* 162, 1001-1010.

- Lalli, G., Gschmeissner, S., and Schiavo, G. (2003). Myosin Va and microtubule-based motors are required for fast axonal retrograde transport of tetanus toxin in motor neurons. *J Cell Sci* 116, 4639-4650.
- LaMonte, B.H., Wallace, K.E., Holloway, B.A., Shelly, S.S., Ascano, J., Tokito, M., Van Winkle, T., Howland, D.S., and Holzbaur, E.L. (2002). Disruption of dynein/dynactin inhibits axonal transport in motor neurons causing late-onset progressive degeneration. *Neuron* 34, 715-727.
- Landgraf, M., Sanchez-Soriano, N., Technau, G.M., Urban, J., and Prokop, A. (2003). Charting the *Drosophila* neuropile: a strategy for the standardised characterisation of genetically amenable neurites. *Dev Biol* 260, 207-225.
- Landgraf, R., and Neumann, I.D. (2004). Vasopressin and oxytocin release within the brain: a dynamic concept of multiple and variable modes of neuropeptide communication. *Front Neuroendocrinol* 25, 150-176.
- Levitani, E.S., Lanni, F., and Shakiryanova, D. (2007). In vivo imaging of vesicle motion and release at the *Drosophila* neuromuscular junction. *Nature protocols* 2, 1117-1125.
- Li, J.Y., and Dahlstrom, A. (2007). Axonal transport of neuropeptides: Retrograde tracing study in live cell cultures of rat sympathetic cervical ganglia. *J Neurosci Res* 85, 2538-2545.
- Llobet, A., Wu, M., and Lagnado, L. (2008). The mouth of a dense-core vesicle opens and closes in a concerted action regulated by calcium and amphiphysin. *J Cell Biol* 182, 1017-1028.
- Lnenicka, G.A., Grizzaffi, J., Lee, B., and Rumpal, N. (2006). Ca²⁺ dynamics along identified synaptic terminals in *Drosophila* larvae. *J Neurosci* 26, 12283-12293.
- Lo, K.Y., Kuzmin, A., Unger, S.M., Petersen, J.D., and Silverman, M.A. (2011). KIF1A is the primary anterograde motor protein required for the axonal transport of dense-core vesicles in cultured hippocampal neurons. *Neurosci Lett* 491, 168-173.
- Loveall, B.J., and Deitcher, D.L. (2010). The essential role of bursicon during *Drosophila* development. *BMC Dev Biol* 10, 92.
- Lukyanov, K.A., Chudakov, D.M., Lukyanov, S., and Verkhusha, V.V. (2005). Innovation: Photoactivatable fluorescent proteins. *Nat Rev Mol Cell Biol* 6, 885-891.
- MacDonald, P.E., and Rorsman, P. (2007). The ins and outs of secretion from pancreatic beta-cells: control of single-vesicle exo- and endocytosis. *Physiology (Bethesda)* 22, 113-121.
- MacGregor, R.R., Hamilton, J.W., and Cohn, D.V. (1975). The by-pass of tissue hormone stores during the secretion of newly synthesized parathyroid hormone. *Endocrinology* 97, 178-188.
- Macia, E., Ehrlich, M., Massol, R., Boucrot, E., Brunner, C., and Kirchhausen, T. (2006). Dynasore, a cell-permeable inhibitor of dynamin. *Dev Cell* 10, 839-850.

- Martin, T.F. (2003). Tuning exocytosis for speed: fast and slow modes. *Biochim Biophys Acta* 1641, 157-165.
- Mattie, F.J., Stackpole, M.M., Stone, M.C., Clippard, J.R., Rudnick, D.A., Qiu, Y., Tao, J., Allender, D.L., Parmar, M., and Rolls, M.M. (2010). Directed microtubule growth, +TIPs, and kinesin-2 are required for uniform microtubule polarity in dendrites. *Curr Biol* 20, 2169-2177.
- McGuire, S.E., Roman, G., and Davis, R.L. (2004). Gene expression systems in *Drosophila*: a synthesis of time and space. *Trends Genet* 20, 384-391.
- Melkonian, K.A., Maier, K.C., Godfrey, J.E., Rodgers, M., and Schroer, T.A. (2007). Mechanism of dynamitin-mediated disruption of dynactin. *J Biol Chem* 282, 19355-19364.
- Michael, D.J., Cai, H., Xiong, W., Ouyang, J., and Chow, R.H. (2006). Mechanisms of peptide hormone secretion. *Trends Endocrinol Metab* 17, 408-415.
- Miller, K.E., DeProto, J., Kaufmann, N., Patel, B.N., Duckworth, A., and Van Vactor, D. (2005). Direct observation demonstrates that Liprin-alpha is required for trafficking of synaptic vesicles. *Curr Biol* 15, 684-689.
- Mimori-Kiyosue, Y., and Tsukita, S. (2003). "Search-and-capture" of microtubules through plus-end-binding proteins (+TIPs). *J Biochem* 134, 321-326.
- Morfini, G.A., Burns, M., Binder, L.I., Kanaan, N.M., LaPointe, N., Bosco, D.A., Brown, R.H., Jr., Brown, H., Tiwari, A., Hayward, L., *et al.* (2009). Axonal transport defects in neurodegenerative diseases. *J Neurosci* 29, 12776-12786.
- Munch, C., Sedlmeier, R., Meyer, T., Homberg, V., Sperfeld, A.D., Kurt, A., Prudlo, J., Peraus, G., Hanemann, C.O., Stumm, G., *et al.* (2004). Point mutations of the p150 subunit of dynactin (DCTN1) gene in ALS. *Neurology* 63, 724-726.
- Neco, P., Fernandez-Peruchena, C., Navas, S., Gutierrez, L.M., de Toledo, G.A., and Ales, E. (2008). Myosin II contributes to fusion pore expansion during exocytosis. *J Biol Chem* 283, 10949-10957.
- Neher, E., and Marty, A. (1982). Discrete changes of cell membrane capacitance observed under conditions of enhanced secretion in bovine adrenal chromaffin cells. *Proc Natl Acad Sci U S A* 79, 6712-6716.
- Ng, Y.K., Lu, X., Gulacsi, A., Han, W., Saxton, M.J., and Levitan, E.S. (2003). Unexpected mobility variation among individual secretory vesicles produces an apparent refractory neuropeptide pool. *Biophys J* 84, 4127-4134.
- Nicholson, L., Singh, G.K., Osterwalder, T., Roman, G.W., Davis, R.L., and Keshishian, H. (2008). Spatial and temporal control of gene expression in *Drosophila* using the inducible GeneSwitch GAL4 system. I. Screen for larval nervous system drivers. *Genetics* 178, 215-234.

- Niwa, S., Tanaka, Y., and Hirokawa, N. (2008). KIF1Bbeta- and KIF1A-mediated axonal transport of presynaptic regulator Rab3 occurs in a GTP-dependent manner through DENN/MADD. *Nat Cell Biol* 10, 1269-1279.
- Okada, Y., Yamazaki, H., Sekine-Aizawa, Y., and Hirokawa, N. (1995). The neuron-specific kinesin superfamily protein KIF1A is a unique monomeric motor for anterograde axonal transport of synaptic vesicle precursors. *Cell* 81, 769-780.
- Pack-Chung, E., Kurshan, P.T., Dickman, D.K., and Schwarz, T.L. (2007a). A *Drosophila* kinesin required for synaptic bouton formation and synaptic vesicle transport. *Nat Neurosci* 10, 980-989.
- Pack-Chung, E., Kurshan, P.T., Dickman, D.K., and Schwarz, T.L. (2007b). A *Drosophila* kinesin required for synaptic bouton formation and synaptic vesicle transport. *Nature neuroscience* 10, 980-989.
- Park, J.J., Koshimizu, H., and Loh, Y.P. (2009). Biogenesis and transport of secretory granules to release site in neuroendocrine cells. *J Mol Neurosci* 37, 151-159.
- Park, J.J., and Loh, Y.P. (2008). How peptide hormone vesicles are transported to the secretion site for exocytosis. *Mol Endocrinol* 22, 2583-2595.
- Perlson, E., Jeong, G.B., Ross, J.L., Dixit, R., Wallace, K.E., Kalb, R.G., and Holzbaur, E.L. (2009). A switch in retrograde signaling from survival to stress in rapid-onset neurodegeneration. *J Neurosci* 29, 9903-9917.
- Perlson, E., Maday, S., Fu, M.M., Moughamian, A.J., and Holzbaur, E.L. (2010). Retrograde axonal transport: pathways to cell death? *Trends Neurosci* 33, 335-344.
- Pfister, K.K., Shah, P.R., Hummerich, H., Russ, A., Cotton, J., Annuar, A.A., King, S.M., and Fisher, E.M. (2006). Genetic analysis of the cytoplasmic dynein subunit families. *PLoS Genet* 2, e1.
- Pouli, A.E., Emmanouilidou, E., Zhao, C., Wasmeier, C., Hutton, J.C., and Rutter, G.A. (1998). Secretory-granule dynamics visualized in vivo with a phogrin-green fluorescent protein chimaera. *Biochem J* 333 (Pt 1), 193-199.
- Praprotnik, D., Smith, M.A., Richey, P.L., Vinters, H.V., and Perry, G. (1996). Filament heterogeneity within the dystrophic neurites of senile plaques suggests blockage of fast axonal transport in Alzheimer's disease. *Acta Neuropathol* 91, 226-235.
- Prokop, A. (2006). Organization of the efferent system and structure of neuromuscular junctions in *Drosophila*. *Int Rev Neurobiol* 75, 71-90.
- Puls, I., Jonnakuty, C., LaMonte, B.H., Holzbaur, E.L., Tokito, M., Mann, E., Floeter, M.K., Bidus, K., Drayna, D., Oh, S.J., *et al.* (2003). Mutant dynactin in motor neuron disease. *Nat Genet* 33, 455-456.

Puls, I., Oh, S.J., Sumner, C.J., Wallace, K.E., Floeter, M.K., Mann, E.A., Kennedy, W.R., Wendelschafer-Crabb, G., Vortmeyer, A., Powers, R., *et al.* (2005). Distal spinal and bulbar muscular atrophy caused by dynactin mutation. *Ann Neurol* 57, 687-694.

Purves, D. (2001). *Neuroscience*, 2nd edn (Sunderland, Mass., Sinauer Associates).

Rao, S., Lang, C., Levitan, E.S., and Deitcher, D.L. (2001a). Visualization of neuropeptide expression, transport, and exocytosis in *Drosophila melanogaster*. *Journal of neurobiology* 49, 159-172.

Rao, S., Lang, C., Levitan, E.S., and Deitcher, D.L. (2001b). Visualization of neuropeptide expression, transport, and exocytosis in *Drosophila melanogaster*. *J Neurobiol* 49, 159-172.

Riviere, J.B., Ramalingam, S., Lavastre, V., Shekarabi, M., Holbert, S., Lafontaine, J., Srour, M., Merner, N., Rochefort, D., Hince, P., *et al.* (2011). KIF1A, an axonal transporter of synaptic vesicles, is mutated in hereditary sensory and autonomic neuropathy type 2. *Am J Hum Genet* 89, 219-230.

Rolls, M.M. (2011). Neuronal polarity in *Drosophila*: sorting out axons and dendrites. *Dev Neurobiol* 71, 419-429.

Roos, J., Hummel, T., Ng, N., Klambt, C., and Davis, G.W. (2000). *Drosophila* Futsch regulates synaptic microtubule organization and is necessary for synaptic growth. *Neuron* 26, 371-382.

Salio, C., Lossi, L., Ferrini, F., and Merighi, A. (2006). Neuropeptides as synaptic transmitters. *Cell Tissue Res* 326, 583-598.

Sanyal, S., Consoulas, C., Kuromi, H., Basole, A., Mukai, L., Kidokoro, Y., Krishnan, K.S., and Ramaswami, M. (2005). Analysis of conditional paralytic mutants in *Drosophila* sarcoplasmic reticulum calcium ATPase reveals novel mechanisms for regulating membrane excitability. *Genetics* 169, 737-750.

Schmid, A., and Sigrist, S.J. (2008). Analysis of neuromuscular junctions: histology and in vivo imaging. *Methods Mol Biol* 420, 239-251.

Shakiryanova, D., Klose, M.K., Zhou, Y., Gu, T., Deitcher, D.L., Atwood, H.L., Hewes, R.S., and Levitan, E.S. (2007). Presynaptic ryanodine receptor-activated calmodulin kinase II increases vesicle mobility and potentiates neuropeptide release. *The Journal of neuroscience : the official journal of the Society for Neuroscience* 27, 7799-7806.

Shakiryanova, D., Tully, A., Hewes, R.S., Deitcher, D.L., and Levitan, E.S. (2005). Activity-dependent liberation of synaptic neuropeptide vesicles. *Nature neuroscience* 8, 173-178.

Shakiryanova, D., Tully, A., and Levitan, E.S. (2006a). Activity-dependent synaptic capture of transiting peptidergic vesicles. *Nature neuroscience* 9, 896-900.

Shakiryanova, D., Tully, A., and Levitan, E.S. (2006b). Activity-dependent synaptic capture of transiting peptidergic vesicles. *Nat Neurosci* 9, 896-900.

- Shin, H., Wyszynski, M., Huh, K.H., Valtschanoff, J.G., Lee, J.R., Ko, J., Streuli, M., Weinberg, R.J., Sheng, M., and Kim, E. (2003). Association of the kinesin motor KIF1A with the multimodular protein liprin-alpha. *J Biol Chem* 278, 11393-11401.
- Siegel, G.J. (1999). *Basic neurochemistry : molecular, cellular, and medical aspects*, 6th edn (Philadelphia, Lippincott Williams & Wilkins).
- Silverman, M.A., Johnson, S., Gurkins, D., Farmer, M., Lochner, J.E., Rosa, P., and Scalettar, B.A. (2005). Mechanisms of transport and exocytosis of dense-core granules containing tissue plasminogen activator in developing hippocampal neurons. *J Neurosci* 25, 3095-3106.
- Smith, R., and Taylor, J.P. (2011). Dissection and imaging of active zones in the *Drosophila* neuromuscular junction. *J Vis Exp*.
- Sobota, J.A., Mohler, W.A., Cowan, A.E., Eipper, B.A., and Mains, R.E. (2010). Dynamics of peptidergic secretory granule transport are regulated by neuronal stimulation. *BMC Neurosci* 11, 32.
- Staal, R.G., Mosharov, E.V., and Sulzer, D. (2004). Dopamine neurons release transmitter via a flickering fusion pore. *Nat Neurosci* 7, 341-346.
- Strom, A.L., Gal, J., Shi, P., Kasarskis, E.J., Hayward, L.J., and Zhu, H. (2008). Retrograde axonal transport and motor neuron disease. *J Neurochem* 106, 495-505.
- Sturman, D.A., Shakiryanova, D., Hewes, R.S., Deitcher, D.L., and Levitan, E.S. (2006). Nearly neutral secretory vesicles in *Drosophila* nerve terminals. *Biophys J* 90, L45-47.
- Thorn, N.A. (1966). In vitro studies of the release mechanism for vasopressin in rats. *Acta Endocrinol (Copenh)* 53, 644-654.
- Tobias, G.S., and Koenig, E. (1975). Axonal protein synthesizing activity during the early outgrowth period following neurotomy. *Exp Neurol* 49, 221-234.
- Tsuboi, T., Kitaguchi, T., Karasawa, S., Fukuda, M., and Miyawaki, A. (2010). Age-dependent preferential dense-core vesicle exocytosis in neuroendocrine cells revealed by newly developed monomeric fluorescent timer protein. *Mol Biol Cell* 21, 87-94.
- Tsuboi, T., McMahon, H.T., and Rutter, G.A. (2004). Mechanisms of dense core vesicle recapture following "kiss and run" ("cavcapture") exocytosis in insulin-secreting cells. *J Biol Chem* 279, 47115-47124.
- Tsuboi, T., and Rutter, G.A. (2003). Multiple forms of "kiss-and-run" exocytosis revealed by evanescent wave microscopy. *Curr Biol* 13, 563-567.
- Vardjan, N., Stenovec, M., Jorgacevski, J., Kreft, M., and Zorec, R. (2007). Subnanometer fusion pores in spontaneous exocytosis of peptidergic vesicles. *J Neurosci* 27, 4737-4746.

- Vaughan, K.T. (2005). Microtubule plus ends, motors, and traffic of Golgi membranes. *Biochim Biophys Acta* 1744, 316-324.
- Vaughan, K.T., and Vallee, R.B. (1995). Cytoplasmic dynein binds dynactin through a direct interaction between the intermediate chains and p150Glued. *J Cell Biol* 131, 1507-1516.
- Vaughan, P.S., Miura, P., Henderson, M., Byrne, B., and Vaughan, K.T. (2002). A role for regulated binding of p150(Glued) to microtubule plus ends in organelle transport. *J Cell Biol* 158, 305-319.
- Wagh, D.A., Rasse, T.M., Asan, E., Hofbauer, A., Schwenkert, I., Durrbeck, H., Buchner, S., Dabauvalle, M.C., Schmidt, M., Qin, G., *et al.* (2006). Bruchpilot, a protein with homology to ELKS/CAST, is required for structural integrity and function of synaptic active zones in *Drosophila*. *Neuron* 49, 833-844.
- Wagner, O.I., Esposito, A., Kohler, B., Chen, C.W., Shen, C.P., Wu, G.H., Butkevich, E., Mandalapu, S., Wenzel, D., Wouters, F.S., *et al.* (2009). Synaptic scaffolding protein SYD-2 clusters and activates kinesin-3 UNC-104 in *C. elegans*. *Proc Natl Acad Sci U S A* 106, 19605-19610.
- Washburn, C.L., Bean, J.E., Silverman, M.A., Pellegrino, M.J., Yates, P.A., and Allen, R.G. (2002). Regulation of peptidergic vesicle mobility by secretagogues. *Traffic* 3, 801-809.
- Wiegand, U.K., Duncan, R.R., Greaves, J., Chow, R.H., Shipston, M.J., and Apps, D.K. (2003). Red, yellow, green gol--A novel tool for microscopic segregation of secretory vesicle pools according to their age. *Biochem Soc Trans* 31, 851-856.
- Wong, M.Y., Shakiryanova, D., and Levitan, E.S. (2009). Presynaptic ryanodine receptor-CamKII signaling is required for activity-dependent capture of transiting vesicles. *J Mol Neurosci* 37, 146-150.
- Wong, M.Y., Zhou, C., Shakiryanova, D., Lloyd, T.E., Deitcher, D.L., and Levitan, E.S. (2012). Neuropeptide delivery to synapses by long-range vesicle circulation and sporadic capture. *Cell* 148, 1029-1038.
- Xia, X., Lessmann, V., and Martin, T.F. (2009). Imaging of evoked dense-core-vesicle exocytosis in hippocampal neurons reveals long latencies and kiss-and-run fusion events. *J Cell Sci* 122, 75-82.
- Ye, B., Zhang, Y., Song, W., Younger, S.H., Jan, L.Y., and Jan, Y.N. (2007). Growing dendrites and axons differ in their reliance on the secretory pathway. *Cell* 130, 717-729.
- Zahn, T.R., Angleson, J.K., MacMorris, M.A., Domke, E., Hutton, J.F., Schwartz, C., and Hutton, J.C. (2004). Dense core vesicle dynamics in *Caenorhabditis elegans* neurons and the role of kinesin UNC-104. *Traffic* 5, 544-559.
- Zhainazarov, A.B., and Cottrell, G.A. (1998). Single-channel currents of a peptide-gated sodium channel expressed in *Xenopus* oocytes. *J Physiol* 513 (Pt 1), 19-31.

Zhang, Z., Bhalla, A., Dean, C., Chapman, E.R., and Jackson, M.B. (2009). Synaptotagmin IV: a multifunctional regulator of peptidergic nerve terminals. *Nat Neurosci* 12, 163-171.

Zhong, Y., and Pena, L.A. (1995). A novel synaptic transmission mediated by a PACAP-like neuropeptide in *Drosophila*. *Neuron* 14, 527-536.

Ziv, N.E., and Garner, C.C. (2004). Cellular and molecular mechanisms of presynaptic assembly. *Nat Rev Neurosci* 5, 385-399.

Zupanc, G.K. (1996). Peptidergic transmission: from morphological correlates to functional implications. *Micron* 27, 35-91.

Zweifel, L.S., Kuruvilla, R., and Ginty, D.D. (2005). Functions and mechanisms of retrograde neurotrophin signalling. *Nat Rev Neurosci* 6, 615-625.